CHAPTER 1 Introduction

The protection of cobalt nanoparticles against surface oxidation has been a focus in our labs for many years. Many methods have been employed to stabilize these particles in organic media making them available for many bioapplications. Such methods include siloxane pendent nitrile complexation with the cobalt nanoparticles.[1,2]

Silicones or siloxanes are widely produced by anionic ring-opening polymerization of cyclic trimers such as hexamethylcyclotrisiloxane (D_3). However, the anionic ring-opening copolymerizations of vinyl substituted cyclic trimers (D_3^v) along with D_3 have not been widely studied. It is known that the reactivity ratios between the two monomers are quite different.[3] Therefore, investigating the copolymerization of these two monomers to prepare well-defined poly(dimethylsiloxane-*b*-methylvinylsiloxane) (PDMS-*b*-PMVS) diblock copolymers has been one goal of this research (figure 1.1). Also, investigating the thermal properties of these materials is key in understanding phase behavior of these copolysiloxanes. This will be discussed in chapter 3.

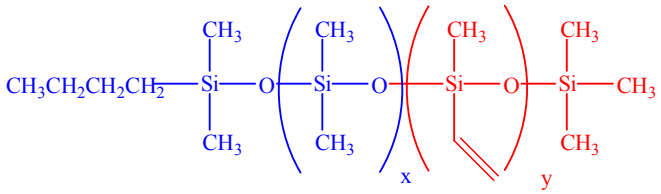

Figure 1.1 Chemical structure of PDMS-PMVS diblock copolymers

Another goal of this research has been to functionalize copolysiloxanes with triethoxysilyl and trimethoxysilyl pendent groups (figure 1.2). This will be discussed in

detail in chapter 4. The thermal and solution properties of these functionalized materials were investigated. It is believed that micellar solutions of these block copolymers may serve as "nanoreactors" for the thermal decomposition and precipitation of cobalt nanoparticles.

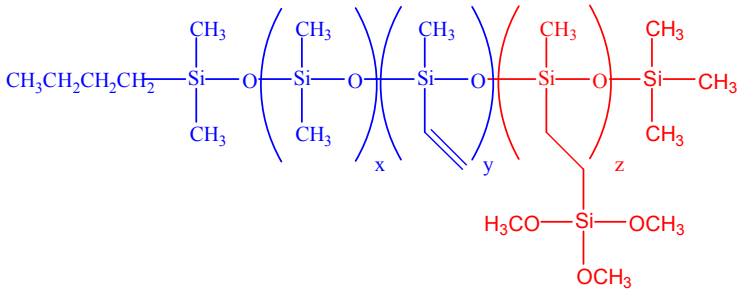

Figure 1.2 Chemical structure of PDMS-PMVS-PMTMS

Previous work in this area has investigated forming "silica-like" thin shells around the cobalt nanoparticles as a possible method to protect against surface oxidation. However, these materials were hydrolyzed and condensed utilizing rather high concentrations of dibutyltin diacetate as the catalyst and this proved to be cytotoxic.[1,4] Therefore, one goal of the present research was to develop a methodology for hydrolysis and condensation without added catalyst was needed. Chapter 5 dicusses these sol-gel reactions of triethoxysilyl and trimethoxysilyl functionalized copolysiloxanes.

Cobalt nanoparticles have been prepared by the thermolysis of dicobalt octacarbonyl in toluene in the presence of a poly(dimethylsiloxane)-*b*-[poly(methylvinylsiloxane-*co*-(methyl-[trimethoxysilyl-2-ethyl]siloxane)] (PDMS-*b*-[PMVS-*co*-PMTMS]) as well as a poly(dimethylsiloxane)-*b*-[poly(methylvinylsiloxane--*co*-(methyl-[triethoxysilyl-2-ethyl]siloxane)] (PDMS-*b*-[PMVS-*co*-PMTES]) copolymers

serving as steric stabilizers (figure 1.3). These reactions produced narrow size distributions of approximately 10 nm diameter particles with high saturation magnetization. It is proposed that the [PMVS-*co*-PMTMS] or [PMVS-*co*-PMTES] form anchor blocks whereas the PDMS tails protrude into toluene providing dispersion stability. The preparation and characterization of these magnetic fluids are discussed in chapter 6.

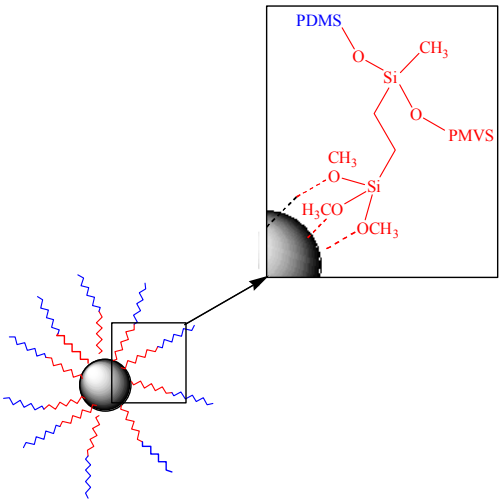

Figure 1.3 Cobalt nanoparticles stabilized with PDMS-*b*-[PMVS-*co*-PMTMS] copolymer.

CHAPTER 2. Literature Review

2.1 Overview

This chapter will discuss areas directly related to the research topic and is divided into five sections. The first section presents an overview of polysiloxane chemistry including physical properties, synthesis of cyclosiloxane monomers including a detailed discussion of the synthesis of vinyl substituted D_3 monomers as it directly applies to this research. The synthesis of polysiloxanes via thermodynamic and kinetic control will be included as well. Siloxane block copolymers and their ability to form micelles in solution will be discussed in detail in the second section. The third section covers sol-gel chemistry due to its implementation in this research as a possible method to inhibit oxidative degradation of stabilized cobalt nanoparticles. In the fourth section, magnetic materials and their properties will be discussed. The final section will discuss the preparation of stable cobalt dispersions via the reduction of $CoCl_2$ and the thermolysis of $Co_2(CO)_8$.

2.2 Introduction to polysiloxane synthesis

2.2.1 Overview of polysiloxanes

Polysiloxanes have been extensively studied over many years. They are comprised of silicon atoms bonded to oxygen. Silicones are intermediates between organic and inorganic compounds, specifically between silicates and organic polymers. The term "silicones" was first coined due to the structural resemblance between R_2SiO and those of "ketones" (R_2CO). However, the Si=O bond is very unstable unlike the C=O bond in ketones.[5] The term "polysiloxane" was proposed based on the structure of the repeating unit in the polymer backbone (Si-O-Si). Silicones can, therefore, be categorized based on their structure:

Table 2.1 Structural Units of Polysiloxanes[6]

Structural Formula	Composition	Functionality	Symbol
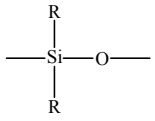	$R_3SiO_{1/2}$	Monofunctional	M
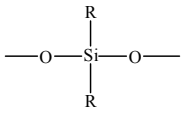	$R_2SiO_{2/2}$	Difunctional	D
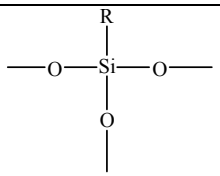	$RSiO_{3/2}$	Trifunctional	T
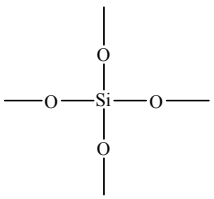	$SiO_{4/2}$	Tetrafunctional	Q

Silicones bring together properties of inorganic and organic materials which give rise to the vast array of industrial applications ranging from aircraft gaskets to auto polishes to construction sealants.[7] Other applications include silicone resins, silicone fluids, siloxane room-temperature-vulcanized (RTV's) rubbers, and siloxane heat-cured rubbers.[7,8] The wide range of applications is summarized in table 2.2.

Table 2.2 Silicones and their applications

Silicone Fluids	*Silicone Resins*
Plastic adhesives	Varnishes
Hydraulic fluids	Protective coatings
Vibration damping	Electric insulations
Release agents	Adhesives
Anti-foamers	Laminates
Dielectric media	Encapsulants
Cosmetic and health product additives	Release coatings
Surfactants	Junction coatings
Greases	Paints
Polishes	

RTV Rubbers	*Heat-Cured Rubbers*
Sealants	Wire-cable insulation
Adhesives	Belting
Gaskets	Tubing and hoses
Foams	Fabric coating
Surgical aids	Extruding
Glazing	Fuel-resistant rubber parts
Medical implants	Medical implants

This wide range of applications is attributable to the unique properties of polysiloxanes (table 2.3).[7] These properties result from its inherent chemical structure and, thus, require a detailed discussion of the basic structure/property relationships of polysiloxanes.

Table 2.3 Unique Properties of Polysiloxanes

Properties
1.) Thermal and oxidative stability 2.) Low temperature properties. Retention of flexibility, elasticity, or flow at temperatures as low as or even lower than -110 °C. 3.) Low surface tension and high surface hydrophobicity 4.) Inertness and biocompatibility 5.) Good electrical insulators and resistance.

Silicon is an amphoteric element and is also known to be one of the most abundant elements at 27.5% of the earth's crust following oxygen at 46.4%.[9] The silicon atom occurs in nature in three isotopic forms. Their natural abundance are listed in table 2.4.

Table 2.4 Silicon Isotope Abundance[10]

Isotope	Abundance	Spin quantum number, l
^{28}Si ^{29}Si ^{30}Si	92.18 4.71 3.21	0 ½ 0

In addition, the silicon atom possesses *d*-orbitals which can accept electron density from other atoms, giving the bonds some double bond character.[5,11,12] The resulting bond is more covalent in nature than ionic. For example, an oxygen atom in an ether shows more basic character than the oxygen in silicones. It also supports the enhanced electrophilicity of a vinyl substituted silicon atom.[9,13] The polarity of the Si-H bond is higher than that of a C-H bond, therefore making it quite susceptible to nucleophilic attack. This has resulted in a wide array of substituted silicon-containing compounds. The Si-O bond has substantial ionic character and has a higher bond strength than that of Si-H or Si-C bonds.[5] This accounts for the high thermal stability of polysiloxanes. For example, the degradation of polydimethylsiloxane, PDMS, begins at 350 °C which is higher than for most organic compounds. This high degradation temperature of polysiloxanes may also be attributed to the higher bond disassociation energies of the Si-O bonds in comparison to the C-C or C-O bonds.

Table 2.5 Mean bond energies in kJ/mol of several bonds of carbon and silicon[14]

Bond	***C***	***Si***
X-X	346	222
X-O	358	452
X-H	413	318

The Si-O skeleton bond is 1.64 Å which is significantly longer than the 1.53 Å C-C single bond. The siloxane bond rotates easily about the Si-O axis, especially when small substituents are present such as a methyl group.[15] This rotational ability creates larger intermolecular distances between dimethylsiloxane chains and smaller intermolecular forces.[16] It has also been shown that these polymers exist in α-helical configurations which allow them to retain their size upon absorbtion of heat. This results in little variation of physical properties such as viscosity with temperature.

In PDMS, the bond angles of 143° in Si-O-Si and 110° in O-Si-O are significantly more than the tetrahedral bond angle of 109.5° of hydrocarbon chains. This gives rise to an open structure and low rotational barrier. This accounts for their low glass transition temperature (≈-125 °C for PDMS) and low surface tension (≈20 mN/m for PDMS).[17,18]

Table 2.6 Silicon and Carbon Rotational Barriers[9,19]

Bond	Energy (kJ/mole)
Si-O	< 0.8
C-O	11.3
Si-CH_3	6.7
C-CH_3	15.1

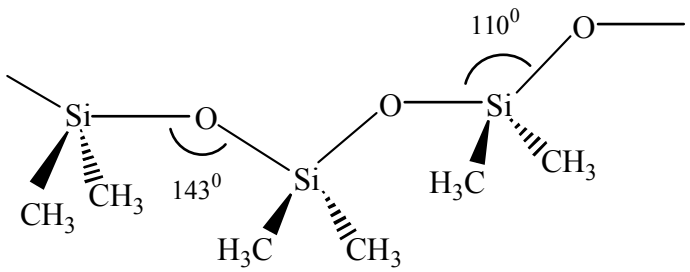

Figure 2.1 PDMS chains indicating bond angles of the siloxane backbone.

Polysiloxanes also possess other highly desirable properties such as electrical resistance. Therefore, these polymers offer great advantages in the electrical industry due to the low relative permittivity of PDMS fluids of approximately 2.75. This is significantly lower than 20.7 and 78.5 for acetone and water, respectively.[20] Along with the low permittivity of PDMS, it also exhibits high hydrophobicity. This property may be altered or enhanced by incorporating different moieties on the backbone. PDMS with pendent methyl groups is a perfect example of hydrophobic groups on the siloxane backbone.

2.2.2. Preparation of Cyclosiloxanes

Cyclosiloxanes can be prepared via several different methodologies. Ladenburg first reported the preparation of a mixture of siloxanes in 1872 after studying the reaction between acidified water and diethyldiethoxysilane.[21] Stock and Somieski, in 1919, were the first reported investigators to obtain a very small amount of liquid, polydimethylsiloxane (PDMS). However, it was Kipping and Lloyd who carried out a systematic study of organosilicon chemistry. They resolved that each silicon was shared by two oxygens and that each oxygen by two silicons.

Hyde and DeLong reported a method by which certain cyclosiloxanes could be converted into industrially useful compounds.[22] The most common method derived from these earlier studies involved the hydrolysis of a reactive silane. This method is still utilized due to the commercial availability of diorganodichlorosilanes. Hydrolysis of a diorganodichlorosilane yields a diol which undergoes condensation to produce mixtures

of cyclosiloxanes and linear polysiloxanes. Dichlorodimethylsilane, for example, can be hydrolyzed to yield an unstable diol which immediately undergoes condensation to yield a mixture of polydimethylsiloxanes and dimethylsiloxane cyclics (Figure 2.2).[23] The cyclics are easily recovered by fractional distillation.

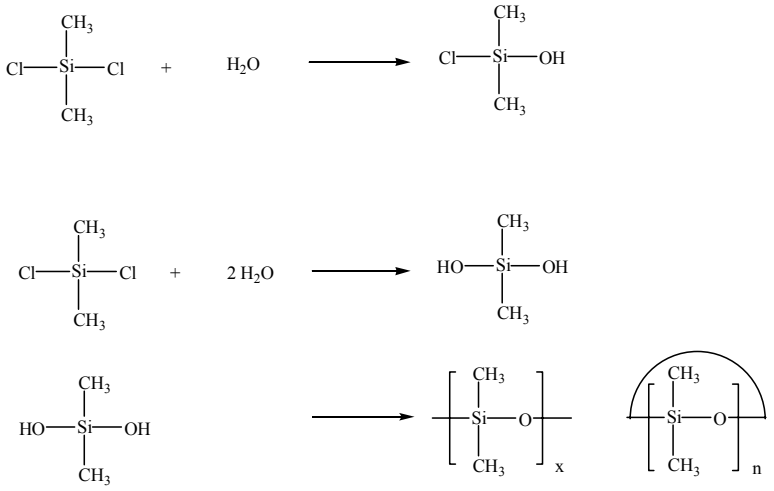

Figure 2.2 Hydrolysis of dichloromethylsilane to produce linear PDMS and dimethylsiloxane cyclics. [23]

However, it is the reaction conditions that dictate the proportion of cyclic to linear species. The distribution of cyclosiloxanes also depends upon the nature of the hydrolyzed compound. It was found that the yield of cyclosiloxanes was optimized when the extent of intermolecular condensation was limited, and intramolecular condensation was induced when the degree of condensation equaled or exceeded 3. Low concentrations of reactants favored intramolecular condensation over intermolecular condensation, and lower temperatures and bulky organic substituents on silicon limited the extent of condensation.[24]

It was also reported that the pH of the reaction medium had significant effects on the product composition. Hydrolysis in strongly acidic media favored the production of

cyclics and low molecular weight polysiloxanes. Hydrolysis in basic media, however, had the opposite effect.[25]

Solvent interactions were investigated as possible methods to control the condensation to form cyclosiloxanes. It was believed that the solvent used in hydrolysis may markedly affect the product composition. Water-miscible solvents favored the formation of cyclic compounds.[26] However, a *very* polar solvent may increase the amount of ring-opening reactions of the cyclic trimer. For example, the condensation of diethyldichlorosilane in ether yielded the trimer, $(Et_2SiO)_3$, and the tetramer, $(Et_2SiO)_4$ in 41 and 31% yields, respectively. However, the same condensation in methanol yielded 70% tetramer.[27]

The thermodynamically favored product, D_4, is typically synthesized commercially by the process discussed above. Due to its cost-effectiveness, the most common method to produce linear PDMS is via equilibration reactions. However, the more reactive trimer, D_3, used for living polymerizations, is produced by several different methodologies. Commercial production of D_3 typically involves 1,3-dihydroxy-1,1,3,3-tetramethyldisiloxane and dichlorodimethylsilane in the presence of pyridine.[28,29] Hexamethylcyclotrisiloxane can also be prepared by using 10% excess zinc oxide in the presence of dichlorodimethylsilane (figure 2.3).[30,31]

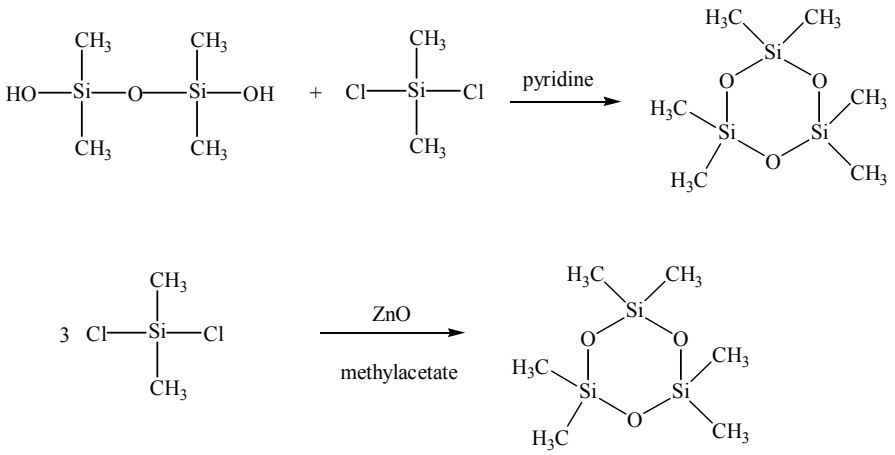

Figure 2.3 Preparation of hexamethylcyclotrisiloxane

In more recent years, various new synthetic approaches have been reported for preparing the reactive trimer. These novel methods involved reaction of dimethylsulfoxide with a dichlorodialkylsilane (figure 2.4). Weber et. al reported higher yields of cyclic trimers in this manner.[3,32-34] The deoxygenation of sulfoxide to sulfide is an important synthetic reaction in organic chemistry and was found to be an efficient method for preparing cyclotrisiloxanes of varying functionality including 1,3,5-trivinyl-1,3,5-trimethylcyclotrisiloxane.[3] These syntheses were usually conducted in chloroform utilizing triethylamine as a proton scavenger. There are other methods involving chlorosilanes and metals, such as Zn, that involve deoxygenation of sulfoxides. These methods have expanded the range of accessible cyclosiloxanes.[35]

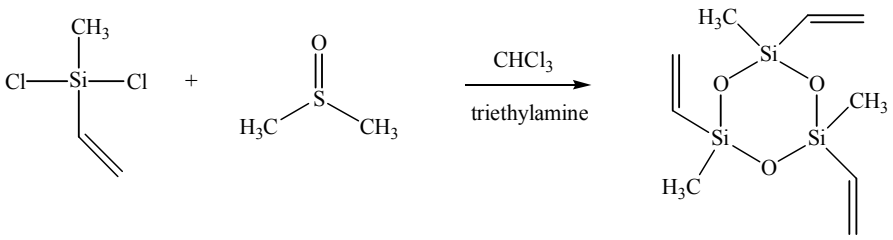

Figure 2.4 Preparation of 1,3,5-trivinyl-1,3,5-trimethylcyclotrisiloxane[3,32]

2.2.3. Ring-Chain Equilibria : Thermodynamic Control

Siloxanes are known for their thermal stability, but in the presence of strong acids and bases a mixture of cyclic and linear polysiloxanes will be obtained. The equilibrium concentration of cyclics is strongly dependent upon the change in both enthalpy and entropy of polymerization. The polymerization enthalpy change is close to zero since no net changes of chemical bonding occur. The polymerization of unstrained cyclics such as D_4, however, is driven by a positive change in entropy that is a summation of entropy changes due to mixing, configurational, and translational entropies.[36] There have also been some reports of using the strained trimer, D_3, in equilibrium reactions.[37]

Equilibration polymerization is dependent on the Gibbs free energy change, ΔG. The Gibbs free energy equation describes this dependency by using fundamental thermodynamic quantities: polymerization enthalpy change (ΔH) and polymerization entropy change (ΔS) with respect to temperature.[38,39]

$$\Delta G = \Delta H - T\Delta S$$

The ΔG must be a negative value for the polymerization to occur or to transform cyclics to linear species. As mentioned, there is no net bonding change for the polymerization of D_4. Therefore, the reaction is driven by entropy changes alone yielding a negative ΔG.[40]

Rearrangement or so-called "redistribution" or "equilibration" of the siloxane bonds occur in the presence of strong acids or bases.[41] The siloxane bonds are continuously broken and reformed until the reaction reaches thermodynamic equilibrium. A distribution of cyclics and linear polymers are produced at equilibrium. The equilibrium composition is dependent on the cyclic monomer. A Gaussian distribution of molecular weights for the linear polymers is obtained.[42]

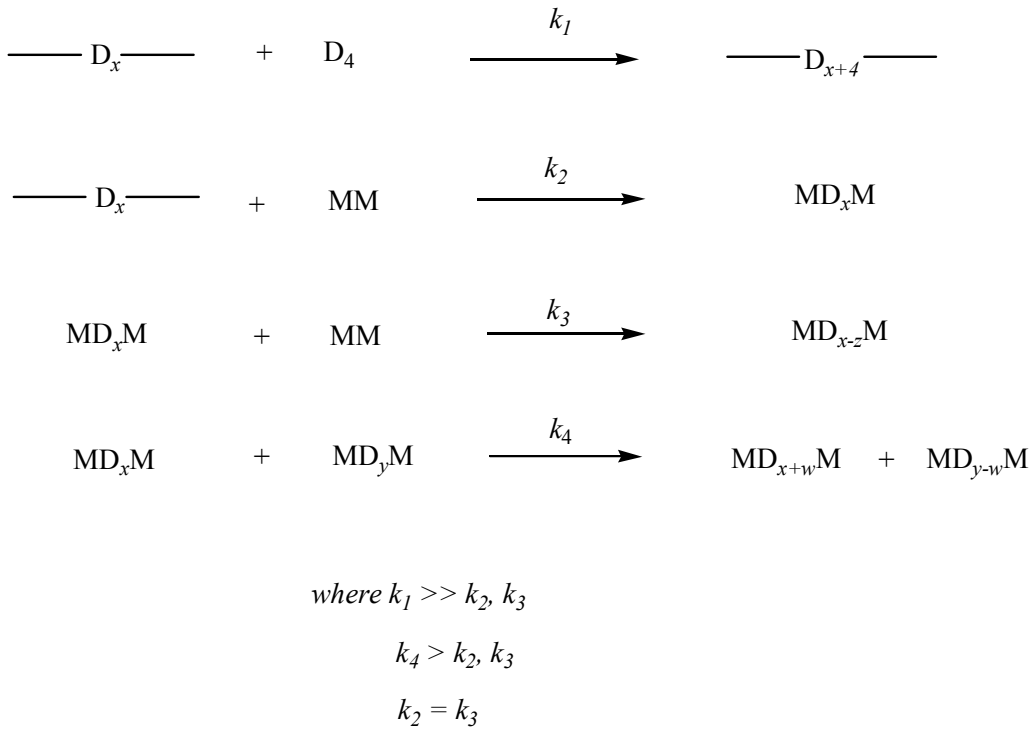

Figure 2.5 Equilibration reaction of siloxanes[41]

The equilibrium concentration also depends strongly on the substituents. Longer and more bulky substituents tend to lead to higher equilibrium concentrations of cyclics. Equilibrium concentrations of common cyclic siloxanes are listed in table 2.7. The percentages of cyclics and linear polymers at equilibrium are also dependent upon the reaction conditions as listed in table 2.8.

Table 2.7 Yields of linear polymers in undiluted equilibrates of siloxanes[37]

R	*R'*	*Approximate Yield %*
Me	Me	82
Me	Et	74
Me	$CF_3CH_2CH_2$	17
Ph	Me	70
Ph	Me	0

Table 2.8 Reaction conditions and their influence on equilibrium position

Conditions	*Linear Polymers*	*D_4*	*D_5-D_9*
135 °C, toluene, KOH[43]	29	33	31
20 °C, benzene, Li cryptate[44]	70	2.7	11.5
20 ºC, CH_2Cl_2, CF_3SO_3H[45]	28	32	27
20 ºC, CH_2Cl_2, CF_3SO_3H-$(CF_3SO_2)_2O$[45]	0	38	22

Another common approach to control the molecular weight of the polymers prepared by the polymerization of unstrained cyclics involves end-blocking reagents. A disiloxane end-block (see general structure in figure 2.6) behaves as a monofucntional monomer in condensation polymerization. It is important that these endblockers contain not only Si-O bonds but also Si-C bonds to prevent any interchange reactions in the equilibration. This method, figure 2.7, is an efficient way to target and control the molecular weights of these polymers. In addition, functional polydimethylsiloxanes may be obtained in this manner to produce siloxane-containing block copolymers or networks.[46,47]

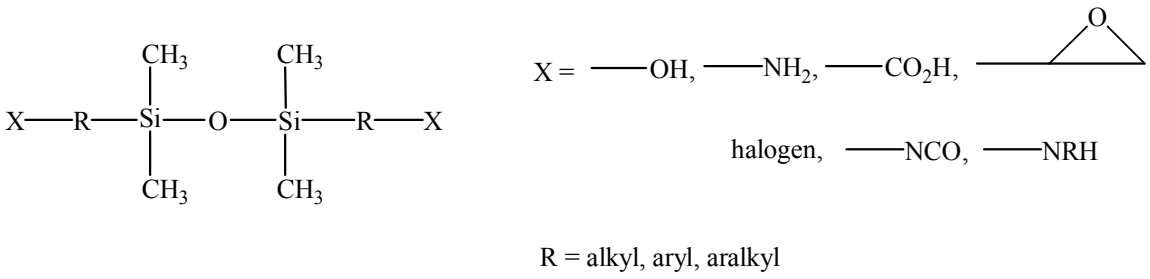

Figure 2.6 End-blocking disiloxanes [42,48]

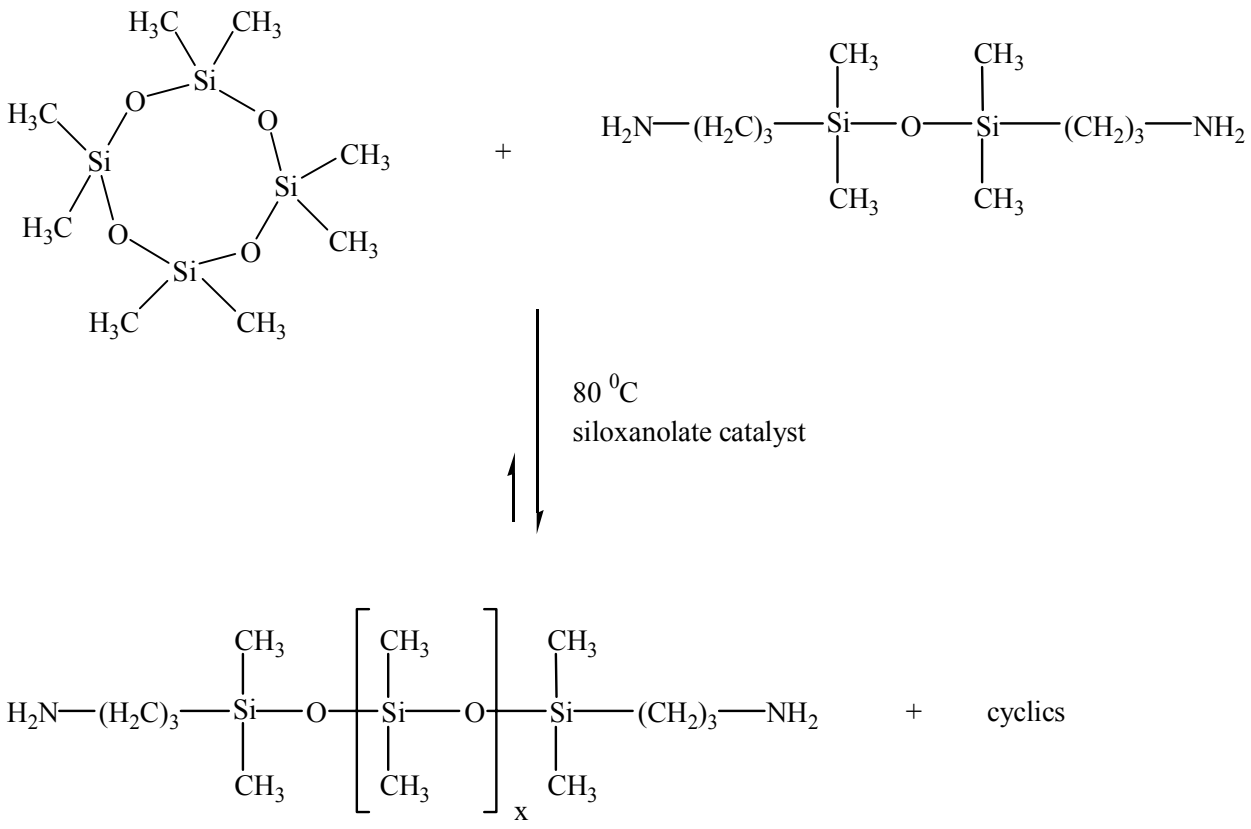

Figure 2.7 Preparation of aminopropyl terminated polydimethylsiloxane via an end-block procedure[44,47,48]

2.2.4 Ring Opening Anionic polymerization : kinetic control

2.2.4.1 Introduction to ring opening anionic polymerization

Several catalysts have been reported for ring opening polymerizations of cyclosiloxanes including strong organic and inorganic acids or bases[49] and metal oxides[50]. Depending on the type of catalyst, the ring opening polymerization can be classified into acid/base polymerization or cationic/anionic polymerization. This section will focus only on anionic polymerization as it pertains to this thesis.

Telechelic polymers with various functional groups are produced by anionic polymerization with exclusively kinetically controlled polymerization and narrow molecular weight distributions.[51] Several catalysts are used in these anionic systems such as alkaline metal hydroxides or silanolates, alkyllithiums, ammonium hydroxides, and phosphonium hydroxides. Cyclic trimers are much preferred to cyclic tetramers due to their higher reactivity attributable to greater ring strain (kinetically favored). For example, the catalyst reacts with the cyclic siloxane to yield oligomeric silanolate chains (chain initiation). It is thought that the silanolate ions then attack the cyclic trimer to form pentacoordinated silicon complexes. These subsequently open to form longer chains. Higher molecular weight polysiloxane chains are produced by propagation; the continuous repeating reaction of chain ends with cyclic timer.

In addition to the ring opening of the cylic monomers, the chain ends also have a reactive affinity towards polymer chains. Backbiting, or reacting on the host chain, occurs in such systems, causes depolymerization, and yields various sized cyclics. However, when the silanolate ions attack other chains, a redistribution of chains occurs (figure 2.8).[52] A reaction that takes place between two silanolate ions is known as specific redistribution. This reaction is faster than a reaction between a siloxane unit in a linear polysiloxane and a silanolate; known as normal reshuffling reactions.[53] The unusual reactivity of the specific redistribution can be explained by the transition state. There is a silicone resonance structure which stabilizes this transition state (figure 2.9).[54,55]

The amount of backbiting, redistribution, and reshuffling is dependent upon the concentration of cyclics in solution. At initial stages of the reaction, the concentration of cyclics is high, therefore, polymerization predominates. However, as the concentration of

cyclics steadily decreases over time, redistribution and reshuffling become important finally reaching an equilibrium between rings and chains. The polysiloxanes produced upon polymerization may be isolated by the addition terminating agents such as chlorosilanes.

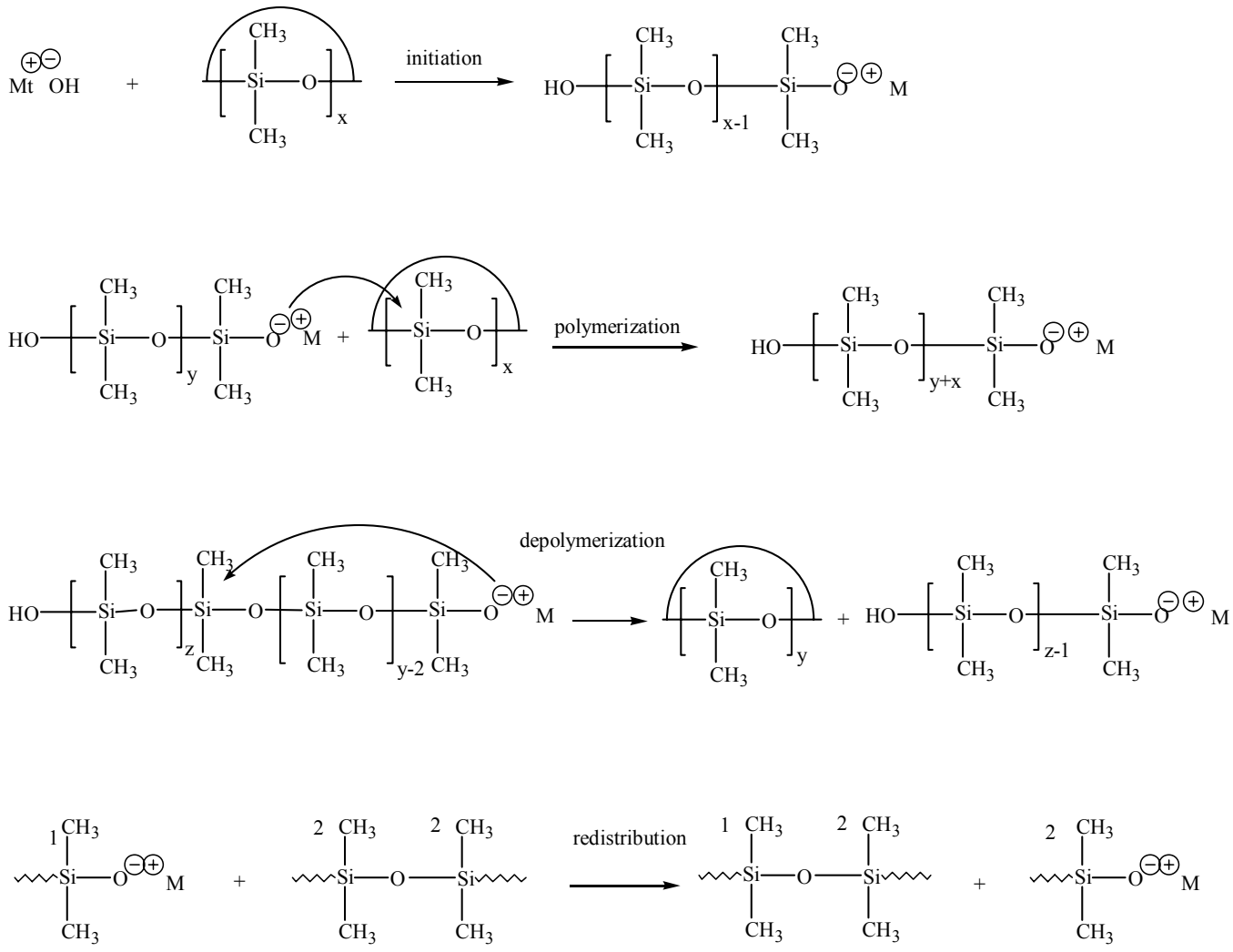

Figure 2.8 Anionic polymerization mechanism of cyclosiloxanes[52,55]

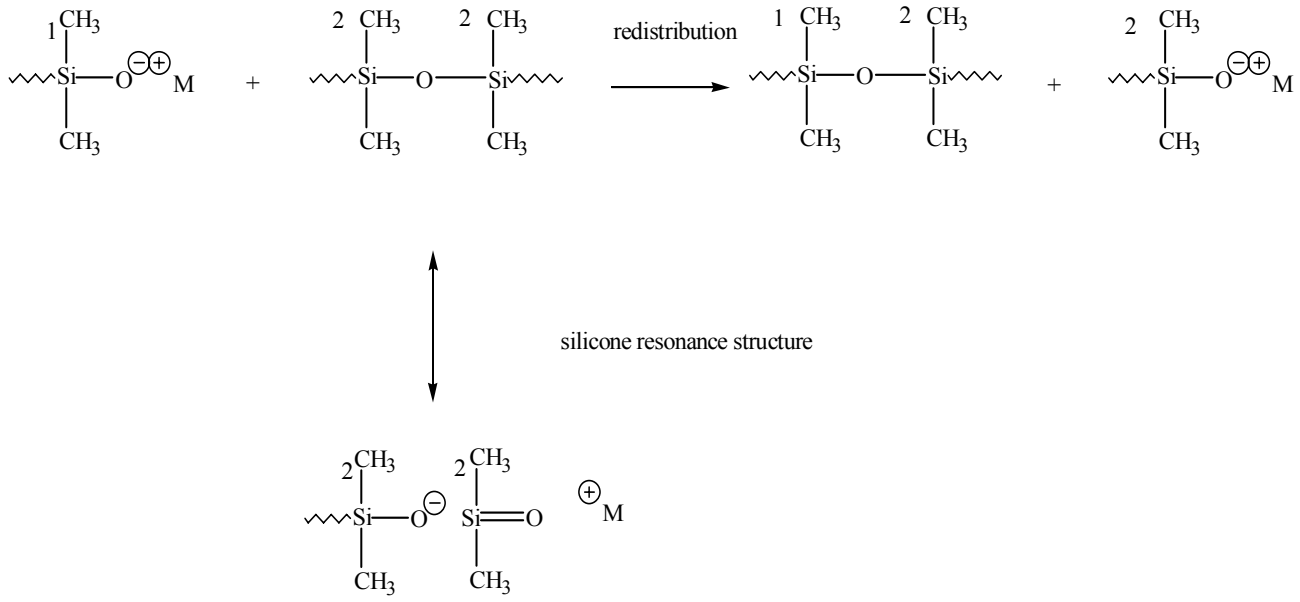

Figure 2.9 Specific redistribution mechanism

The active propagating center for anionic polymerization is an ionic aggregate of silanolate ions rather than free ions. This was determined from various studies including polymerization reaction kinetics and conductivity experiments.[37,56] The rate law suggests that there is an equilibrium established between free silanolate ions and ionic aggregates which lies in favor of aggregates (figure 2.10)

$$\frac{d\,[\text{monomer}]}{dt} = \frac{[\text{Silanolate}]^{1/n}}{(nK_n)^{1/n}} \quad (k_p[\text{monomer}] - k_{\text{depolym.}})$$

Figure 2.10 Rate law of anionic polymerization of cyclosiloxanes[37]

Ionic systems are unique from other polymerization mechanisms in that a variety of species may co-exist and simultaneously contribute to polymerization.[57] These ion pairs will have their own characteristic behavior and exist as free ions, ion pairs, triple ions, and ion pair dimers (figure 2.11).[58] The contributions of aggregates and free ions in solution as well as the rate of polymerization are attributed to the reactivity differences between their counter-ions. The reactivity of counter-ions increases as size of the cation increases.

$$Cs^+ > Rb^+ > K^+ > Na^+ > Li^+$$

The ionic equilibria are influenced by many factors including concentration, cationic or anionic strength, dielectric constant, presence of salts or cation binding ligands, pressure, temperature, and solvent.

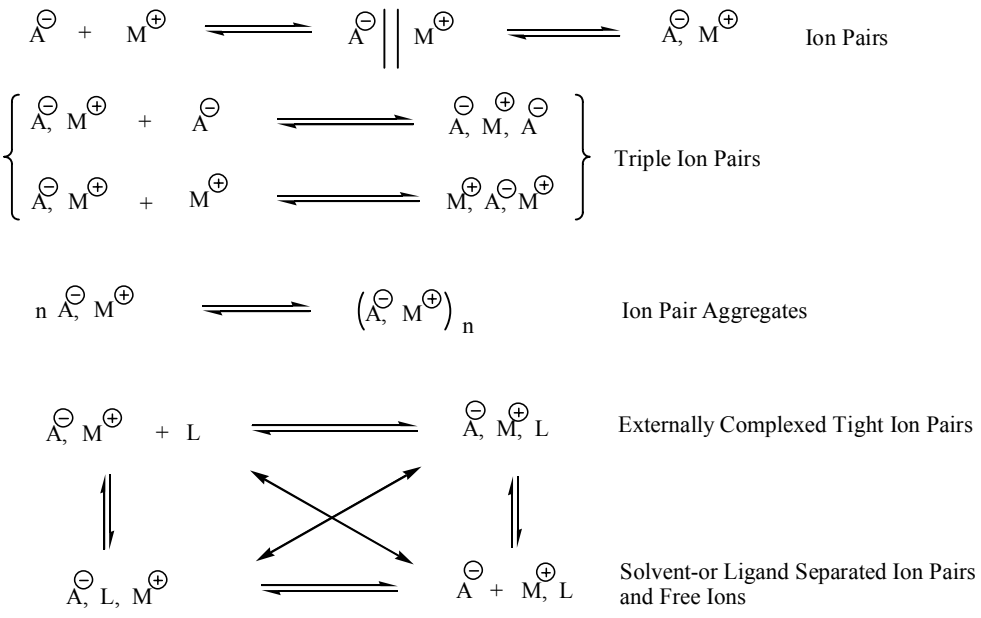

Figure 2.11 Ionic Species present during polymerization[58]

Solvents play an important role in the contributions of these species. Highly polar solvents are not appropriate for these polymerizations for many reasons. Firstly, polar protic solvents such as H_2O, CH_3OH, CH_3CH_2OH, etc., will donate protons and terminate the propagating anionic species, and, secondly, ethers and acetone can form highly stable complexes with the initiator. Therefore, these polymerizations are usually conducted in hydrocarbon solvents of low polarity.

Electron donating compounds increase the rate of polymerization attributed to solvating the cations and increasing the concentration of free silanolate anions. The resulting silanolates are solvent-separated or loose ion pairs. These promoters have large dipole moments and include elements such as oxygen and nitrogen. Monodentate promoters, e.g., tetrahydrofuran (THF)[59], dimethylether[60], hexamethylphosphoramide (HMPA)[60], dimethylsulfoxide (DMSO)[61]and triglyme[62] are typically utilized. It has been reported that multidentate promoters such as poly(ethylene glycol), cryptands[63] and crown ethers[64] can be more effective promoters than the aforementioned monodentates[40]

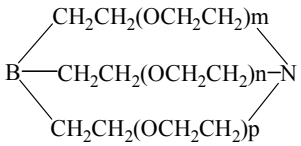

Figure 2.12 Crytate [2,2,1] where m=n=2 and p=1

2.2.4.2 Living Anionic Polymerization

Living anionic polymerization is defined as a base initiated polymerization without any chain transfer or termination reactions.[40] In the mid 1950's, Szwarc et. al. demonstrated that carbanionic polymerizations could be prepared using electron transfer initiation and coined the term "living" for these termination free processes.[57] Stavely and co-workers utilized an alkyllithium initiator to polymerize isoprene with 90% *cis*-1,4 units.[39] What were essentially living polymerizations were reported earlier by Ziegler[65] in 1929 and later by Mark and Dostal[66], and Flory[67]. Anionic living polymerizations have the following ideal features :

1.) The rate constant of initiation (k_i) is greater than or equal to the propagation rate constant (k_p).
2.) The initiator participates only in reactions involving the formation of active centers.
3.) Termination reactions are excluded (termination rate constant, k_t, is 0).
4.) Chain transfer reactions are excluded as well ($k_{tr} = 0$).

These active chain ends are known to have indefinite lifetimes.[40] Living polymerizations are often carried out in solvent of low to moderate polarity such as cyclohexane or hexane. These polymerizations also exhibit a linear increase in molecular weight with percent conversion attributable to the fast initiation process in tandem with the absence of termination reactions (figure 2.13.)

Termination of the living chain can occur by introducing suitable materials such as water, methanol, chlorosilanes. Tailoring block copolymer architecture is achieved by terminating these living polymerizations with functional end groups.

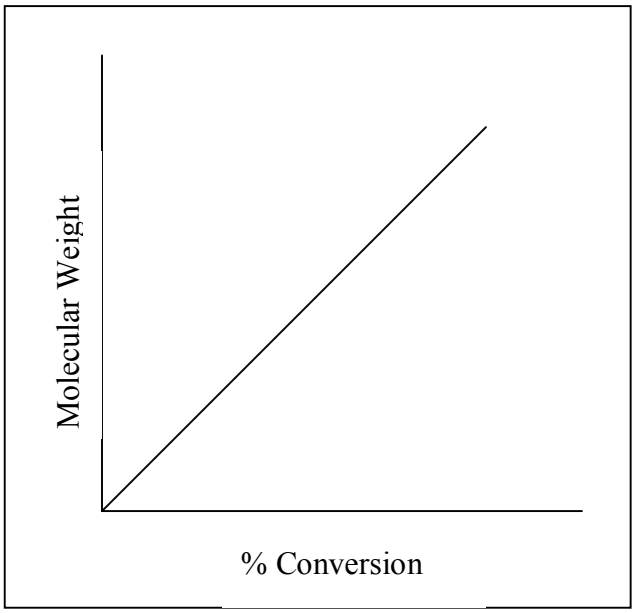

Figure 2.12 Variation of molecular weight with conversion for living anionic polymerizations.

2.2.4.3 Living anionic polymerization of D_3

In the 1980's two groups, Sigwalt and Chojnowski studied the mechanism of cyclic siloxane polymerization.[37,68-70] It was believed that there is a multiplicity of species responsible for chain formation. However, mechanism elucidation is difficult due to the short lifetime of active species due to fast exchange reactions.

Polysiloxane polymerizations rely greatly on the cyclic monomers that exhibit high ring strain as it minimizes side reactions such as redistribution. It has been reported that these monomers, such as D_3, are more reactive in such systems. D_3, in particular,

contains highly reactive Si-O bonds, is somewhat strained, and has a significantly exothermic polymerization (figure 2.13) [53]

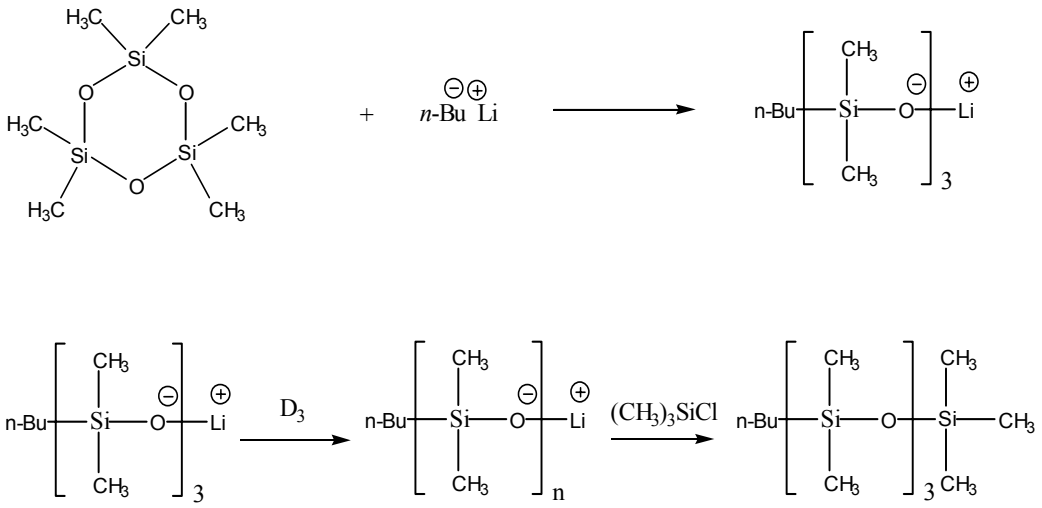

Figure 2.13 Living anionic polymerization of D_3[44]

Organolithium initiators, specifically *n*-butyllithium and *sec*-butyllithium, are the most common initiators for these systems.[3,32] *Sec*-butyllithium forms tetramer aggregates in cyclohexane whereas *n*-butyllithium forms hexamer aggregates in the same solvent.[71]

Precedence was established for the anionic polymerization of D_3 by Sylvie Boileau.[72] She found that D_3 in benzene disappears according to a first-order rate law at least up to 80% conversion. The kinetics of propagation were studied by dilatometry under high vacuum.[73] The R_p (rate of propagation)/ [M] plotted versus [C] was linear(figure 2.14). Therefore, the reaction order in active centers was equal to 1. Two conclusions that can be drawn from this data: one type of active species is present such as

cryptated ion pairs and it may be that there are different types of active centers which may have the same reactivity.

Boileau et. al. also demonstrated that the addition of a promoter or cryptad accelerated the propagation rate of D_3. The polymerization was initiated with *n*-BuLi in benzene. This further supported the idea that electron donating agents, especially multidentate promoters, aid in reaction rates (figure 2.15)

Table 2.9 Polymerization of D_3 initiated by n-BuLi, in benzene at room temperature[72]

D_3 (g)	*nBuLi (10^3 mol)*	*Benzene/THF (v/v)*	*[2,1,1]*	*Propagation Time (hr.)*
5.1	3.95	27/26	0	7
6.0	4.27	26/0	11	1

Viscosity measurements were conducted to clarify the reaction kinetics. Living and deactivated solutions of PDMS were performed in toluene with Li^+ and [2,1,1] as counterion. There was no significant change observed, therefore, the fraction of aggregates was negligible. Conductance experiments of model silanolates in THF determined that the fraction of free aggregates was low. Therefore, the main ionic species is cryptated ion pairs and k_p can be defined as follows :

$$k_p = \frac{R_p}{74} = k_{\pm} = 1.41 \text{ mol}^{-1} \text{ sec}^{-1}$$

In addition, cyclic oligomers are formed as by-products through redistribution and backbiting during propagation. The cyclic concentrations have been determined via GLC

analysis. The conversion of D_3 monomers and the formation of linear polymers, D_4, D_5, and D_6 as a function of time was determined. Showing the formating of polymer to be quite significant.

2.3 Preparation of Block Copolymers

Block copolymers have offered several advantages to typical polymer blends. Firstly, they contain different segments that are covalently bonded together eliminating interfacial problems. Secondly, the molecular architecture can be controlled, and they also serve to strengthen immiscible blends improving interfacial adhesion.

The potential of block copolymers was realized in the late 1950's by Schollenberger who prepared linear polyurethanes composed of "soft" polyester segments and "hard" polyurethane segments.[75] These polymers were found to be soluble in organic solvents even though these materials behaved as crosslinked rubbers.

The development of controlled living anionic polymerization also aided in the development of well-defined block copolymers. This technique was successful in producing diblock and multiblock structures.[76] Polymer properties were found to be dependent on the molecular architecture of the resulting polymer. Milkovich reported that there is a significant difference between diblock and triblock copolymers and their properties (figure 2.14).[77]

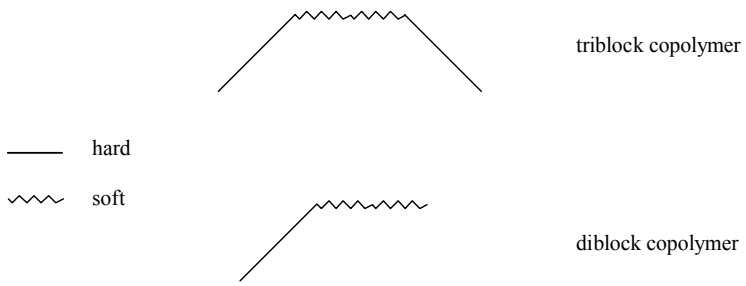

Figure 2.14 Triblock and diblock copolymer architectures.

He also found that the triblock copolymer behaved as a crosslinked elastomers unlike the diblock copolymers. This prompted many investigations and developments of new materials consisting of multiblock copolymers for high performance materials.[78]

Block copolymers show unique properties including transition and elastomeric behavior. Phase separated block copolymers may have two glass transition temperatures, T_g's, corresponding to the two respective blocks. The modulus-temperature behavior of homogeneous and microphase separated systems illustrate this phenomenon.

The elastomeric behavior of block copolymers is characterized by a number of features including thermoplasticity and rubbery behavior. These materials must be two-phase physical networks that evolves the thermoplastic elastomeric behavior. In other words, these systems contain a small fraction of hard block and a large fraction of soft block where the hard blocks aggregate to create microdomains that serve as physical crosslinks. It should be noted that these sites are thermally reversible unlike chemically crosslinked materials. All thermoplastic elastomers are based on the A-B-A, $(A\text{-}B)_n$, or $(AB)_x$ star architectures.[51]

As mentioned, the living anionic polymerization technique has allowed for the advancement of block copolymer technology. McGrath et. al. have led this area of polymer chemistry. This technique produces controlled architectures which is critical to develop desired properties. Anionic polymerization is preferred due to its freedom from termination reactions and side products. Living techniques employed are usually alkyllithium initiated polymerizations. It was first developed for the sequential copolymerization of styrene and diene monomers (figure 2.15).

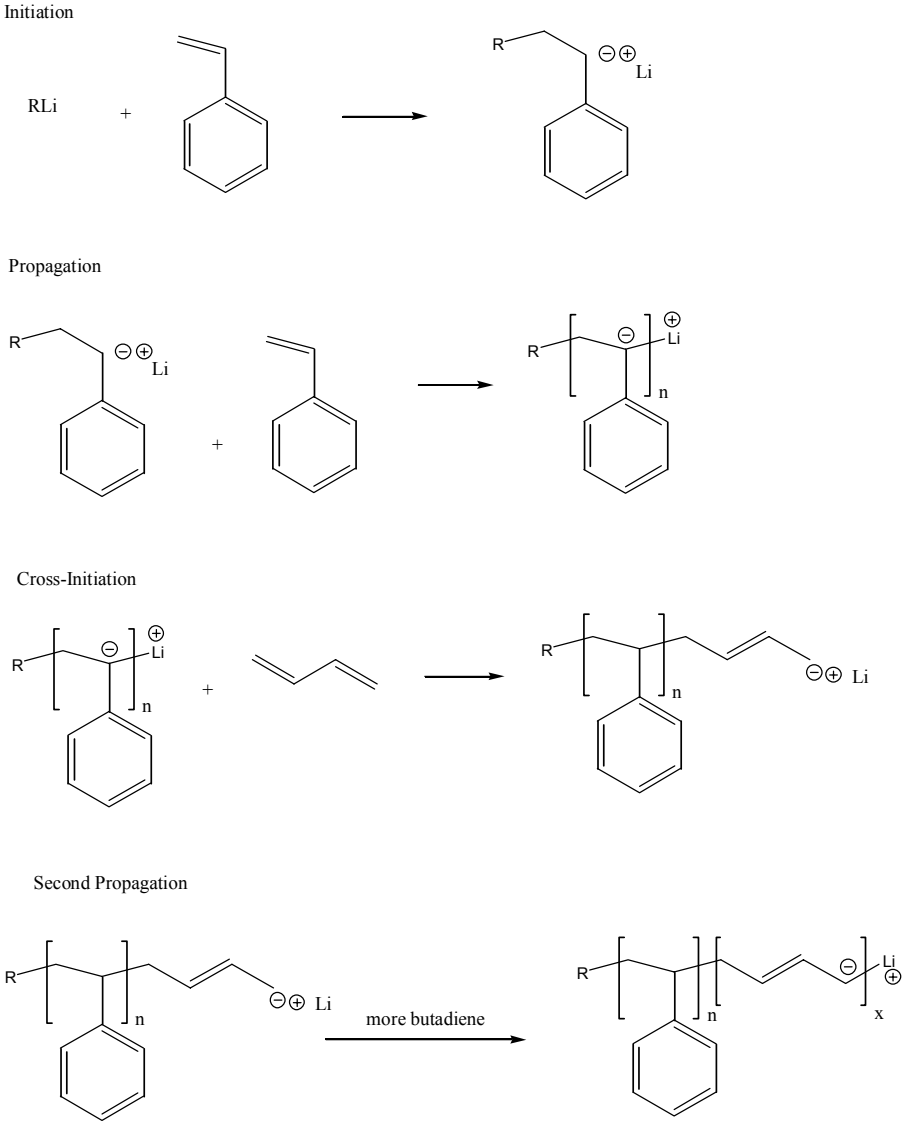

Figure 2.15 Sequential polymerization of styrene and 1,3 butadiene[78]

2.3.1 Siloxane-containing block copolymers

Block copolymers can be prepared with cyclic monomers to form well-defined structures. Examples of these materials include polysiloxanes, polylactones, and poly(alkylene sulfides). Specifically, block copolymers with well-defined siloxane segments have been prepared anionically utilizing the cyclic trimer of dimethylsiloxane. These cyclics can be polymerized with controlled molecular weight and narrow molecular weight distributions. Polysiloxane-polysiloxane copolymers have been prepared with a wide variety of blocks such as polysiloxane with poly(oxyalkylene), polyolefin, polycarbonate, and poly(silphenylenesiloxane).[79]

Polysiloxane-polysiloxane block copolymers have been focused upon in recent years.[80,81] Sequential anionic copolymerization of different cyclotrisiloxanes using lithium silanolates or organolithium initiators yield well-defined block copolymers.

Chojnowski has investigated the controlled synthesis of poly(dimethylsiloxane-*b*-vinylmethylsiloxane) block copolymers via sequential addition.[3,81] These reactions were done in cyclohexane at room temperature using *n*-butyllithium as the initiator. The first monomer, D_3, was polymerized until 90% conversion was reached and then the addition of the second monomer, D_3^v, followed (figure 2.16). It was found that there was little to no contamination of the second block formation if sequential polymerization was carried out. These materials are well-defined diblock copolymers.[3,81] It is necessary to polymerize the D_3 first in these reactions. This may be due to the alkyllithium species

reacting with the vinyl moiety on the cyclic trimer versus initiating polymerization. However, if a propagating siloxanolate is present addition of the vinyl monomer, no reaction of the strong basic butyllithium with the vinyl group occurs. Chojnowski[3], Weber[32], and Kickelbick[82] support the validity of this hypothesis. They utilized lithium siloxanolate and *n*-butyl initiators to polymerize D_3^v.

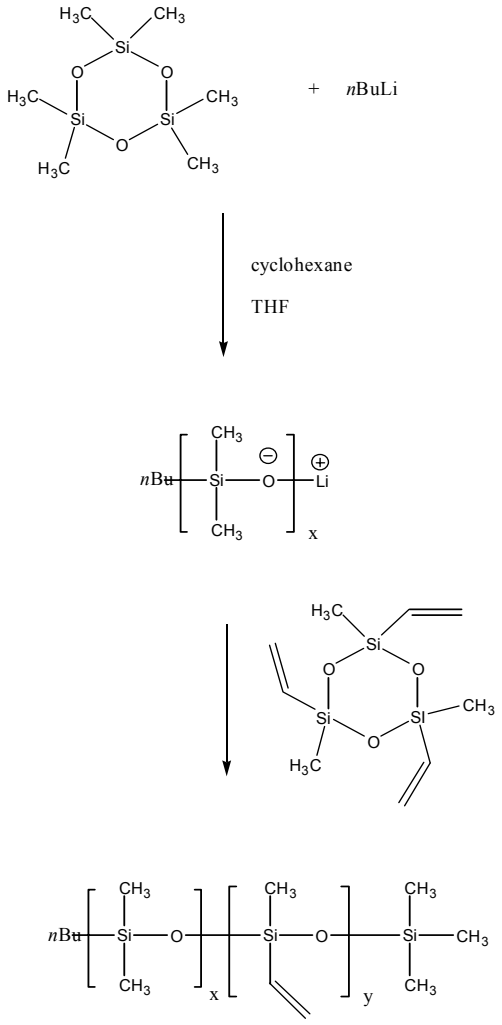

Figure 2.16 Sequential copolymerization of D_3 and D_3^v

In addition, these copolymers may be functionalized.[83] These materials may be further functionalized via hydrosilation reactions to create polymers with pendant carboxyl, organosulfur, phosphine, etc. groups. Functionalization of poly(dimethylsiloxane-*b*-methylvinylsiloxane) has been reported by Kickelbick[82], Chonjowski[81], and Weber[32]. Specifically, functionalized polysiloxane-polysiloxane copolymers are attractive materials in biomedical applications.[1]

2.3.2 Micelle Formation

Micelle formation occurs when amphiphilic molecules are placed in aqueous environments. Their hydrophobic regions segregate from the water by associating into aggregate structures known as micelles.[84] Block copolymers can often times function as amphiphilic molecules where one block is preferentially solvated to form aggregates (micelles) in solution.[85] These micelles are non-covalently bonded macromolecular aggregates which dynamically exchange polymer amphilphiles in solution.[74,86] This dynamic aggregation process depends on the amphiphilic species and the solution conditions. When a specific concentration of amphiphilic molecules or surfactants is exceeded, the formation of oriented colloidal aggregates or micelles occurs. The narrow concentration range in which this micellization occurs is called the critical micelle concentration or CMC.[87] At concentrations below the CMC, insoluble blocks in block copolymer surfactants migrate to the surface of the solution in an attempt to leave the medium while the soluble block protrudes down into the solution (figure 2.17). This concentration of surface aggregated blocks is dependent on pressure, temperature, pH,

type of copolymer/surfactant and solvent.[88] At concentrations above the CMC, sudden changes occur in solution that cause a change in properties such as surface tension, osmotic pressure, and electrical conductivity.[89]

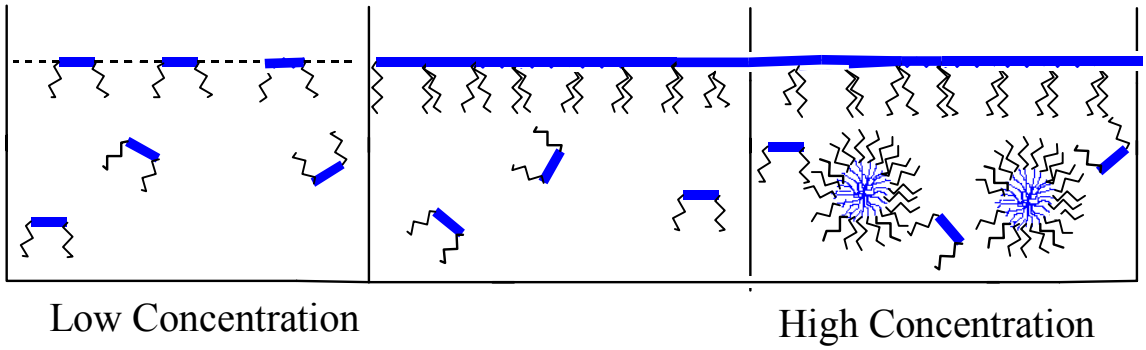

Figure 2.17 Increasing concentration of surfactant in solution

There are two theories that treat micellar behavior depending on whether the micelle is regarded as a chemical species or as a separate phase.[90] The first model, the *mass action model,* depicts the micelles as a chemical species. However, this model assumes constant numerical values for each micelle association or employs the monodispersity of the micelle aggregation number.[84,91] The second model, the *phase separation model*, regards micelles as a separate phase[92] and assumes that the surface tension or surfactant activity remains constant above the CMC.[92,93]

The macromolecular aggregate structures have aided in understanding micellar solution behavior.[90] Several people have proposed aggregate morphologies such as Hartley[94], Harkins et. al[95], and McBain[96]. Hartley proposed that micelles are spherical having charged groups located at the surface of the micelles. McBain determined that

there is a coexistence of spherical forms with lamellar structures. However, X-ray studies by Harkins et. al. suggested that the micellar aggregates exist only as lamellae. Debye and Anacker later proposed rod-shaped micelles versus the previously accepted spherical aggregates.[97]

Techniques such as NMR, ESR, and neutron scattering have aided in elucidating the real structures of micelles. Hartley's theory of spherical micelles has been upheld for ionic surfactants such as sodium dodecyl sulfate.[98,99] It was determined that the ion concentration greatly affected the morphology of the micelles. As the concentration increased the ionic micelles changed from spherical to cylindrical to hexagonal to lamellar. However, for nonionic surfactants, the shape changed from spherical directly to lamellar (figure 2.18).[100]

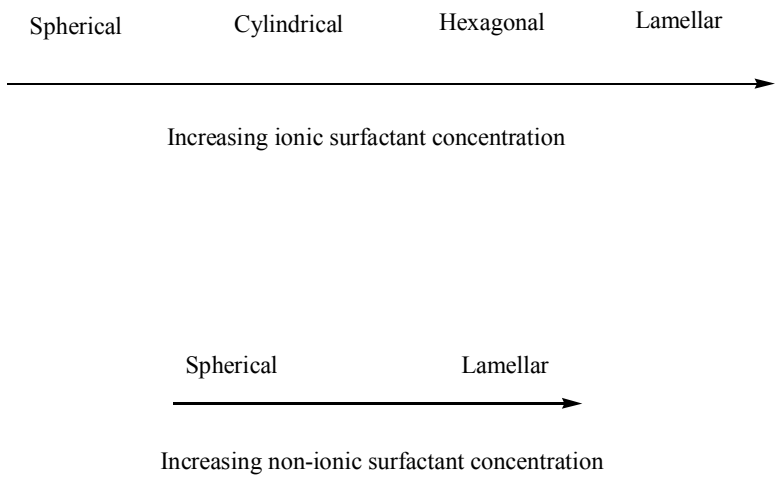

Figure 2.18 Micellar morphology as concentration of surfactant increases

Block copolymers are known to self-associate in solution leading to very useful microstructures analogous to colloids formed by short-chain surfactants.[39] A diblock

copolymer of polymethylbutene and polyethylbutene produces a variety of morphologies in solution such as cylindrical and lamellar. Recent investigations have shown that polysiloxane block copolymers form micelles in solution as determined by surface tension measurements and dynamic light scattering. Nose et. al. have studied the micelle formation of polystyrene-b-polydimethylsiloxane (PS-b-PDMS) in hexane as a function of temperature using dynamic light scattering.[101] The PS existed as the micelle core whereas the PDMS was the micelle corona. At high temperatures, the copolymer formed spherical domains, but as the temperature was decreased the copolymer formed hollow cylinder morphologies.

Riffle et. al. have investigated triblock copolymers comprised of a polycyanopropylmethylsiloxane center block with PDMS chains as tail blocks (PDMS-*b*-PCPMS-*b*-PDMS) (figure 2.19). Both dynamic light scattering and surface tension measurements were performed on these polymers in toluene solutions.[2] Toluene is known to be a good solvent for PDMS, but a poor solvent for the central PCPMS block, allowing the PCMPS block to form the micelle cores and the PDMS tail blocks protrude outward into the toluene to form micelle coronas. At significantly low concentrations, the surface tension of the copolymer solution was that of the value for pure toluene, 28 mN m^{-1}. However, as the concentration of copolymer was increased to values dropped indicating the presence of a surface active agent. The critical micelle concentration were calculated to be about 0.01-0.1 g l^{-1}. [1] Experiments evaluating the change in CMC as a function of temperature were also performed. The CMC's of each copolymer run were significantly lower as a function of temperature.[1,102]

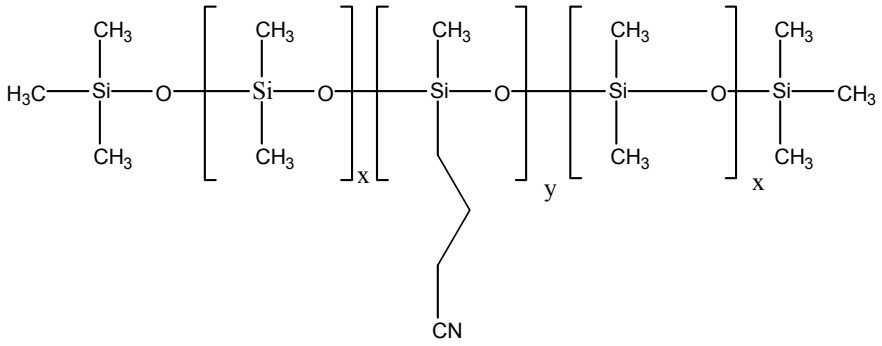

Figure 2.19 PDMS-*b*-PCPMS-*b*-PDMS triblock copolymer

Dynamic light scattering data further supported the formation of micellar structures for these polysiloxanes. At low molecular weight PDMS blocks the hydrodynamic radii increased from ≈ 3-4 nm at 0.001 g l^{-1} to approximately 11-12 nm at 0.01 g l^{-1}. The smaller hydrodynamic radii is indicative of small molecules whereas the larger domain sizes indicate the presence of macromolecular aggregates. These changes were observed in the concentrations of the CMC's determined by surface tension.[1]

2.4 Sol-gel chemistry

2.4.1 An introduction

Brinker and Scherer defined sol-gel as the fabrication of ceramic materials by the preparation a sol, gelation of the sol, and the removal of the solvent.[103] They have also defined a sol as being a colloidal suspension of solid particles in a liquid analogous to an aerosol which is a colloidal suspension of particles in a gas such as fog. The sol-gel process involves precursors for the preparation of colloids that consist of metal or metalloid elements surrounded by various types of ligands. Metal alkoxides belong to a family of metalorganic compounds which contain an organic ligand attached to the metal or metalloid element. The most common example of metal alkoxides is the tetraethoxysilane (TEOS), $Si(OC_2H_5)_4$.[104]

The earliest report of using TEOS in a sol-gel process came from Ebelman in 1846.[105] He observed monolithic products resulting from the hydrolysis and condensation of TEOS over several months. In the 1930's, Geffcken recognized that alkoxides could be employed for the preparation of oxide films.[106] Schroeder further supported this in his reviews of Geffcken's work in the late 60's.[107]

During the 1960's and 1970's, the ceramics industry focused on gels formed from the controlled hydrolysis and condensation of alkoxides. Multicomponent glasses were independently developed by Levene and Thomas[108], and Dislich[109]. Developing an understanding of the sol-gel mechanisms technology has been the focus of academic and industrial research.

Sol-gel reactions using the class of organometallic precursors are usually performed in an inert solvent such as ethanol due to incompatibility of TEOS with H_2O. However, the reaction media produce several different products.[110] The concentrations of catalyst, solvent, water, and TEOS influence the product structure.[104]

The sol-gel process for siloxane and silicate formation proceeds via hydrolytic polycondensation of an alkoxysilane performed the parent alcohol of the alkoxysilane. There are six exchange reactions that are possible in these systems (figure 2.20).[111]

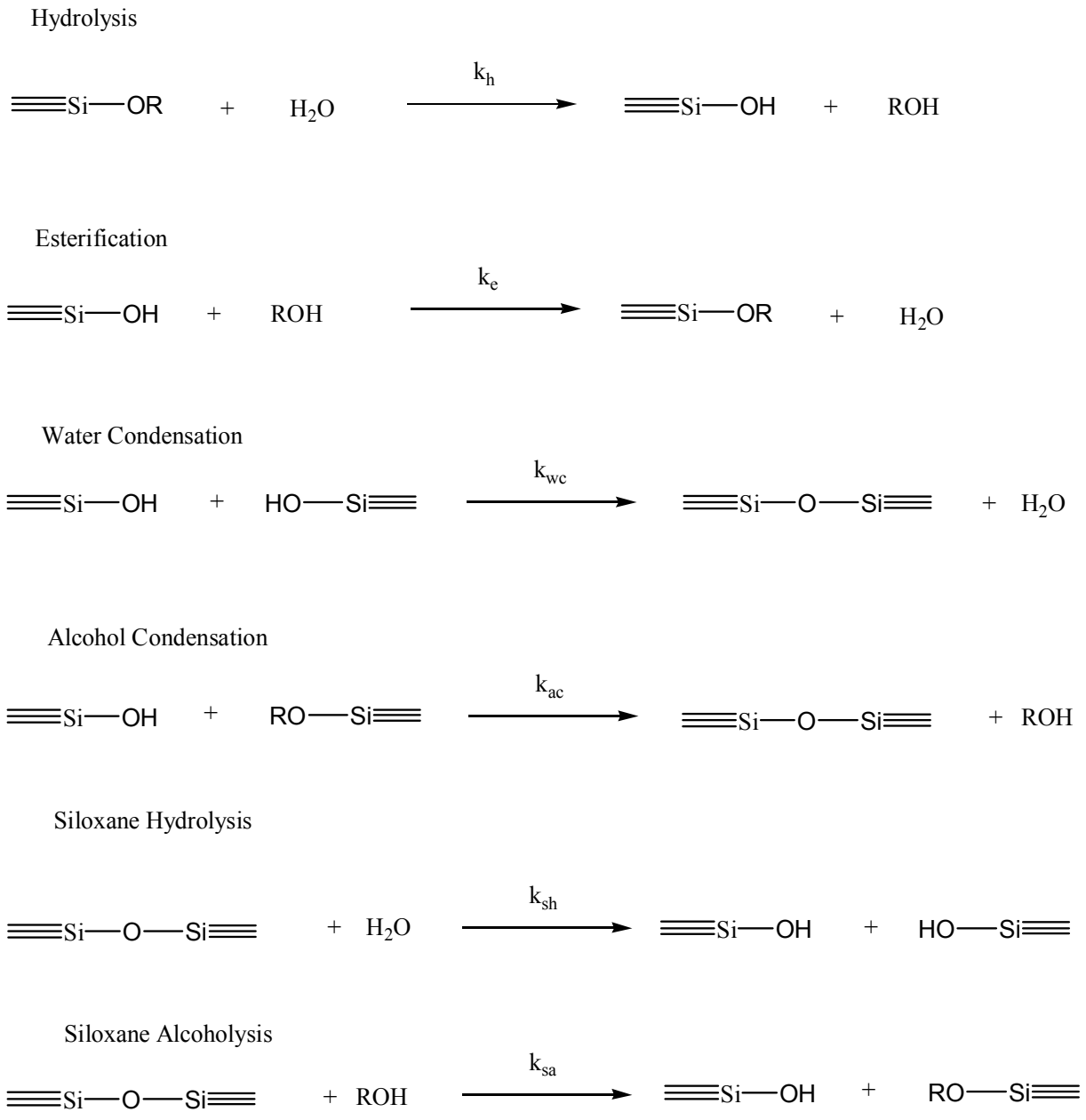

Figure 2.20 Exchange reactions in the hydrolytic polycondensation of alkoxysilanes

Theoretically, the tetravalent silicon monomer may begin with one to four hydrolysable OR groups. The process occurs via two main pathways, hydrolysis and condensation, to produce the desired silica network. The reaction proceeds by producing trialkoxysilanols, dialkoxysilanediols, and alkoxysilanetriols for the TEOS system. Finally, the processing of these materials involves densifying these gels by heating them to a higher temperature (figure 2.21)

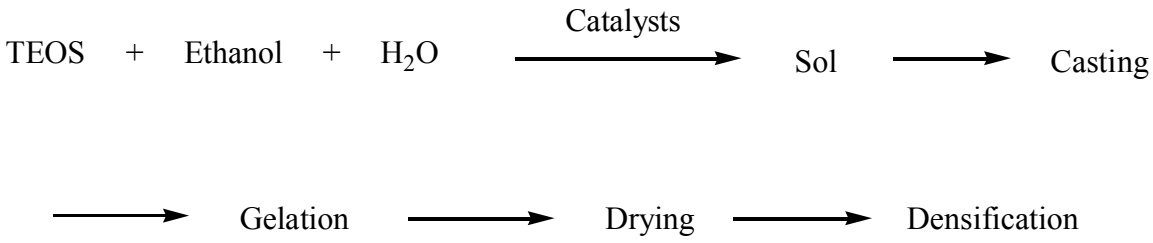

Figure 2.21 Processing for the TEOS-ethanol-water system[112]

2.4.2 Acid- and base- catalyzed sol-gel reactions

Alkyltrialkoxysilanes are known to undergo hydrolysis and condensation reactions in aqueous solution.[113] These hydrolytic condensations are catalyzed by metal salts, acids, or bases. Acid- and base-catalyzed reactions are more common than those catalyzed by metal salts. However, when room-temperature, mild, neutral reaction conditions are needed, metal salts such as dibutyltin diacetate or dibutyltin dilaurate is used.

There have been several studies in an attempt to understand hydrolysis and condensation reactions in aqueous media.[114,115] These investigations were not conclusive due to the difficulty in separating the hydrolysis from the condensation reactions. Therefore, Pohl and Osterholtz et. al., utilized fundamental S_N1 and S_N2 mechanism to elucidate the hydrolytic condensation mechanisms. In an effort to understand these sol-gel mechanisms, only two key steps, hydrolysis and condensation, will be considered here.

2.4.2.1 Hydrolysis reactions

The experiments performed with aryl- and alkyltrialkoxysilanes by McNeil and Pohl suggested that hydrolysis must proceed in a step-wise manner. The first step of the hydrolysis formed aryl- or dialkylalkoxysilanols and was rate-determining step due to the faster hydrolysis reactions forming silanediols and silanetriols. It was found that the hydrolysis in dilute aqueous solution occurred via pseudofirst order kinetics and are general base and specific acid catalyzed.[116] Pohl examined the effect of pH on the hydrolysis of γ-glycidoxypropyltrimethoxysilane in aqueous solution. This study also aided in determining kinetics and mechanisms for acid and base catalyzed hydrolysis.

His experiments determined, that under acidic environments, the hydrolysis rates of γ-glycidoxypropyltrimethoxysilane was ten times faster than n-propyl-tris-(2-methoxyethoxy)silane. The rate equation for the disappearance of the γ-glycidoxypropyltrimethoxysilane was determined by the extraction method which was

able to monitor solely the first step of hydrolysis. The rate of disappearance of the γ-glycidoxypropyltrimethoxysilane followed this equation :

$$- \frac{d[\text{silane}]}{dt} = k^{OH}[^{-}OH][\text{silane}] + k^{H}[H^{+}][\text{silane}] + k_b[B][\text{silane}]$$

where [B] is the concentration of the conjugate base which is calculated from the pH, pK, and total buffer concentration.

Acid-catalyzed hydrolysis is proposed to proceed via a bimolecular nucleophilic substitution mechanism which involves a pentacoordinate intermediate catalyzed via the hydronium ion. The rate of hydrolysis is, therefore, increased if the steric hindrance around the silicon atom is decreased. Substituents which stabilize the negative charge developed in the transition state also increase the hydrolysis rate which suggests that smaller substituents such as methoxy groups are more labile and have faster reaction rates.

The first step of the reaction involves the protonation of the alkoxy group to form an oxonium ion intermediate (figure 2.22). This protonation converts the –OR group into a good leaving group (weak base), -ROH. Water subsequently attacks the oxonium ion intermediate, displaces the alcohol and generates a protonated silanol intermediate. This reaction proceeds through a pentacoordinate transition state followed by the removal of the proton from the protonated silanol species resulting in a dialkoxylsilanol and the parent alcohol.

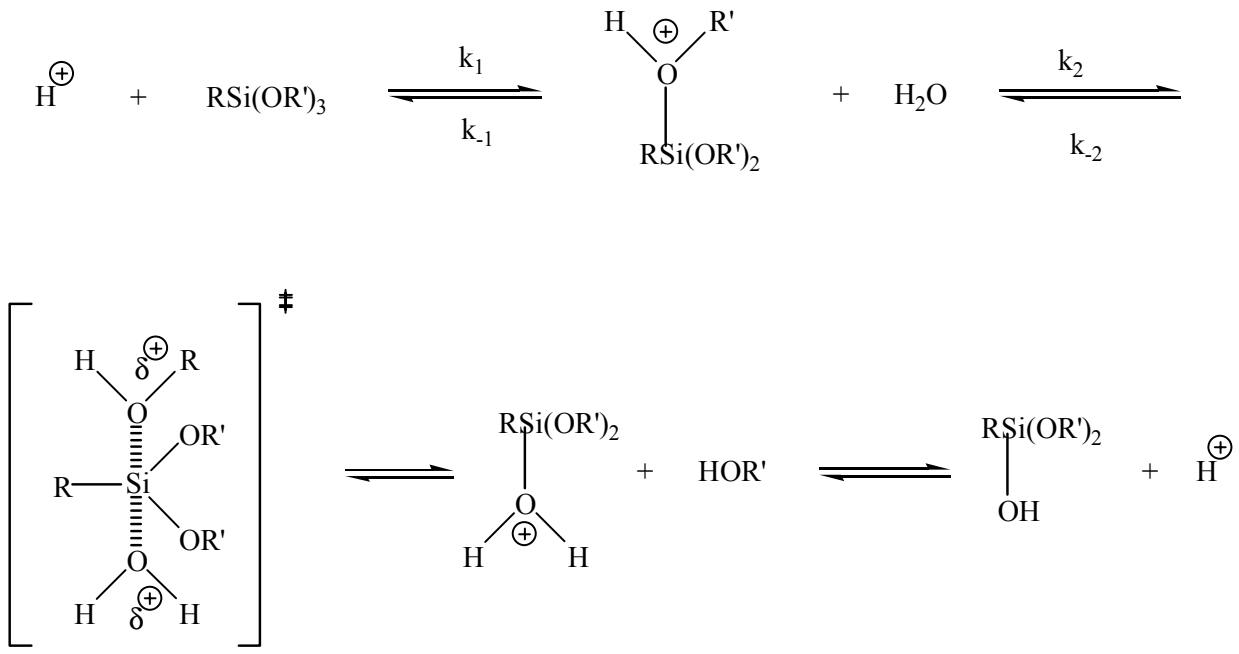

Figure 2.22 Acid-catalyzed hydrolysis mechanism[116]

The base-catalyzed reactions is catalyzed by the hydroxide anion and proceeds via a bimolecular nucleophilic substitution reaction (S_N2) with a pentacoordinate intermediate (figure 2.23).[116] The hydrolysis is initiated by attack of the hydroxide ion on the electropositive silicon atom. It proceeds through a transition state yielding a pentacoordinate intermediate where the silicon adopts a negative charge. The intermediate then breaks down through another transition state where the alkoxide anion is cleaved resulting in a dialkoxysilanol and an alkoxide ion. The hydroxide anion catalyst can be re-generated by proton abstraction of water by the alkoxide ion (forming the parent alcohol).

As with the acid-catalyzed mechanisms, the substituents play a large role in the reaction kinetics. The rate is enhanced when substituents that stabilize the negative charge on the pentacoordinate intermediate are bonded to the silicon atom. Also, a rate enhancement is observed when these substituents are sterically unhindered, e.g. trimethoxy groups.

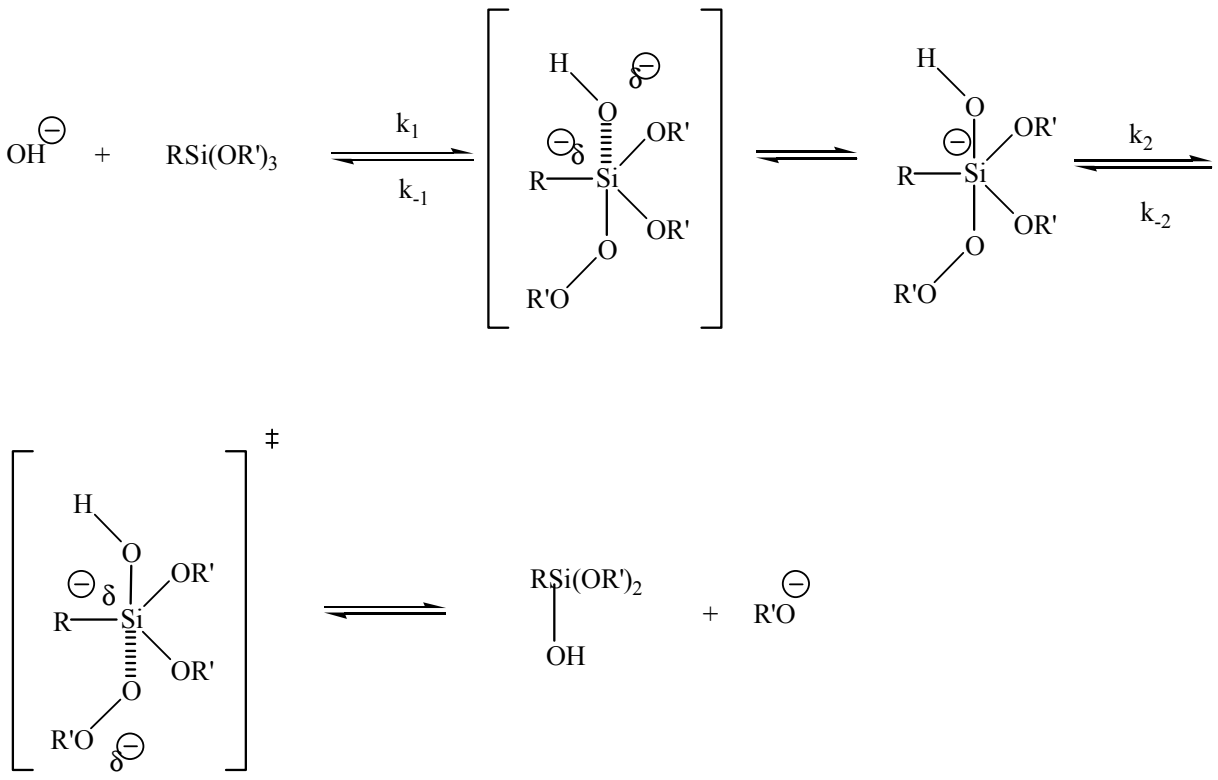

Figure 2.23 Base-catalyzed hydrolysis mechanism[116]

2.4.2.2 Condensation reactions

Condensation reactions, acid- and base-catalyzed, are not as understood as their hydrolyses counterparts due to the difficulty in studying these reactions. There have been studies performed on silanols to form siloxanes specifically γ-methacryloxypropylsilanetriol and γ-glycidoxypropylsilanetriol using deuterium labeling. The reaction rates for condensation, determined by Pohl et. al., were first order in the catalyst concentration and second order in the silanetriol concentration as shown below.

$$-\frac{d[\text{silanetriol}]}{dt} = k_c^{DO}\,[DO^-][\text{silanetriol}]^2 + k_c^{D}\,[D^+][\text{silanetriol}]^2$$

Base-catalyzed condensation reactions were proposed to undergo an S_N2 mechanism whereby the deutroxide anion begins by abstracting a deuterium from the trialkoxysilane yielding a silanolate ion. This silanolate ion functions as the nucleophile as it attacks a secondary trialkoxysilane or neutral silanol to produce a siloxane dimer and a deutroxide anion. Swain et. al. proposed that the reaction proceeds through yet another negatively charged pentacoordinate intermediate with the first reaction step faster than the second (figure 2.24).[117] Grubbs et. al. proposed that the condensation of trimethylsilanol in methanol occurred by backside attack of an electron donor molecule and displacing one of the substituents on the silicon.[118] The resulting siloxane dimer did not undergo further condensation due to the increased steric hindrance at the reaction site.

Pohl et. al. reasoned that base-catalyzed condensations are reversible reactions of silanetriols with deutroxide anion and is assumed to be rapid in accordance with Swain.[116] This leads to an equilibrium concentration of silanolate anion. The second step is slower and yields an equilibrium concentration of silanolate anion and siloxane dimer. No further condensation of the alkoxy groups was observed.

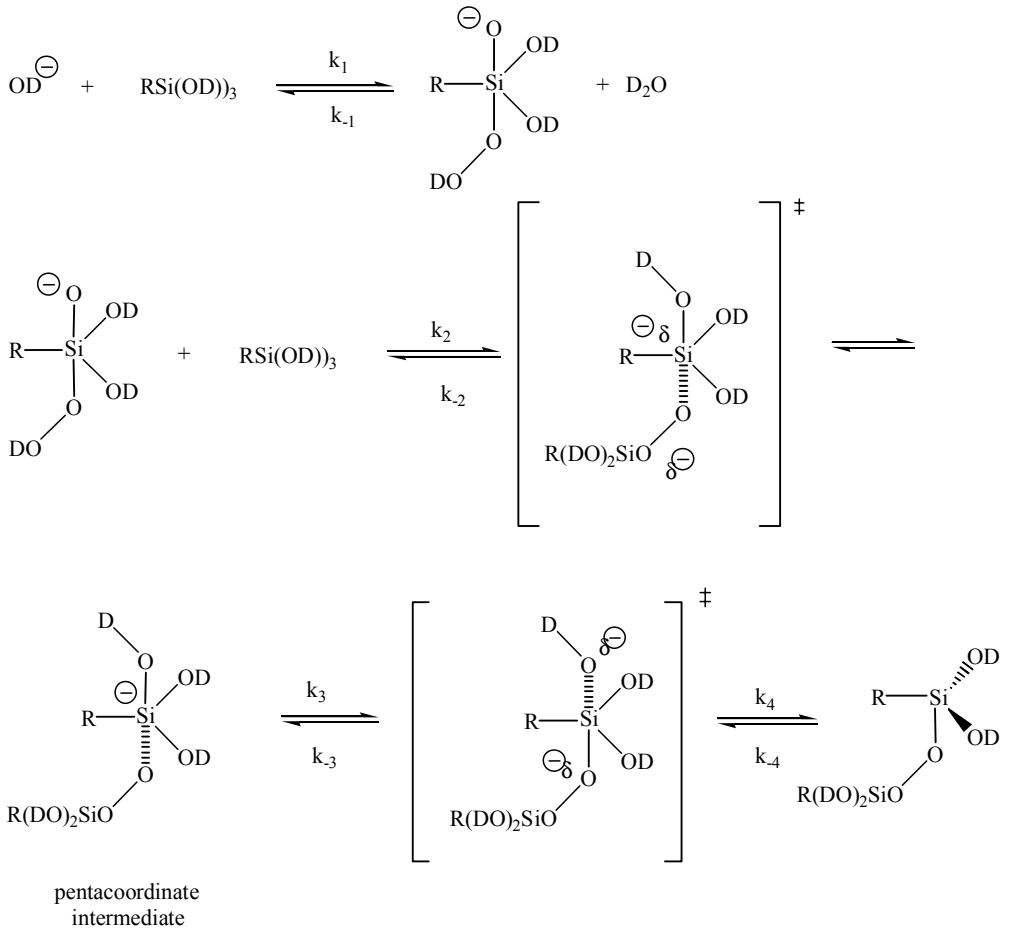

Figure 2.24 Base-catalyzed condensation mechanism[116,117]

Bimolecular nucleophilic substitution reactions are also utilized to explain acid-catalyzed condensation reactions. The reaction rate is second order in silanetriol concentration and first order in deuterium ion concentration. The protonated species involved in the reaction are assumed to be in a non-rate determining equilibrium. The results from studies performed by Pohl et. al. are consistent with either an S_N2**-Si or an S_N2-Si mechanism.[116,117]

The reaction begins by the protonation of the deuterated alkoxy group on the silicon yielding a deuterated water leaving group (figure 2.25). This reaction is fast and non-rate determining. Another neutral trialkoxysilane acts as a nucleophile and attacks the deuterated silanol, proceeding through a triangular bipyramidal transition state which is slow and rate determining. Upon decomposition of the transition state, a protonated siloxane dimer is produced. D_2O abstracts the deuterium ion from the protonated siloxane dimer which regenerates the acid catalyst. These reactions are assumed to be in dynamic equilibrium.

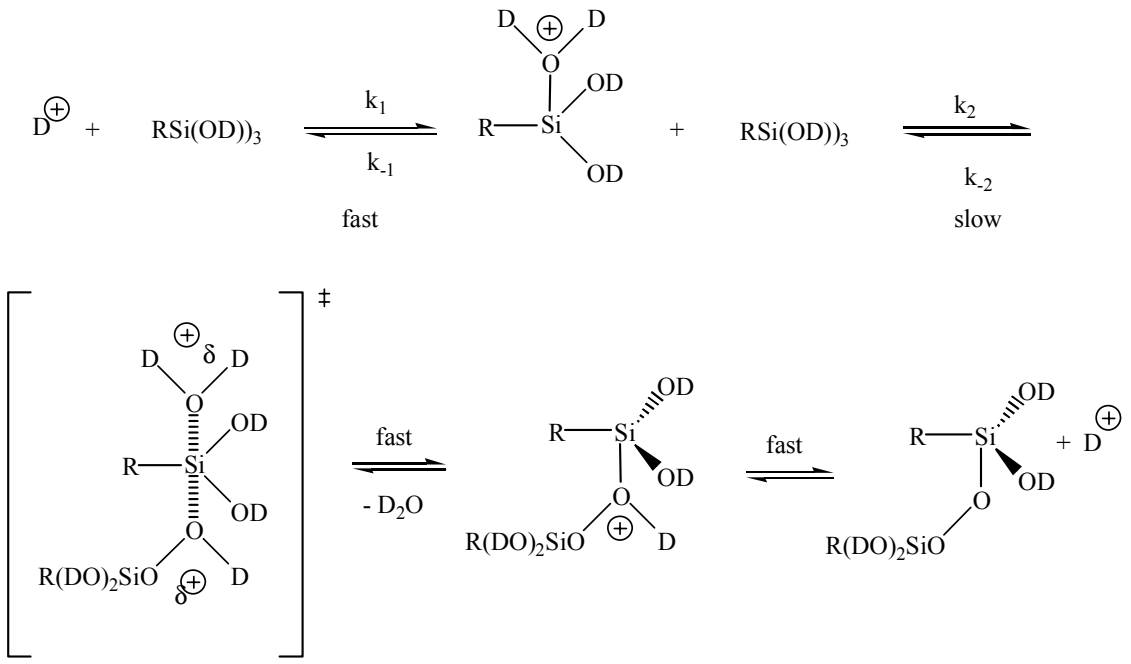

Figure 2.25 Acid-catalyzed condensation mechanism[116,117]

2.5 Magnetic materials and their properties

2.5.1 Overview of magnetic materials

The earliest reports of magnetic materials involved magnetite, an iron oxide or Fe_3O_4. These iron ore materials were fundamental in defining modern day magnetic materials. It is said if two objects attract each other and also repel each other, depending on orientation, that they are magnets. However, objects that are attracted to but not repelled by magnets are magnetic materials. These materials also must not be attracted or repelled by each other.[119]

Magnetic materials are classified by various terms. These terms are important in revealing the magnetic behavior of several materials. The magnetization of an object can be expressed in terms of dipole strength or magnetic moment. For magnetic fields arising from small magnetized objects, the *magnetic field strength, H* at large distances of *r*

varies inversely with r^3.[120] The magnetic field strength of an object can therefore be defined tangentially or radially :

$$H_\theta = \frac{2M \cos\theta}{r^3}$$

$$H_r = \frac{M \sin\theta}{r^3}$$

The magnetic field strength is measured in A/m for SI units (International System of Units) and Oersteds in cgs units (a system based on centimeters, grams, and seconds). The intensity of magnetization or *magnetization*, M, is defined as the magnetic moment, *m,* per unit volume; M = m/V. The permeability of the medium, μ, is important to define the *magnetic induction*, *B*, which is the net magnetic response of a medium to an applied field. The permeability in free space is equal to $4\pi \times 10^{-7}$ H/m. The relationship is given by the following equations depending on units used.

$$B = \mu_o (H + M) \quad \text{[SI units]}$$

The magnetic induction is measured in Tesla (T) for SI units and based on the permeability of a medium. The magnetic induction may be defined in terms of intensity of magnetization with B, H, and M all co-directional.

$$B = H + 4\pi M \quad \text{[cgs units]}$$

Here, magnetic induction is measured in gauss (G) for cgs units.[120]

However, when the magnetic material has zero magnetic moment (M) where B = H, the magnetic permeability is redefined as shown in the following equation :

$$\mu = B/H$$

and the susceptibility

$$\kappa = M/H \ (emu/cm^3 \ Oe)$$

The magnetic susceptibility, κ ,also characterize magnetic materials by varying M with H. Being that M is the magnetic moment, κ also refers to unit volume and is sometimes referred to as volume susceptibility. [121]Other susceptibilities are defined as follows:

$\chi = \kappa/\rho$ = mass susceptibility (emu/g Oe), where ρ is density,

$\chi_A = \chi A$ = atomic susceptibility (emu/g atom Oe), where A is atomic weight,

$\chi_M = \chi M'$ = molecular susceptibility (emu/g mol Oe), where M' is molecular weight

Both χ and μ are important parameters in describing magnetic materials. Magnetic materials having large values of χ and μ are desirable as they show high response to an external magnetic field.

Another important parameter in characterizing magnetic materials are the magnetization curves generated from magnetic measurements. Typical curves vary M vs. H. At large values of H, the magnetization, M, becomes constant and is known as its

saturation magnetization, M_s. Also, the curves demonstrate the degree of irreversibility. In other words, the curve shows whether the magnetic material may still retain magnetic properties even after the field strength, H, is reduced to zero. Also, if the applied field is reversed, the induction will decrease to zero when the negative applied field equals coercivity or H_c. This is defined as the field necessary to force or coerce the magnetic material back to zero induction.

Magnetic materials are classified into different categories based on their values of χ and μ. To further the understanding of magnetic materials, separating these materials on the basis of negative and positive values of χ is necessary. Large positive values of χ are categorized separately.

Classifications are also based on critical temperatures, the temperature at which the susceptibility changes. As the temperature increases, the susceptibility decreases and their magnetic moments randomize. For materials at sufficiently high temperatures, they follow the following relationship :

$$X = \frac{C}{T \pm \theta}$$

where θ and C are positive constants and vary for each material.[120]

Therefore, materials can be classified into five different categories depending on the aforementioned values. Materials are usually categorized as diamagnetic, paramagnetic, ferromagnetic, antiferromagnetic, and ferromagnetic.[119,121] *Diamagnetic* materials possess atoms that have no net permanent dipole or magnetic moments. In other words, two electrons that have two distinct dipole moments cancel each other since their spins align in opposite directions. However, the other categories exhibit net

magnetization due to only partial cancellation of their magnetic dipoles. *Paramagnetic* materials have atoms that do permanent dipoles and are randomly oriented at any temperature in the absence of an external magnetic field. In *ferromagnetic* materials, the moments align parallel to each other whereas the moments in *antiferromagnetic* materials, the moments align anti-parallel. Ferrimagnetic materials also exhibit anti-parallel alignment of dipoles, however, the magnitude of the moments are unequal. Table 2.10 depicts these descriptions as well as examples of compounds exhibiting these magnetic characteristics.

Table 2.10 Classification of magnetic materials based on magnetic properties

Class	Critical Temperature	Structure	Examples
Diamagnetic	None	Atoms have no permanent dipole	Inert gases, Cu, Hg, Si, P, S, salts
Paramagnetic	None	Atoms have permanent dipole	Cr, Mn, NO, rare earth metals
Ferromagnetic	Below Θ : yes, follows universal curve. Above : none	Atoms have permanent dipoles with parallel alignment	Co, Fe, Ni
Antiferromagnetic	None	Anti-parallel alignment of dipoles	MnO, CoO, NiO, MnS
Ferrimagnetic	Below Q : yes, but doesn't follow universal curve. Above : none	Unequal moment magnitude with anti-parallel alignment	Fe_3O_4 (magnetite), γ -Fe_2O_3 (maghemite)

2.5.2 Magnetic Fluids

Magnetic fluids are stable suspensions of solid particles in liquid or colloidal solutions. Their stability is dependent and ensured by the Brownian motion of the particles which must be small to experience this motion. Ferromagnetic particles are known to coalesce due to attractive forces, however, this aggregation can be prevented by

coating the surface of the particle with a surfactant.[122] Therefore, a magnetic fluid is usually a stable colloidal solution with small (30 – 100 Å) coated ferromagnetic particles dispersed in a carrier fluid. Table 2.11 lists common carrier fluids and surfactants used in this technology.

Table 2.11 Common surfactants and carrier fluids[122]

Carrier	Surfactant
Hydrocarbons	Oleic Acid, Aerosol TR
Aromatic hydrocarbons	Polyphosphoric acid derivative
Perfluoropolyethers	Perfluoropolyether acid
Kerosene	polyisobutene

Career fluids are important in creating stable magnetic fluids, therefore, must possess certain desired properties. These properties include low evaporation rate, low melting point and viscosity, inertness, high thermal stability, and high dispersing capability. However, all of these characteristics are not fulfilled by one single carrier fluid. For example, hydrocarbons have excellent chemical and dispersive stability, however, their high viscosities, high melting temperatures, and/or high vapor pressures limit their applications.[123] Silicone fluids present promising results as potential fluids for magnetic particles. Silicone is preferred especially for its high thermal stability. Riffle et. al. have prepared silicone magnetic fluids with polysiloxanes as steric stabilizers.[1,2]

Magnetic fluids sometimes possess special magnetic properties. The magnetic moments are completely randomized in the absence of an external magnetic field and are not magnetized. The magnetic moments of small particles have the ability to rotate along the gradient of the applied field and have the ability to increase the overall magnetic strength. *Superparamagnetic* fluids possess magnetic moments that completely randomize once the field is removed (figure 2.26). These materials usually exhibit high magnetic susceptibility, and they do not show magnetic hysteresis.

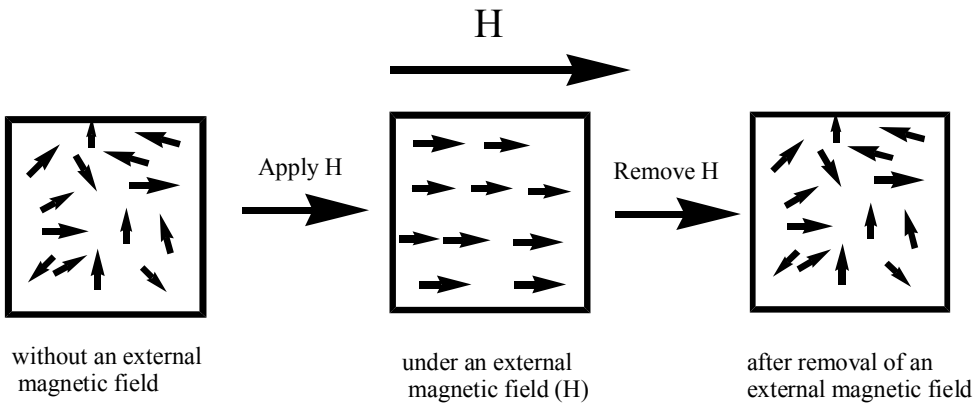

Figure 2.26 Superparamagnetic fluid properties

2.5.3 Magnetic Fluid Stabilization

As previously mentioned, ferrofluids are colloidal suspensions of small particles on that order of nanometers. It is necessary to sustain the dispersive capability of the magnetic fluid. It is possible to find an upper limit of particle size in which aggregation stability of a colloidal solution is maintained. This is defined as the following equation :

$$(\Delta\rho)VgL = kT$$

where $\Delta\rho$ is the density difference of solid and liquid phases (kg/m^3); $V = \pi d^3/6$ and is the volume of a spherical particle of diameter d (m^3); g is the acceleration due to gravity (m/s^2); L is the liquid layer height at which the number of particles per unit volume decreases as compared to the layer at the bottom of the vessel; k is the Botlzman constant, and T is the temperature.[124] For example, the upper limit to particle size for uncoated magnetite is approximately 5.5 nm.[124] This estimate is acquired assuming monodispersed spherical non-interacting particles. In addition, particle interactions such as attractive and repulsive forces play an important role in dispersive stability. Therefore, a detailed discussion of these interactions will be provided.

2.5.3.1 Particle Interactions – Attractive Forces

Stability of magnetic fluids is largely dependent on particle size. Magnetic fluids are stable if the particle size is small and less than its critical value such that the particles are of single domain structure.[125] The critical size is around 3-10 nanometers for the majority of magnetic materials. Single domain structure is defined as each particle having one single dipole of a particular magnitude. These dipoles induce magnetic dipole-dipole interactions or *E*. As the size of particles increase, the magnetic moment of each particle increases and the dipolar interaction is also increased.[126] Dipolar interactions may be estimated using an equation based on the distance between particles, r, and the magnetic moments, μ. The value of *E* is usually negative for attractive dipolar interactions. Figure 2.27 describes two situations where attractive forces are experienced.

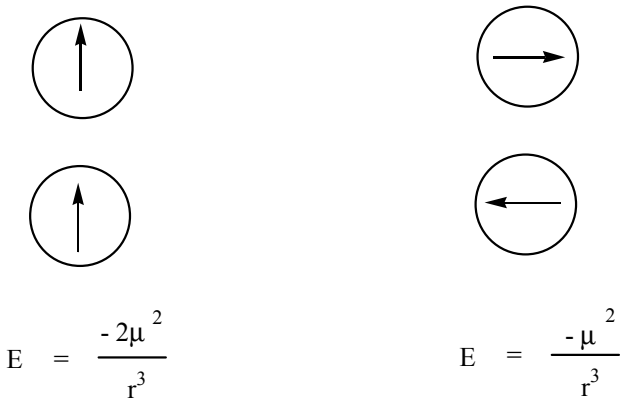

Figure 2.27 Dipolar interaction energy E between two spheres of equal magnetic moment. Attractive interaction is experienced.[126]

As mentioned in the introduction to this section, Brownian motion also plays an important role in the stability of magnetic particle suspensions. Brownian motion, thermal motion, can not prevent the agglomeration of magnetic particles or the formation of chains if the mean particle size is above its critical value.[122] Therefore, the particles must obey the following equation relating dipolar interaction energy to that of thermal energy.

$$| E_i + E_d | \leq kT$$

If the dipolar interactions are less than the energy of thermal motion, the particles will remain as non-interacting particles and prevent sedimentation.[124] In addition to Brownian motion and dipolar interactions, London-type van der Waal's forces also exist as attractive forces in magnetic colloids. This attractive force is a result of the interaction between instantaneous electric dipoles or dispersion forces. These forces may not be

overcome by thermal motion due to the large negative potential energy experienced when particles are in close contact. In the early 1930's London found that the attraction energy decreased proportional to l^{-6} with increasing distance, l, between the dipoles. It is important, then, to have repulsive forces that prevent agglomeration.[124]

2.5.3.2 Particle interactions - repulsive forces

There are several ways to induce repulsive forces in magnetic fluids. Electrostatic repulsion may be used where each particle contains the same surface charge. Electrostatic repulsion results because the particle surfaces tend to adsorb ions of different charge and repel ions of the same charge (figure 2.28). This is also known as the Coulomb repulsion of charged surfaces. It is dependent upon the surface potential, particle size, and concentration of ions or salts in the liquid.[127] This ion exchange and adsorption leads to an electric double layer where the inner layer is the Stern layer consisting of tightly bound ions. The diffusion layer or outside layer is comprised of scattered ions of opposite charge.

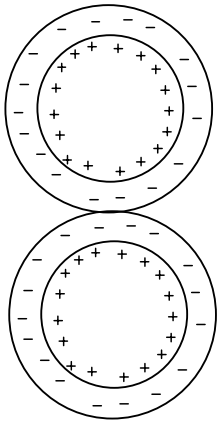

Figure 2.28 Electrostatic stabilization[127]

Moreover, the stability of magnetic colloids may be achieved by coating the spherical particles with a surfactant. This induces steric repulsion. The adsorbed surfactant inhibits the approach to each other so that the attractive energy distance is larger in comparison to the disordering energy of thermal motion.[124] Generally, surfactants are long flexible molecules attached to the surface of the particle. These molecules are usually linear chains with anchor blocks or groups at one end such as fatty acids or long polymers or copolymers. The anchor section functions in binding the surfactant to the particle surface whereas the rest of the chain extends out into the fluid performing thermal motion. Therefore, their stability is determined by an entropic mechanism. When two particles approach each other, the chains have to bend and restrict their motions which decreases disorder and ultimately decreases the entropy or negative ΔS. This negative entropy influences the Gibbs free energy around the particle. The enthalpic effect is negligible, therefore, the Gibbs free energy has a positive value, preventing particle agglomeration (figure 2.29).[127]

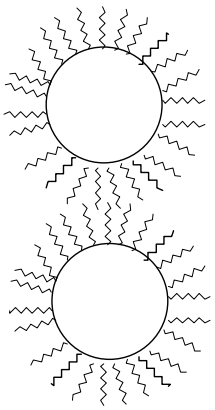

Figure 2.29 Steric repulsion[127]

2.6 Cobalt magnetic fluids

In recent years, solid state chemistry has been presented with a new challenge; the synthesis of nanoparticles with low size distributions. These materials show novel properties that are different from the bulk or atomic structures.[128] Since the 1980's scientists have been able to obtain and exhibit some control the characteristic sizes of inorganic particles.[129] These nanoparticles have shown great promise as they are desirable for many applications such as data storage devices and sensors. The production of controlled nanometer sized magnetic particles is a goal of modern research.

Specifically, cobalt nanoparticles are of great interest due to their high spin density resulting in their excellent magnetic properties. Colloidal chemistry is well suited to synthesize nanoparticles.[129,130] There are two very well known synthetic methodologies for preparing cobalt nanoparticle dispersions; the reduction of cobalt salts and the

thermolysis of cobalt carbonyls. These two reactions occur within micelles or colloids in solution. Generally, these reactions must have a suitable polymer stabilizer, cobalt precursor, and inert solvent. Riffle et. al. have lead the investigations of amphiphilic block copolymers as steric stabilizers for the thermal decomposition of dicobalt octacarbonyl. It is believed that the cobalt precursor decompose in the cores of micelles as long as the polymer solution is above the critical micelle concentration or CMC. [1] In addition, these polymers must be soluble in the selective solvent and both ambient and high temperatures.

It has been established that PDMS-*b*-PCPMS-*b*-PDMS triblock copolymers function well stabilizing cobalt nanoparticles of uniform size distributions. These triblock copolymers contain a nitrile containing anchor block, PCPMS, that adsorbs onto the particle surface. The tail blocks, PDMS, protrude out into the solvent and provide steric stability.[1,2] They also have been shown to form micelles in toluene and D_4.

2.6.1 $CoCl_2$

The preparation of cobalt magnetic fluids has been reported using a variety of methods. One method in particular, the reduction of $CoCl_2$, has drawn great attention in recent years for its synthetic feasibility. This method is known to produce stable cobalt dispersions with narrow size distributions. The reduction of $CoCl_2$ reduction involves the use of reducing salts such as borohydride (eg. sodium borohydride[131] and superhydride[132], alkaline metals[133], and polyols[134]). Hoffman et. al. has reported reducing cobalt salts to cobalt nanoparticles via electrochemical methods.[135]

The most common approach to the reduction of cobalt salts is the inverse micelle technique. This reaction normally involves the use of a surfactant, usually didodecyldimethylammonium bromide (DDAB), $CoCl_2 \cdot 6H_2O$, and $NaBH_4$. The DDAB is dissolved in toluene or another appropriate organic solvent to create the inverse micellar solution.[131] The inverse micelle reactions produce narrow size distributions of particles. It is thought that the particle sizes are controlled by the amount of water/surfactant ratio in the system. However, this is not entirely correct. Higher concentrations lead to the formation of Co_2B instead of Co metal inside the micelles. Sorenson et. al. found the germ-growth method better controlled the particle size as well as ensured the production of cobalt metal while keeping the water/surfactant ratio constant. The cobalt particles are germinated in the first stages of the reaction and serve as nucleation sites for larger particles to grow.[131]

Pileni et. al. have investigated the use of surfactants such as sodium bis(2-ethylhexyl) sulfosuccinate (AOT) to produce controlled sized nanocobalt particles.[136] Pileni reported that ternary systems such as hydrocarbon/AOT/water systems present better advantages than the normal approaches previously described. The particles are spherical and monodisperse. He found that the addition of the AOT surfactant along with the water, DDAB, and hydrocarbon solvent, produced superparamagnetic nanoparticles of 3-4 nm in diameter coated with a monolayer of AOT. The volume of solubilized water in the system controlled the size inverse micelles (water-in-oil) and thus controlled the size of the particles produced.

The mechanism of cobalt salt reductions via borohydrides is unclear. The reaction is dependent upon the reactions conditions especially the amount of water, pH, and

oxygen present.[137,138] Borohydrides are known to be very reactive to oxygen and water as they are used extensively in the organic reduction reactions to produce alcohols. Mochalov et. al. presented a concise overall reaction for these reductions.[139]

$$2\,BH_4^- + 2\,Co^{2+} + 9\,H_2O \longrightarrow Co_2B + 3\,H_3BO_3 + 12.5\,H_2$$

Later studies by Pileni et. al[140] and Gomez-Lahoz et. al [141] elucidated other reactions that attempt to solidify the molar ration of borohydride to cobalt salts.

2.6.2 Thermal decomposition of $Co_2(CO)_8$

Magnetic fluids can also be prepared by the thermal decomposition of metal carbonyls to form magnetic particles in various organic media such as esters or benzene. Carbonyls are carbon oxide compounds complexed with transition metals. They are usually comprised of iron or cobalt with a varying number of carbon monoxide groups forming ligands to the metal. Table 2.12 shows common carbonyls along with their decomposition temperatures and suitable reaction solvents.[142]

Table 2.12 Common carbonyls and decomposition temperatures[142]

Carbonyl	Decomposition Temp. ^{0}C	Density, g/cm^3	Solvent
$Fe(CO)_5$	60-250	1.47	Ester, benzene
$Fe_2(CO)_9$	95-100	2.08	Ester, benzene
$Fe_3(CO)_{12}$	140	2.00	Ester, benzene
$Co_2(CO)_8$	25-52	1.82	Benzene, alcohol
$Co_4(CO)_{12}$	60	-	Pentane, benzene

The implementation of carbonyls created a feasible methodology to create magnetic particles with a diameter of several fractions of a micron. As mentioned, a stable magnetic fluid must possess particles that do not aggregate or settle out of solution. The particle size ranges have been achieved by thermolyzing metal carbonyls in polymer solutions.[143] The polymer prevents aggregation of the particles due to steric repulsion and stabilization. It also facilitates in producing nano-sized cobalt particles. It has been reported that particle size can be controlled by varying the molecular weight and/or composition of the polymer. Also, the formation of single-domain cobalt particles is sensitive to the ratio of [polymer] : [solvent] : [metal]. More importantly, as it pertains to this thesis, the size of the cobalt particles is dependent on the concentration of polar groups in the polymer. Large concentrations of polar groups have been show to produce cobalt nanoparticles with diameters less than 10nm.[142]

Cobalt magnetic fluids may also be prepared via thermolysis in toluene. These magnetic fluids have been studied by various groups. Firstly, a Russian group studied the effects of different stabilizers, polystyrene and polybutylmethacrylate, on the magnetization and sizes of cobalt nanoparticles. They employed molecular weights of 300, 000 g/mol and 100, 000 g/mol respectively for the polymer surfactants. Table 2.13 lists the results of these experiments.

Table 2.13 Cobalt thermolysis in the presence of polymer stabilizers in toluene

Characteristics	Stabilizer	
	polystyrene	polybutylmethacrylate
Polymer content g/cm^3	0.0006	0.005
Magnetization, Gs	0.63	0.3
Particle radius, nm	7.5	5
Viscosity, cP	3	1.7

Riffle et. al. have extensively studied the use of polysiloxanes as stabilizers in thermolysis reactions of $Co_2(CO)_8$. They have shown that triblock copolymers of PDMS-PCPMS-PDMS form stable superparamagnetic fluids with size ranges of 10 nm and high saturation magnetization values.[1,144] The thermal decomposition under inert atmospheres has been documented for many years. It is believed that at temperatures below 90 °C, the decomposition occurs in two separate steps (figure 2.30). Many investigators have reported an initial and rapid CO gas evolution that corresponds to the transformation of $Co_2(CO)_8$ into $Co_4(CO)_{12}$.[145]

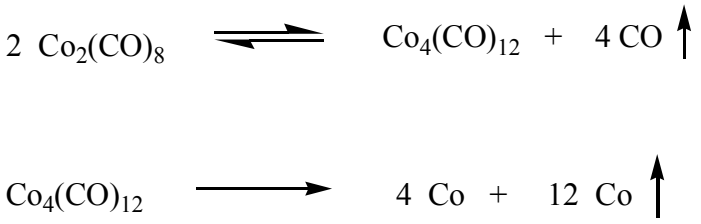

Figure 2.30 Decomposition of $Co_2(CO)_8$ below 90 °C.

The rate of decomposition slowly decreases and becomes equal to a constant. After some time, the rate of production of CO rises again which is owed to the metal formation. The end of the reaction is marked by a cessation in CO gas evolution.[1,142]

The reaction and the products are affected by temperature of decomposition, solvent, composition and concentration of surfactant, gas pressure, and concentration of carbonyl. The most appropriate solvents are organic aromatic compounds. Aliphatic solvents fail to produce stable magnetic fluids.[142] These solvents also must be able to dissolve the cobalt carbonyl precursor as well as the polymer stabilizer. In addition they must be chemically unreactive towards the cobalt carbonyl and polymer.[146] Typical chemically inert solvents are listed in Table 2.14.

Table 2.14 Common classes of solvents for cobalt carbonyl thermolysis[146]

Classes	Examples
Benzene and alkyl derivatives	monoalkyl benzene, dialkyl benzene
Halogenated derivatives of benzene	chlorobenzene, *o*-dichlorobenzene, *p*-dichlorobenzene
Aliphatic and cyclic hydrocarbons	decane, octane, pentane, hexadecane, isooctane, neopentane, cyclohexane, decalin, and tetraline
Ethers and alcohols	THF, dialkyl ether, ethyleneglycolmonomethylether, butanol, hexanol, cyclohexanol
Esters	alkyl acetate, alkyl propionate, alkylbutyrate
Ketones	cyclohexanone, mesityl oxide

As previously described, surfactants play key roles in these reactions. These surfactants are commercially available and affect the sizes of nanoparticles produced, however, in all cases the surfactant achieved size ranges lower than 10 nm (table 2.15).

Table 2.15 Colloidal stability influenced by commercial surfactants for the thermolysis of $Co_2(CO)_8$ in toluene.[142]

Surfactants	Commercial Names	Colloid Stability	Size range, nm
Sodium sulfosuccinate	AOT-Na	+	6.8 ± 0.8
Cesium sulfosuccinate	AOT-Cs	+	9.2 ± 1.2
4-(1-butyloctyl)-2-ethylbenzoyl-1-sodium sulfonate	Texas-2	+	6.7 ± 0.8
octyl-benzoyl sodium sulfonate	OBS	-	-
dodecyl benzoyl sodium sulfonate	DDBS	+	7.1 ± 1.6
dodecyl ammonium propionate	DAP	+	10.1 ± 1.9
octyl sodium sulfate	--	-	-
octyl sodium sulfonate	--	-	-
octyl phenolpolyethoxyethanol	Triton X-45	-	-

CHAPTER 3. Synthesis and characterization polysiloxane diblock copolymers

3.1 Synopsis

This chapter describes the synthesis and characterization of diblock copolysiloxanes comprised of poly(dimethylsiloxane-*b*-methylvinylsiloxane) (PDMS-*b*-PMVS). These diblock copolymers served as the precursors for polymer modifications, then the modified polymers were used as dispersion stabilizers for cobalt nanoparticles in toluene.

Sequential living polymerizations to form well-defined, diblock copolysiloxanes were carried out by first ring-opening D_3, then polymerizing D_3^v (figure 3.1). Molecular weights and molecular weight distributions were analyzed by GPC with a universal calibration, and their thermal transitions were determined by DSC.

1a.)

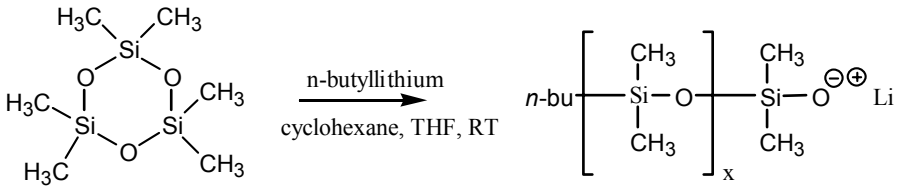

1b.)

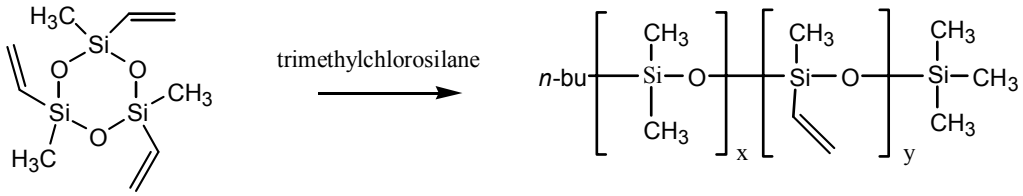

Figure 3.1 Diblock copolymers were formed by anionic polymerization of D_3 (1a.) followed by living anionic polymerization of D_3^v (1b.), then termination with trimethychlorosilane.

3.2 Experimental

Hexamethylcyclotrisiloxane (D_3, Gelest, Inc., FW 222.47 g mol^{-1}, mp 64-66 °C, bp 134 °C, d 1.02 g mL^{-1}) was purified by stirring over calcium hydride at 80 °C overnight, then fractionally distilled under nitrogen into a pre-weighed flame dried flask. The initiator, n-butyllithium (FW 64.06 g mol^{-1}, bp 80° C, d 0.775 g mL^{-1}), was kindly donated by FMC Corporation and was approximately 2.45M in cyclohexane. It was titrated with diphenylacetic acid in THF to determine the molar concentration and used as received. 1,3,5-Trivinyl-1,3,5-trimethylcyclotrisiloxane (D_3^V, Gelest, Inc., FW 258.50 g mol^{-1}, 80 °C/20 mTorr, d 0.9669 g mL^{-1}) was fractionally distilled under vacuum into a pre-dried flask, purged with nitrogen, sealed with a septum, and stored in a dessicator. Dichlorovinylmethylsilane (Gelest, Inc., FW 153.09 g mol^{-1}, bp 118-119 °C, d 1.0813) was used as received. Dimethylsulfoxide (Aldrich, 99.9%, FW 78.13 g mol^{-1}, mp 18.4 °C, bp 189 °C, d 1.4790 g mL^{-1}), was dried over $MgSO_4$ for 24 h and then fractionally distilled just prior to use. Triethylamine (Aldrich, 99.5%, FW 101.49 g mol^{-1}, mp -115 °C, bp 88.8 °C, d 0.726 g mL^{-1}) was dried over calcium hydride for 24 h and then fractionally distilled. It was maintained in a dark dessicator until used to prevent degradation. Chloroform (Aldrich, 98%, FW 119.38 g mol^{-1}, mp -63 °C, bp 60.5-61.5 °C, d 1.492) was washed with concentrated sulfuric acid and dried over $MgSO_4$ for 24 h. It was distilled just prior to use. Cyclohexane (Aldrich, 99%, FW 84.16 g mol^{-1}, mp 6.5 °C, bp 80.7 °C, d 0.779 g mL^{-1}) was stirred with concentrated sulfuric acid for 48 h, washed with water, dried over $MgSO_4$, then over sodium, and distilled just prior to use. Tetrahydrofuran (THF, 99.5%, E.M. Sciences, FW 72.11 g mol^{-1}, mp -108 °C, bp 65-67 °C, d 0.889 g mL^{-1}) was dried over calcium hydride overnight, then refluxed over sodium

in the presence of benzophenone until the solution was a deep purple. The THF was distilled just prior to use. Trimethylchlorosilane (Gelest, Inc.) used as the terminating reagent for the diblock copolymers was distilled before use. A Pt^0[1,3-divinyl-1,1,3,3-tetramethyldisiloxane]$_{1.5}$ complex catalyst in xylene (2.1–2.4 wt % Pt) (Gelest, Inc., FW 389.49 g mol^{-1}, mp 12-13 °C, bp 138 °C, d 0.885 g mL^{-1}) was used as received. Triethoxysilane and trimethoxysilane (Gelest, Inc.) were used as received. Toluene (Aldrich, 99.8%, FW 92.14 g mol^{-1}, mp -93 °C, bp 110.6 °C, d 0.865 g mL^{-1}) was washed twice with concentrated sulfuric acid and neutralized with water. It was dried over $MgSO_4$ for one hour, then over calcium hydride overnight and distilled just before use.

3.2.1 Synthesis of 1,3,5-trivinyl-1,3,5-trimethylcyclotrisiloxane

This synthetic procedure was based on that provided previously by Chojnowski [3]and Weber [32]and was modified to increase product yield. Dichlorovinylmethylsilane (DVMS) (20g, 0.14 mol) was added via glass syringe to a flame dried, three-neck, 250-mL, round bottom flask equipped with a magnetic stir bar, nitrogen inlet, an addition funnel, and a condenser. Triethylamine (TEA) (28g, 0.28 mol) and 80 mL chloroform were also charged via glass syringe to the reaction vessel. This solution was stirred for approximately 15 minutes. The TEA functioned as an HCl scavenger to prevent acid degradation of the cyclosiloxane product. A solution of dimethylsulfoxide (DMSO)(12g, 0.15 mol) in 50 mL chloroform was prepared separately and added to the addition funnel. The DMSO solution was added dropwise over 1.5 h to the reaction mixture. The reaction was stirred at 25 °C for an additional 3 h. A white solid precipitated as the reaction proceeded. The reaction mixture was purified and recovered by washing several times

with water, then dried over $MgSO_4$ for approximately 1.5 h. It was then filtered to remove precipitates and the solvents were removed by rotary evaporation. The product was fractionally distilled at 72 °C under vacuum at 11 mm Hg. The yield was 40%.

3.2.2 Characterization of 1,3,5-trivinyl-1,3,5-trimethylcyclotrisiloxane

3.2.2.1 ^{1}H NMR

All ^{1}H NMR spectra were obtained on a Varian Unity 400 MHz NMR spectrometer operating at 400 MHz. The NMR parameters included a pulse width of 28.6° and a relaxation delay of 1.000 sec at ambient temperature. The samples were dissolved in *d*-$CHCl_3$ for obtaining the spectra.

3.2.2.2 Gas Chromatography

All GC samples were run on a Hewlett Packard 5890A Gas Chromatograph equipped with a non-polar short column and a He mobile phase. The samples were ramped from room temperature to 250 °C at 10 °C per minute. The GC was equipped with an FID detector.

3.2.3 Synthesis of poly(dimethylsiloxane-*b*-methylvinylsiloxane) (PDMS-*b*-PMVS)

A synthetic procedure for preparing a diblock copolymer with a targeted number average molecular weight of 7000 g mol^{-1} comprised of 5000 g mol^{-1} PDMS and 2000 g mol^{-1} PMVS is provided. A series of diblock copolymers with different molecular weights were prepared by varying the ratio of n-butyllithium to D_3 to control the M_n of

the PDMS block, and by varying the amounts of D_3^V relative to D_3 to control the M_n of the PMVS block (table 3.1). The first part of the synthesis involved preparing a controlled PDMS block with one terminal lithium siloxanolate. D_3 (15.64, 0.003 mol) was distilled into a flame dried, 250-mL, round bottom flask equipped with a magnetic stir bar, which had been purged with dry nitrogen and sealed with a septum. Cyclohexane (18 mL) was added via syringe as a solvent to dissolve the D_3. Once dissolved, 1.26 mL of a 2.45 M solution of n-butyllithium (0.003 mol) in cyclohexane was charged to the reaction flask via syringe, and stirred for 15 minutes at 25 ^{0}C. THF (18 mL) was added as a promoter and the reaction was allowed to proceed at room temperature until the complete conversion of D_3 monomer to polymer, as determined by ^{1}H NMR. This required approximately 8 h reaction time for this composition. D_3^V (6.2 mL, 0.003 mol) was charged to the reaction flask and the copolymerization was allowed to proceed at room temperature until conversion reached approximately 95% (≈8 h), as measured by ^{1}H NMR. The diblock copolymer was terminated with an excess of trimethylchlorosilane (0.76 mL, 0.006 mol) via syringe and stirred for approximately 30 minutes. The solution clouded upon adding the trimethylchlorosilane due to the precipitation of insoluble LiCl salt. The polymer solution was diluted with chloroform (300 mL) and placed in a separatory funnel. It was washed with water several times to remove LiCl. Approximately 80% of the chloroform was removed by rotary evaporation, then the polymer was precipitated and purified by pouring the remaining solution into stirring methanol (200 mL) twice. The clear liquid copolymer sank to the bottom of the vessel. The methanol was decanted and the polymer was dried under vacuum at approximately 500 mTorr at 60 °C for 24 h.

Table 3.1 Concentrations of initiator, monomer, and endcapping reagent utilized to synthesize a series of diblock PDMS-PMVS copolymers with systematically varied block lengths.

Target MW PDMS-*b*-PMVS ($g\ mol^{-1}$)	D_3 (g)	n-butyllithium (mol)	D_3 (mol)	D_3^v		trimethylchlorosilane (mL)
				mol	mL	
5000 – 2000	15.64	0.0031	0.003	0.003	6.21	0.76
5000 – 2000	14.87	0.0029	0.0029	0.0029	6.00	0.73
5000 – 3000	10.12	0.0020	0.0020	0.0020	4.14	0.51
10000 – 2000	10.42	0.0010	0.0010	0.0010	2.07	0.25
10000 – 2000	20.20	0.0020	0.0020	0.0020	4.14	0.51
14000 – 2000	10.72	0.0011	0.0011	0.0011	2.28	0.28
16000 – 2000	17.28	0.0011	0.0011	0.0011	2.28	0.28
16000 – 2000	11.20	0.0007	0.0007	0.0007	1.45	0.18
16000 – 2000	14.20	0.0009	0.0009	0.0009	1.86	0.23

3.3 Molecular weight determination

3.3.1 Nuclear magnetic resonance spectroscopy

3.3.1.1 ^{1}H NMR

All ^{1}H NMR spectra were obtained on a Varian Unity 400 MHz NMR spectrometer operating at 400 MHz. The NMR parameters included a pulse width of 28.6° and a relaxation delay of 1.000 sec at ambient temperature. The samples were all dissolved in *d*-$CHCl_3$ for obtaining the spectra.

3.3.1.2 ^{29}Si NMR

All ^{29}Si NMR spectra were obtained on a Varian Unity 400 MHz NMR spectrometer operating at 80 MHz. The samples for ^{29}Si NMR were prepared with 0.63g copolymer, 0.52 g $Cr(Acac)_3$, and 2.4 mL *d*-$CHCl_3$. Quantitative silicon NMR spectra were obtained with the aid of the relaxation agent, $Cr(Acac)_3$ with a pulse width of 168.0° and a relaxation delay of 10.000 sec.

3.3.2 Gel permeation chromatography

Gel permeation chromatograms were obtained in chloroform at 30 °C on a Waters Alliance Model 2690 chromatograph equipped with a Waters HR 0.5 + HR 2 + HR 3 + HR 4 styragel column set. A Viscotek viscosity detector and a refractive index detector were utilized with polystyrene calibration standards to generate a universal molecular weight calibration curve for absolute molecular weight analyses. Samples were prepared by dissolving 15-20 mg sample in 10 mL HPLC grade chloroform.

3.3.3 Differential Scanning Calorimetry

DSC scans were performed on a TA Instruments DSC Q1000 under constant flow of Helium. The samples (10-15 mg) were ramped from -150 to 25 °C using hermetically sealed DSC pans. Two scans were performed on each sample and the T_g's were take from the inflection points on the second scans.

3.4 Results and Discussion

3.4.1 Synthesis of 1,3,5-trivinyl-1,3,5-trimethylcyclotrisiloxane

Syntheses of the strained cyclosiloxane trimers such as D_3^V have been of great interest in recent years due to their utility for preparing homopolymers and block copolymers with narrow molecular weight distributions [3,32,82]. This synthesis involves deoxygenation of dimethylsulfoxide by reaction with a dichlorosilane, and ring-closure of the six-membered ring. Triethylamine functions as an acid scavenger to prevent any degradation of the cyclosiloxane product and triethylammonium chloride salt precipitates during the reaction. The procedure also yields larger cyclosiloxanes and the eight and ten membered rings (i.e., D_4^V and D_5^V) can be separated by fractional distillation (figure 3.2).

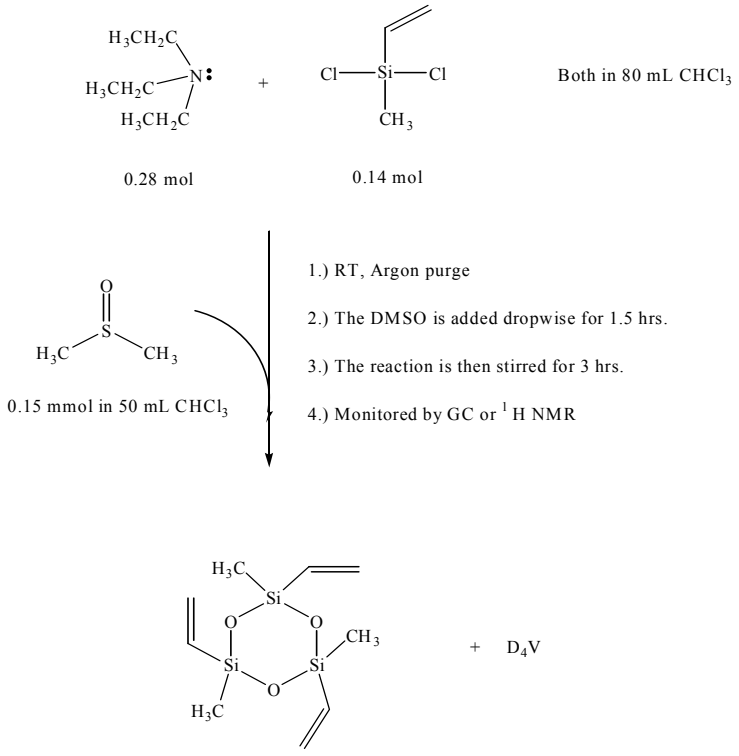

Figure 3.2 Synthesis of D_3^V

Sulfoxides are known to undergo oxygen transfer reactions[147,148]. The electrophilic silicon of the dichlorosilane accepts the oxygen with elimination of chloride. This may be followed by substitution of the remaining chlorine with the Si-O, and ring closure. Ring-closure of the six-membered ring is disfavored thermodynamically due to the strain energy of the resultant cyclic. Its yield was approximately 40% which was similar to previously report yields (30-35%).[32] The reaction forms a mixture of cyclosiloxanes of different sizes and linear species with cyclics being the major products. The methylvinyldichlorosilane was diluted with chloroform to enhance the cyclic yields. The low molecular weight cyclosiloxanes were separated from the mixture by fractional vacuum distillation.

These reactions were kept under nitrogen to prevent contamination with water. When the exothermic reaction commenced, the temperature rose from room temperature to approximately 60 °C, and this temperature was maintained for the duration of the reaction by controlling the rate of addition of the DMSO.

Formation of D_3^v in the reaction was monitored by gas chromatography and compared with a known standard (figure 3.3). The standard was separated/purified by fractional distillation (b.p. of D_3^v at 11 mmHg 72 °C) from a mixture of cyclics. It is important to note that higher membered cyclics have increased boiling points, and it was therefore easy to obtain a pure sample of the D_3^v GC standard. The retention time was 4.45 minutes for D_3^v and 6.09 minutes for D_4^v. GC of the purified product showed no peaks after 4.45 minutes.

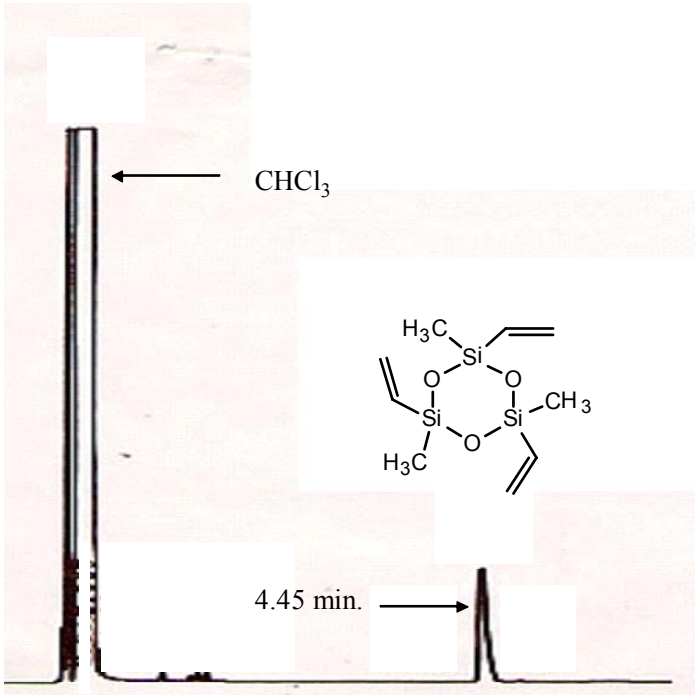

Figure 3.3. Gas chromatogram of D_3^V obtained after purification.

As the reaction proceeded, the retention peak at 4.45 minutes increased in area corresponding to the formation of D_3^V (figure 3.4). The reaction was considered complete when this peak area became constant (≈3 hours). The product structure and composition were confirmed by comparing the ^{1}H NMR spectra to those previously reported by Weber et al. (figure 3.5).[32] The –CH_2 on the vinyl moiety resonated at 5.95 ppm and the –CH resonated at 6.11 ppm. The methyl resonances appeared at three distinct chemical shifts corresponding to *cis* or *trans* stereochemistry. The *trans* methyl protons resonated at 0.24 ppm and 0.26 ppm whereas the *cis* methyl protons resonated at 0.28 ppm. It is important to note that the methyl resonances of the D_4^V cyclics and higher were shifted further upfield to approximately 0.18 ppm. In addition, the vinyl D_4^V –CH_2 protons were shifted upfield to approximately 5.79 ppm and the –CH protons resonated at 6.00 ppm. [32] This allowed for quantitative characterization of the cyclic trimer.

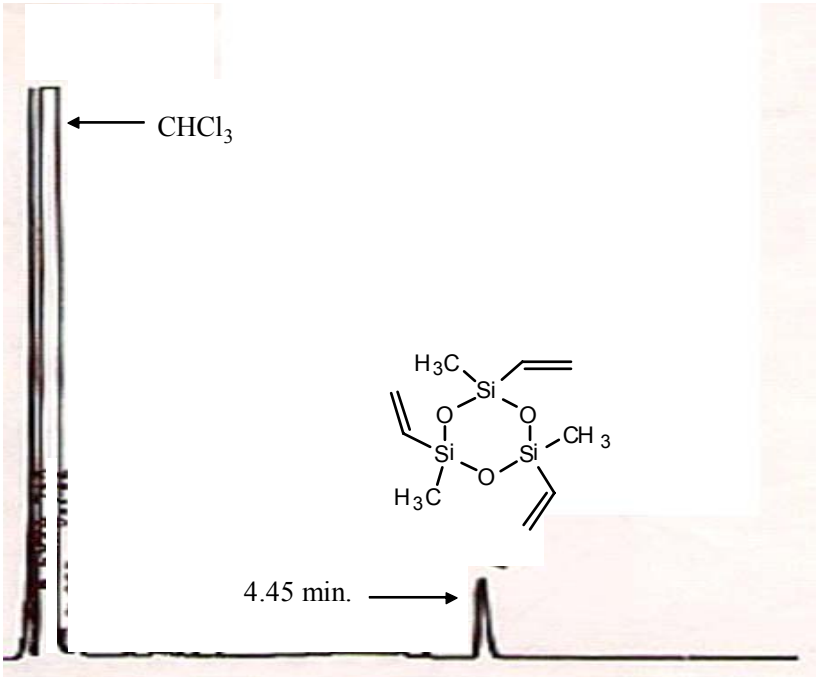

Figure 3.4. Gas chromatogram of the D_3^v reaction.

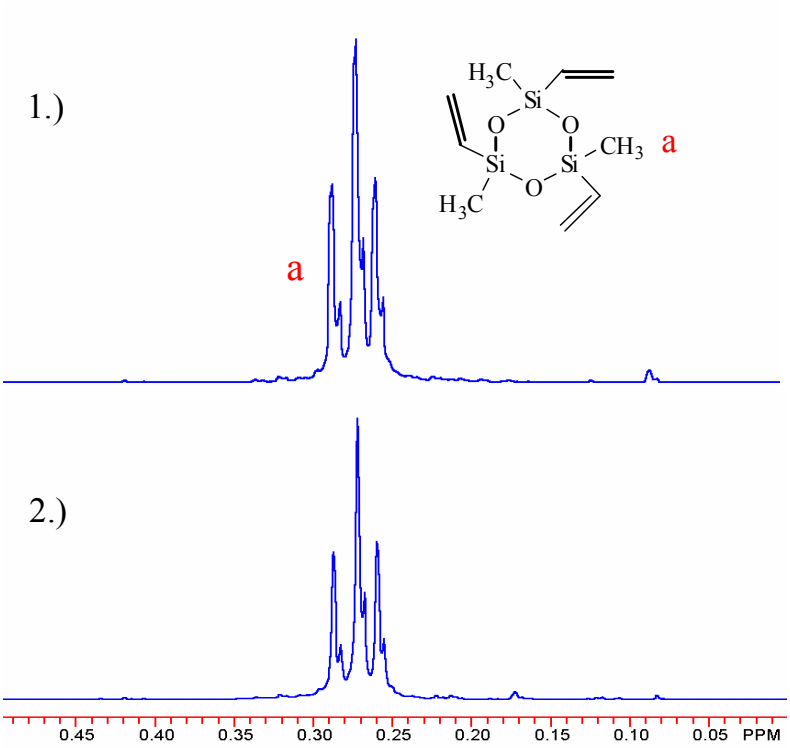

Figure 3.5 Comparison of the ^1H NMR spectra of the D_3^v monomer (1) to the standard (2).

3.4.2 Synthesis of poly(dimethylsiloxane-*b*-methylvinylsiloxane)

It is well-known that the polymerization of D_3 can be living under the conditions utilized in this work. [72,149] The PDMS-*b*-PMVS copolymers were prepared at room temperature in cyclohexane utilizing THF as a co-solvent (figure 3.7). THF was added as a promoter to aid in disassociating the tight ion-ion interactions and to increase the reaction rates. The synthesis of these PDMS-*b*-PMVS diblocks produced copolymers with narrow molecular weight distributions, suggesting that the polymerization of the PMVS block was also living. Data reported in recent work by Kickelbick supports this premise by demonstrating a linear dependence of molecular weight with monomer conversion. [82]

The reactions to open cyclosiloxane trimers are promoted by enthalpic and entropic mechanisms. The enthalpic contribution to ring opening D_3 has been attributed to relief of ring strain, [53,150] and it is reasonable to hypothesize that the 1,3,5-trimethyl-1,3,5-trivinylcyclotrisiloxane is also strained. The entropy also increases as the reaction proceeds, resulting in an overall $-\Delta G$ (figure 3.6).

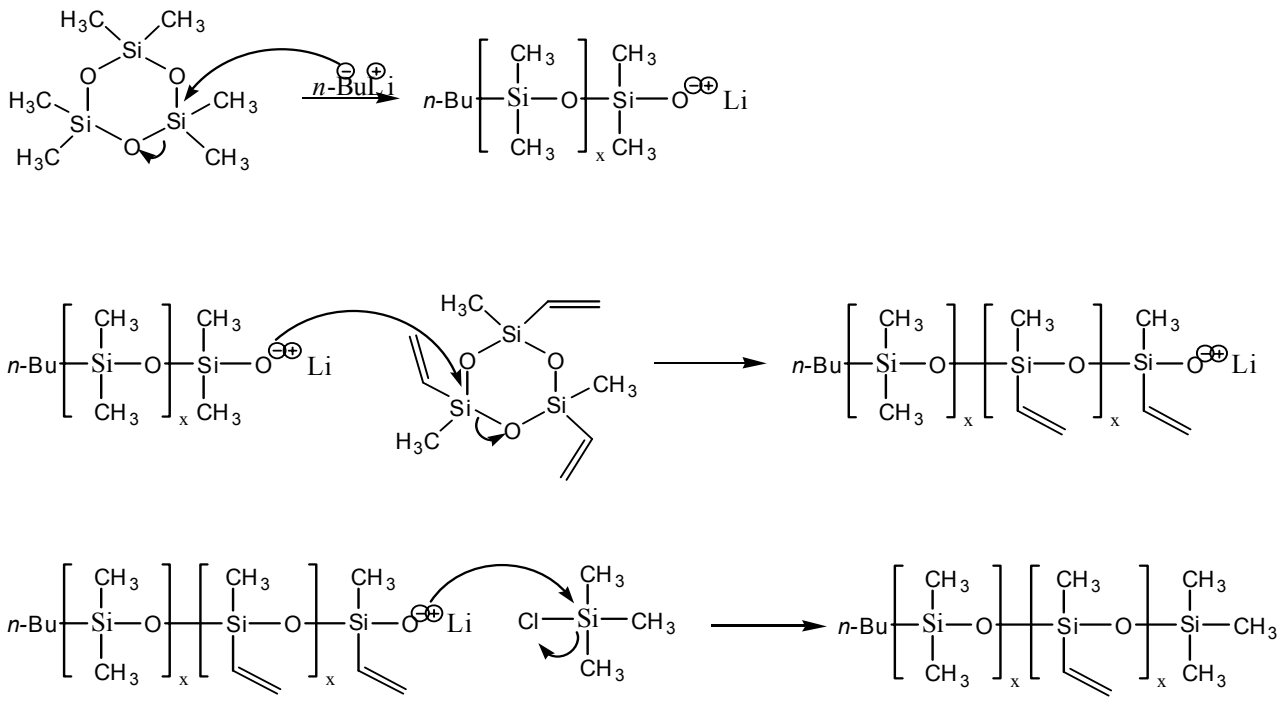

Figure 3.6 Anionic block copolymerization to obtain diblock PDMS-*b*-PMVS copolymers.

The diblock copolymers were prepared by sequential anionic ring opening polymerizations of D_3 and D_3^v, respectively. The synthesis of the PDMS block first was important for controlling the chemical structure of these polymers. Chojnowski et al. analyzed the reaction kinetics of the two monomers and found that the rate of ring opening of 1,1,3,5-tetramethyl-3,5-divinylcyclotrisiloxane was faster than for D_3. [3] The polymerization wherein D_3^v was polymerized first produced multi-modal GPC peaks. This may be due a side reaction of the alkyllithium initiator reacting with the vinyl silane. By constrast, when D_3 then D_3^v were polymerized sequentially, narrow molecular weight distributions suggested well-defined polymers. Weber [32] and Kickelbick[82] homopolymerized D_3^v by intiating the reactions with a weakly basic lithium silanolate, thus avoiding any reaction of an alkyllithium with the vinyl moieties.[82]

The copolymerizations were conducted under rigorously anhydrous conditions to prevent any reaction of the strongly basic initiator with water (which would form LiOH and *n*-butane). Lithium hydroxide can initiate ring-opening of D_3 and form *two* siloxanolate chain ends. This would result in undesirable triblock copolymers with central PDMS blocks and terminal PMVS blocks, which would complicate our analysis of the metal-polymer suspensions. This would also give rise to lower average molecular weights of the PMVS components. The molar ratio of *n*-butyllithium to the weight of D_3 controlled the polymer molecular weights. One mole of *n*-BuLi was used for one mole of endgroups. The use of Li^+ as the counterion, rather than Na^+ or K^+, was to take advantage of more closely associated ion pairs and preserve the living nature of these reactions.

D_3 ring-opening was closely monitored with ^1H NMR by observing the decrease of the methyl peak of the cyclic monomer at 0.14 ppm and the concurrent increase of the resonance peak corresponding to the methyl protons of the linear species at 0.06 ppm (figure 3.7). The D_3 was allowed to react until nearly 100% conversion was achieved. This ensured no contamination of the second block with D_3.

D_3^V was charged to the same reaction vessel sequentially in a "one-pot" copolymerization. The molar ratios of linear PDMS to grams of D_3^V controlled the PMVS block molecular weights. This reaction was also monitored via ^1H NMR. The diblock copolymers were terminated by adding trimethylchlorosilane at approximately 90% conversion of the D_3^V. This somewhat early termination was done to avoid any backbiting or intermolecular chain-chain substitutions which might have occurred at

extremely low monomer concentrations. The end-capping reagent was added in excess to ensure complete termination of all the chains.

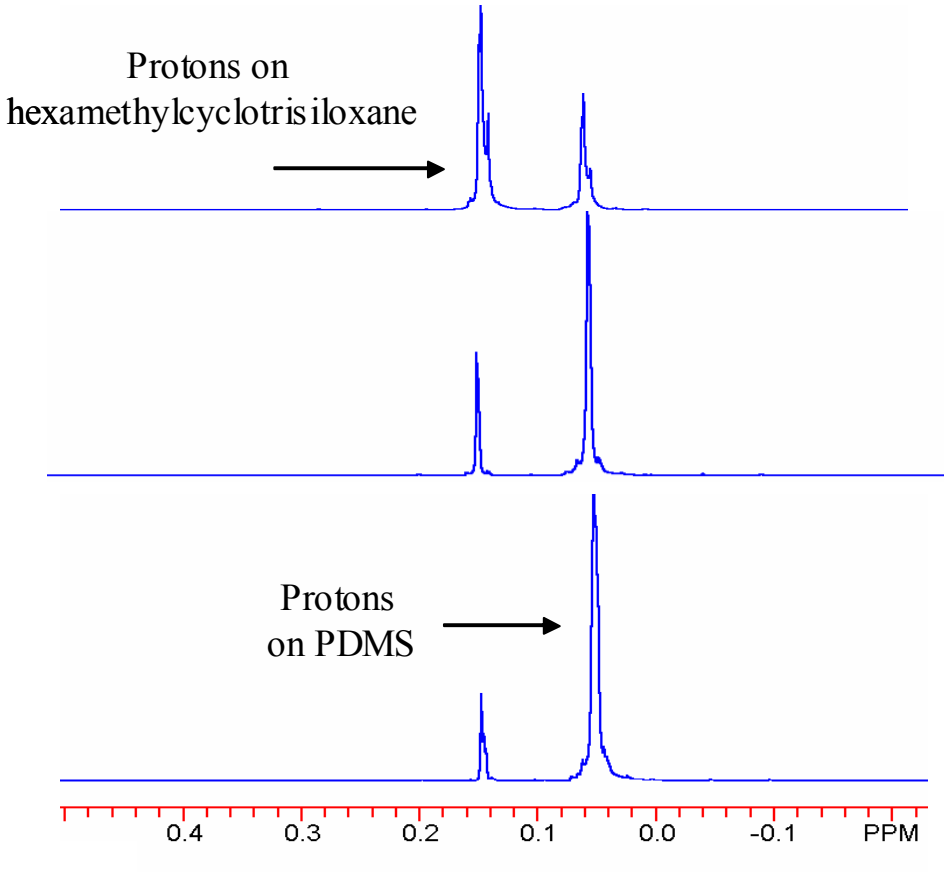

Figure 3.7 The living anionic polymerization of D_3 and the formation of PDMS blocks was monitored by ^1H NMR.

3.4.2.1 Characterization of PDMS-*b*-PMVS

3.4.2.1.1 Molecular weight and molecular weight distribution

The copolymers were rigorously extracted to remove unreacted monomer, promoter, and solvent. The relative compositions of each block in the diblock copolymers were determined by a combination of ^{1}H and ^{29}Si NMR. In the ^{1}H NMR spectra, the integrals from the poly(dimethylsiloxane) methyl resonances at 0.06 ppm were compared to the methyl resonances of the poly(methylvinylsiloxane) at 0.08 ppm. The number average molecular weights were determined by ratioing the butyl endgroup integrals to the methyl resonance integrals. In all cases, the calculated M_n's paralleled the targeted values (Table 3.2), confirming good control over the chemistry. An ^{1}H NMR spectrum of an exemplary block copolymer is depicted in figure 3.8.

Table 3.2 Comparisons of targeted vs. experimental number average molecular weights (M_n) of the PDMS-PMVS diblock copolymers determined via ^{1}H NMR.

Targeted M_n of PDMS-*b*-PMVS (g mol^{-1})	M_n by ^{1}H NMR (g mol^{-1})
5000 – 2000	4200 – 1800
5000 – 2000	4900 – 2100
5000 – 2000	5300 – 2000
10,000 – 2000	10,500 – 2200
10,000 – 2000	11,000 – 2000
14,000 – 2000	13,000 – 2000
16,000 – 2000	13,200 – 2100
16,000 – 2000	17,000 – 3000
16,000 - 2000	15,900 - 1700

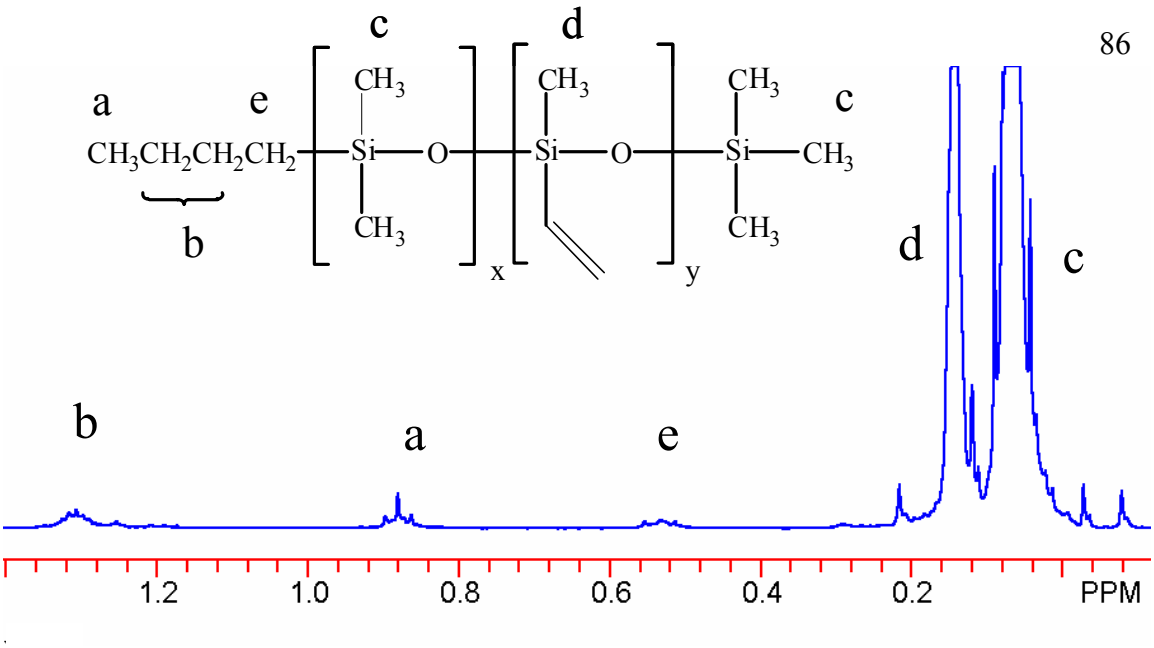

Figure 3.8 ^{1}H NMR spectrum of a PDMS-*b*-PMVS diblock copolymer

^{29}Si NMR was utilized to aid in determining the block compositions as well as to yield block number average molecular weights. ^{29}Si NMR provides a valuable tool for characterizing siloxanes because of its wide frequency range. The PDMS silicons are well-separated from the PMVS silicons in the ^{29}Si NMR. The diblock copolymers should possess one silicon per butyl endgroup and one silicon per trimethylsilyl endgroup. The endgroup peaks were observed at 8.59 ppm and 7.86 ppm, respectively (figure 3.9). Accurate determination of block composition was obtained by ratioing the repeat unit integrals corresponding to each block to the end groups. In all cases, the block M_n's derived from ^{29}Si NMR paralleled the targeted M_n's and those determined via ^{1}H NMR (table 3.3).

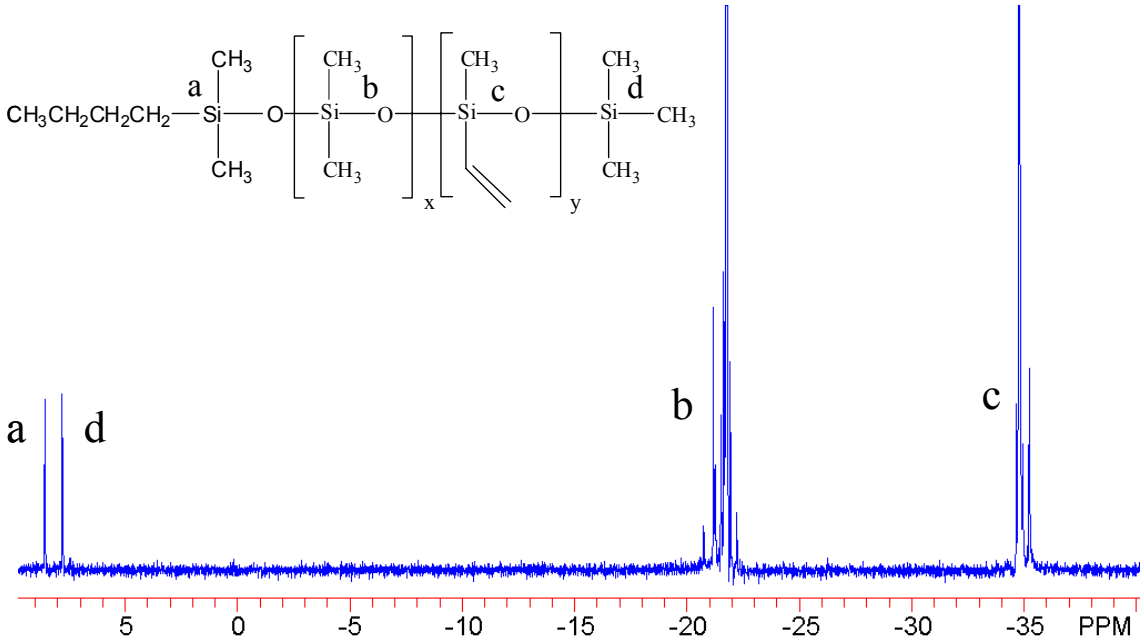

Figure 3.9 ^{29}Si NMR of a PDMS-*b*-PMVS diblock copolymer.

Molecular weight distributions were determined by Gel Permeation Chromatography using polystyrene standards and a universal calibration. For each diblock copolymer, the molecular weight distribution was close to 1(figure 3.10). A summary of all number average molecular weights from ^{1}H and ^{29}Si NMR as well as molecular weight distributions are listed in table 3.4.

Table 3.3 Targeted M_n's of the PDMS-*b*-PMVS diblock copolymers as compared to experimental values.

Targeted M_n of PDMS-*b*-PDMS (g mol^{-1})	M_n by ^{1}H NMR (g mol^{-1})	M_n by ^{29}Si NMR (g mol^{-1})
5000 – 2000	4200 – 1800	4200 – 1800
5000 – 2000	4900 – 2100	5000 – 2000
5000 – 2000	5500 – 2500	5200 – 2900
10,000 – 2000	10,500 – 2200	10,500 – 2000
10,000 – 2000	11,000 – 2000	11,000 – 1500
14,000 – 2000	13,000 – 2000	14,000 – 2000
16,000 – 2000	13,200 – 2100	16,200 – 2200
16,000 – 2000	17,000 – 3000	16,000 – 3000
16,000 - 2000	15,900 - 1700	14,500 - 2000

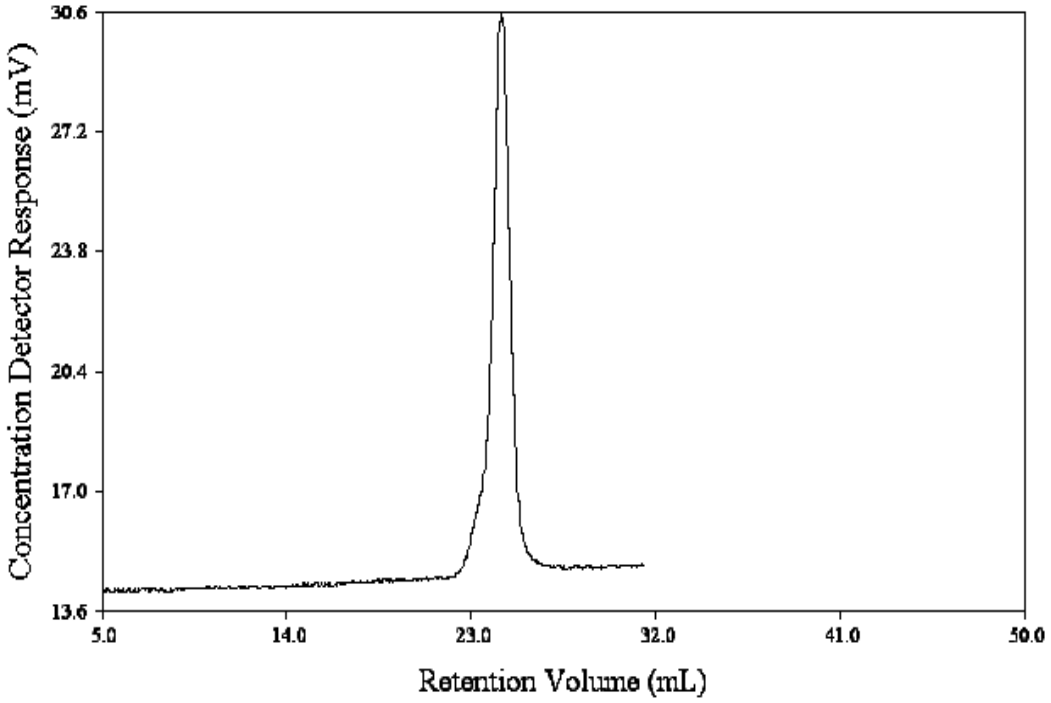

Figure 3.10 Gel permeation chromatogram of a PDMS-*b*-PMVS diblock copolymer

Table 3.4 M_n's and molecular weight distributions of PDMS-*b*-PMVS diblock copolymers.

Targeted M_n (g mol^{-1})	M_n by ^1H NMR (g mol^{-1})	M_n by ^{29}Si NMR (g mol^{-1})	M_n by GPC (g mol^{-1})	Molecular Weight Distribution
7000	6000	6000	7800	1.03
7000	7000	6300	9000	1.05
8000	8500	9000	8700	1.01
12,000	12,700	12,500	13,000	1.02
12,000	13,000	12,500	14,700	1.01
16,000	15,000	16,000	13,700	1.06
18,000	15,200	18,500	17,500	1.01
18,000	20,000	19,000	22,000	1.09
18,000	17,000	16,500	17,200	1.03

3.4.2.3 Characterization of thermal properties

Bulk thermal properties of each diblock copolymer were measured via Differential Scanning Calorimetry. The PMVS block molecular weight was constant in this experiment at approximately 2000 g mol^{-1} and the PDMS block molecular weights ranged from 5000 to 16,000 g mol^{-1}. For each copolymer, only one glass transition temperature (T_g) was observed at approximately -126 °C (figure 3.11 and table 3.5). Since two T_g's would be expected for microphase separated block copolymers, this suggested that the PDMS and PMVS blocks were miscible.

Literature has reported similar T_g's for PDMS homopolymers. [32,151] The T_g of a 1000 g mol^{-1} PMVS homopolymer was observed at approximately -137 °C (figure 3.12). These low T_g's reflect the mobility of both siloxane backbones and the absence of long range order in the PMVS. Semlyen et al., [151] Riffle et al., [152] and Weber et. al. [32]have also reported low glass transition temperatures of PMVS homopolymers. The atactic nature of the stereocenters in the PMVS blocks prevents any crystallization of the PMVS homopolymers.

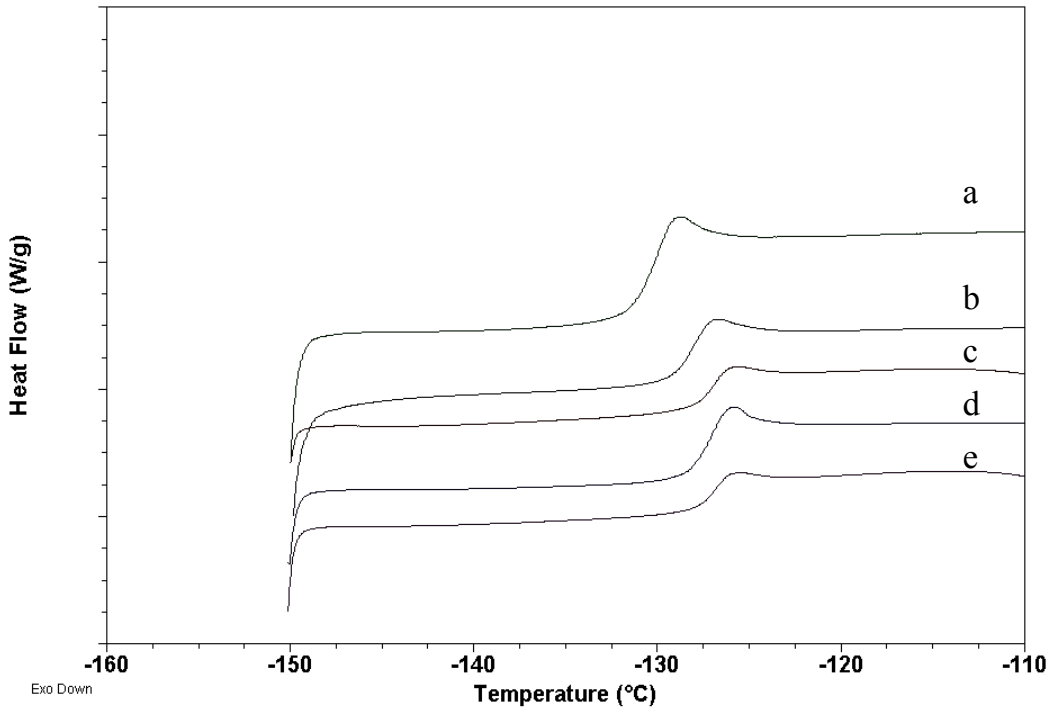

Figure 3.11 DSC thermograms of PDMS-*b*-PMVS diblock copolymers; a.) 5000 g mol^{-1} PDMS-*b*-2000 g mol^{-1} PMVS, b.) 10000 g mol^{-1} PDMS-*b*-2000 g mol^{-1} PMVS, c.) 13,000 g mol^{-1} PDMS-*b*-2000 g mol^{-1} PMVS, d.) 16,000 g mol^{-1} PDMS-*b*-2000 g mol^{-1} PMVS, e.) 18000 g mol^{-1} PDMS-*b*-2000 g mol^{-1} PMVS

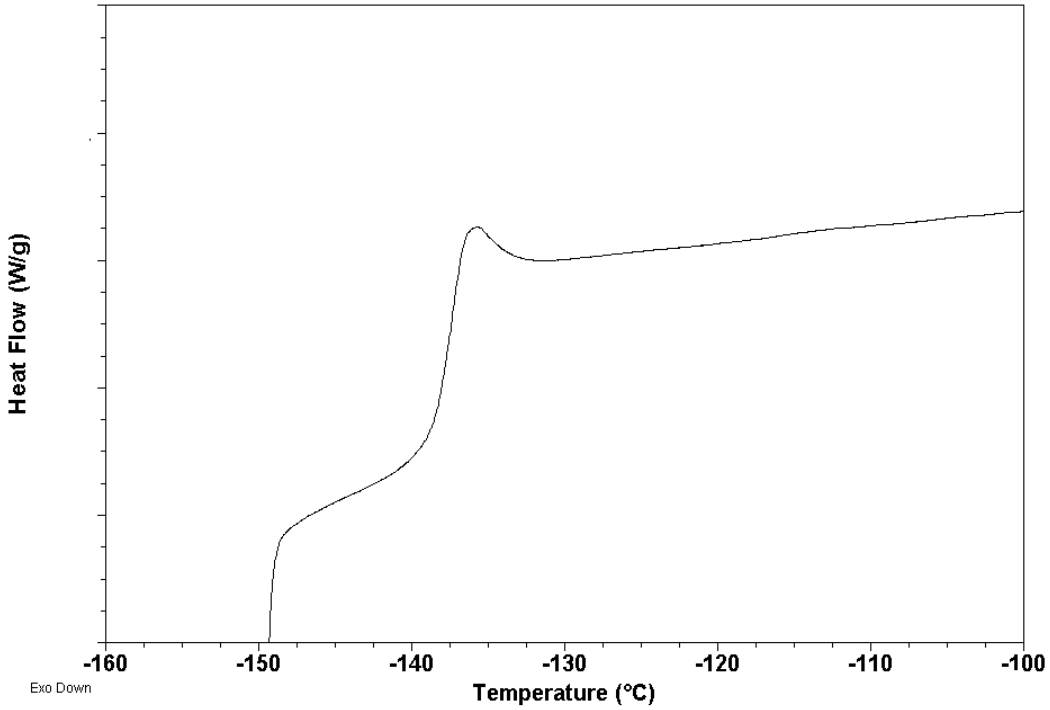

Figure 3.12 DSC thermogram of a 1000 g mol^{-1} PMVS homopolymer

Table 3.5 Glass transition temperatures of a PDMS-*b*-PMVS series

M_n PDMS (g mol^{-1})	M_n PMVS (g mol^{-1})	M_n Total (g mol^{-1})	T_g (°C)
4200	1800	6000	-129
5000	2000	7000	-129
5000	2900	8000	-129
10,500	2200	12,700	-128
11,000	2000	13,000	-128
13,000	2000	15,000	-127
16,200	2200	18,400	-127
17,000	2500	19,500	-127
14,500	2000	16,500	-127

CHAPTER 4 Functionalization of Poly(dimethylsiloxane-*b*-methylvinylsiloxane) Diblock Copolymers with Trialkoxysilethyl Substituents

4.1 Synopsis

Poly(dimethylsiloxane-*b*-methylvinylsiloxane) (PDMS-*b*-PMVS) diblock copolymers have been functionalized with triethoxysilethyl- or trimethoxysilethyl pendent moieties and the melt and solution properties of the copolymers have been investigated. These functionalized diblock copolymers were subsequently utilized to generate micellar solutions in toluene and the formation of cobalt nanoparticles in the solutions was demonstrated.

4.2 Experimental

A Pt^0 [1,3-divinyl-1,1,3,3-tetramethyldisiloxane]$_{1.5}$ complex catalyst in xylene (2.1 – 2.4 wt% Pt) (Gelest, Inc., d 0.885 g mL^{-1}) was used as received. Triethoxysilane and trimethoxysilane (Gelest, Inc.) were used as received. Toluene (Aldrich, 99.8%, FW 92.14 g mol^{-1}, mp -93 °C, bp 110.6 °C, d 0.865 g mL^{-1}) was washed twice with concentrated sulfuric acid and neutralized with water. It was dried over $MgSO_4$ for one hour, then over calcium hydride overnight and distilled just before use.

4.2.1 Synthesis of poly[(dimethylsiloxane–*b*- poly(methyl-(2-triethoxysilethyl)siloxane] (PDMS-*b*-PMTES) via hydrosilation

Functionalized diblock copolymers were prepared from the PDMS-*b*-PMVS diblock copolymers. The molar ratios of triethoxysilane or trimethoxysilane relative to the number of vinyl groups determined the degree of hydrosilation. A exemplary procedure for quantitative hydrosilation is described. Firstly, 0.3g of the polymer precursor, a 5000 g mol^{-1} PDMS and 2500 g mol^{-1} PMVS diblock copolymer, was weighed into a 6 dram vial equipped with a magnetic stir bar. The vial containing the copolymer was sealed with a septum and flame dried under nitrogen. Toluene (10 mL) was added via syringe and mixture was stirred until the polymer dissolved. Triethoxysilane (0.21 mL, 0.0012 mol) was added via syringe to the reaction vial followed by the addition of 10μL of Pt^0 (Karstedt) catalyst in xylene. The reaction was stirred at 60 °C until complete hydrosilation occurred as evidenced by ^{1}H NMR. The solvent was evaporated under vacuum and the PDMS-b-PMTES diblock copolymer was stored under nitrogen.

4.2.2 Synthesis of poly(dimethylsiloxane)-*b*-[poly(methylvinylsiloxane)-*co*-poly(methyl-(2-trimethoxysilethyl)siloxane] (PDMS-*b*-[PMVS-*co*-PMTMS]) via hydrosilation

An exemplary synthesis to prepare a diblock copolymer wherein only half the pendent vinyl groups on the polymer precursor were functionalized is provided. A 5000 g mol^{-1} – 2500 g mol^{-1} PDMS-*b*-PMVS diblock copolymer was utilized. Firstly, 0.3g of the polymer precursor, a 5000 g mol^{-1} PDMS and 2500 g mol^{-1} PMVS diblock copolymer, was weighed into a 6-dram vial equipped with a magnetic stir bar. The vial containing the copolymer was sealed with a septum and flame dried under nitrogen. Toluene (10 mL) was added via syringe and the mixture was stirred until the polymer dissolved. Trimethoxysilane (0.15 mL, 0.0012 mol) was added via syringe to the reaction vial followed by addition of 10 μL of the Pt^0 (Karstedt) catalyst in xylene. The amount of catalyst is based on 10^{-3} moles of Pt^0 per mole vinyl. The reaction was stirred at 60 °C until complete hydrosilation occurred as evidenced by ^{1}H NMR. The solvent was evaporated under vacuum and the PDMS-*b*-[PMVS-*co*-PMTMS] diblock copolymer was stored under nitrogen.

4.2.2.1 Characterization

4.2.2.2 ^{1}H NMR

All ^{1}H NMR were obtained on a Varian Unity 400 MHz NMR spectrometer operating at 400 MHz. The NMR spectra were collected with a pulse width of 28.6° and a relaxation delay of 1.000 sec at ambient temperature. The samples were dissolved in *d*-$CHCl_3$ for obtaining the spectra.

4.2.2.3 Differential Scanning Calorimetry

DSC scans were performed on a TA Instruments DSC Q1000 under constant flow of Helium. The samples (10-15 mg) were ramped from -150 to 25 °C using hermetically sealed DSC pans. Two scans were performed on each sample and the T_g's were take from the inflection points on the second scans.

4.2.2.4 Surface Tension Analysis

The copolymer solutions were prepared in toluene with concentrations of 1g L^{-1} to 10^{-6} g L^{-1} for surface tension measurements. The solution measurements were made by measuring the lowest concentration first then moving to the highest concentration. These measurements were conducted at 24 °C using a platinum Wilhelmy plate. Surface tensions were calculated using the relationship $\Delta F = \gamma P \cos\theta$ where ΔF was the difference in weight between the wet plate and the wet plate in contact with the solution, γ was the surface tension, P was the perimeter of the plate, and the contact angle θ was assumed to be zero degrees.

4.3 Results and Discussion

4.3.1 Functionalization of the PMVS blocks with trimethoxysilane or triethoxysilane

The poly(methylvinylsiloxane) blocks in the PDMS-*b*-PMVS copolymers were quantitatively hydrosilated with triethoxysilane or trimethoxysilane to yield PDMS-*b*-PMTES or PDMS-*b*-PMTMS respectively (figure 4.1). Alternatively, the PDMS-*b*-PMVS precursor copolymers were only partially hydrosilated (figure 4.2). In these cases, the resulting diblock copolymers were comprised of a PDMS block linked to a poly(methylvinylsiloxane-*co*-methyltrialkoxysilethylsiloxane) wherein the sequences of methylvinylsiloxane and methyltrialkoxysilethylsiloxane units in the second blocks were random. These partially hydrosilated diblock copolymers will be designated PDMS-*b*-[PMVS-*co*-PMTES] (for the cases of hydrosilation with triethoxysilane) and PDMS-*b*-[PMVS-*co*-PMTMS] (for the cases of hydrosilation with trimethoxysilane).

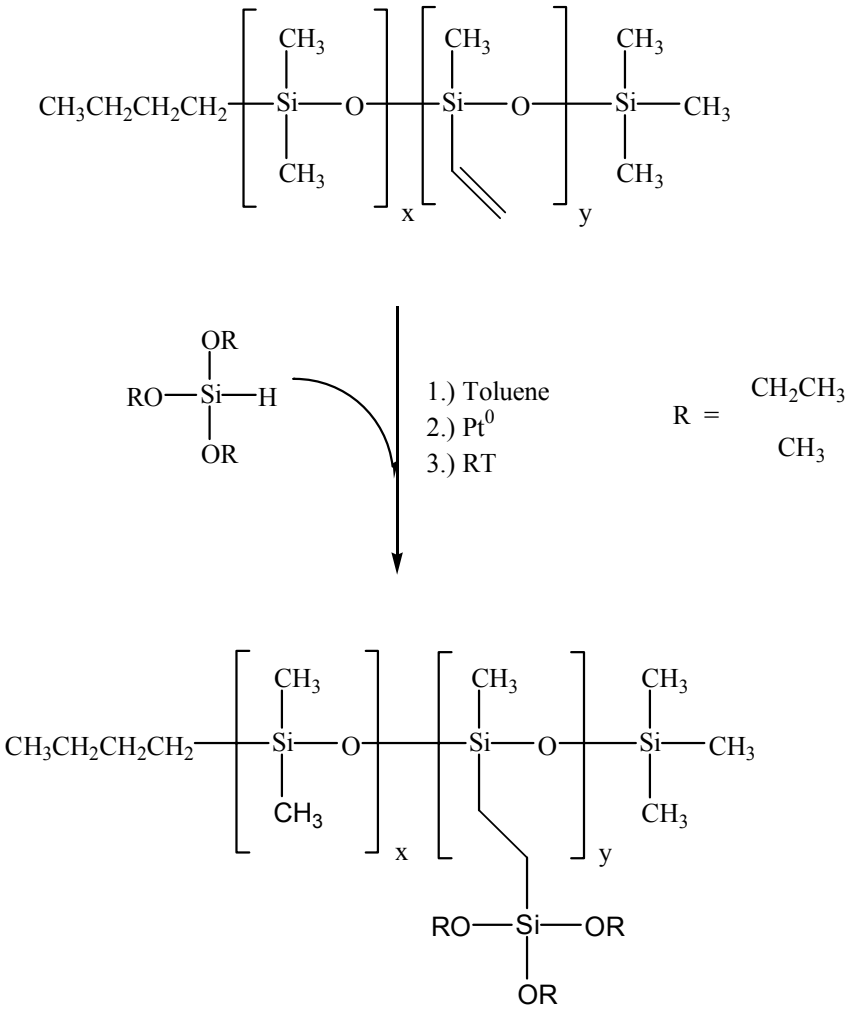

Figure 4.1 PDMS-b-PMVS copolymers were quantitatively hydrosilated with triethoxysilane or trimethoxysilane to yield PDMS-*b*-PMTES or PDMS-*b*-PMTMS, respectively

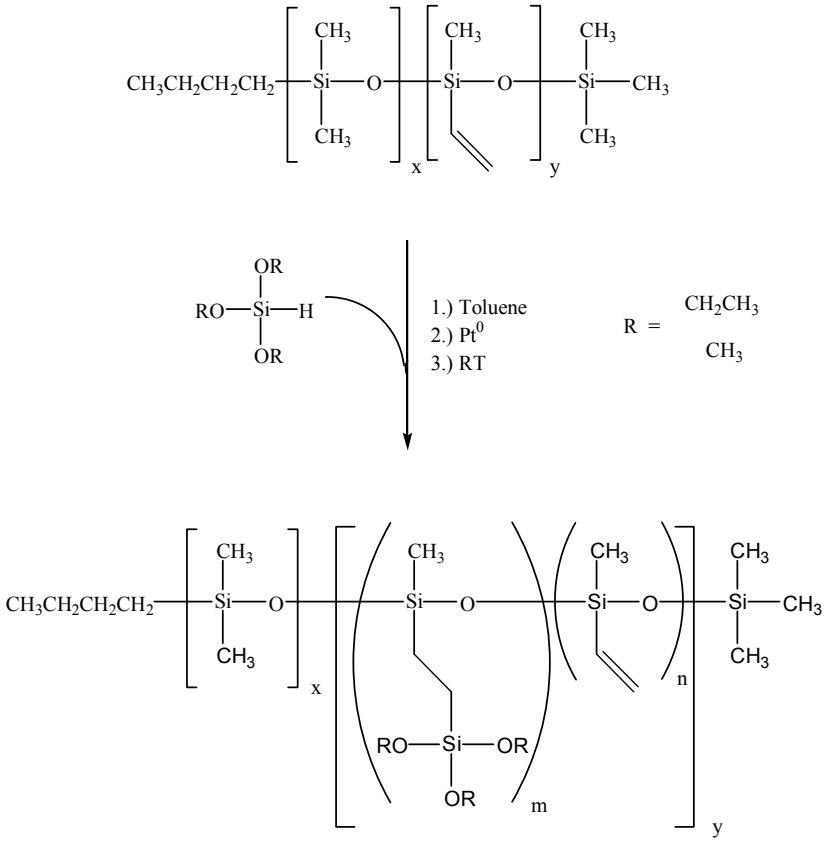

Figure 4.2. Partial hydrosilation of PDMS-*b*-PMVS diblock copolymers with trimethoxysilane or triethoxysilane to form PDMS-*b*-[PMVS-*co*-PMTMS] and PDMS-*b*-[PMVS-*co*-PMTES], respectively.

Hydrosilation reactions are extensively used to prepare monomers with Si-C bonds or to crosslink polysiloxanes. These involve additions of Si-H across vinyl substituents. [150,153] Karstedt's catalyst is Pt^0, usually complexed with divinyltetramethyldisiloxane (figure 4.3). It can be prepared by reacting choroplatinic acid (H_2PtCl_6) with divinyltetramethyldisiloxane. [154] These catalysts are available commercially as solutions in either organic solvents such as xylene or polysiloxane oligomers. Such complexed catalysts are soluble in polysiloxane media and have high reactivity.

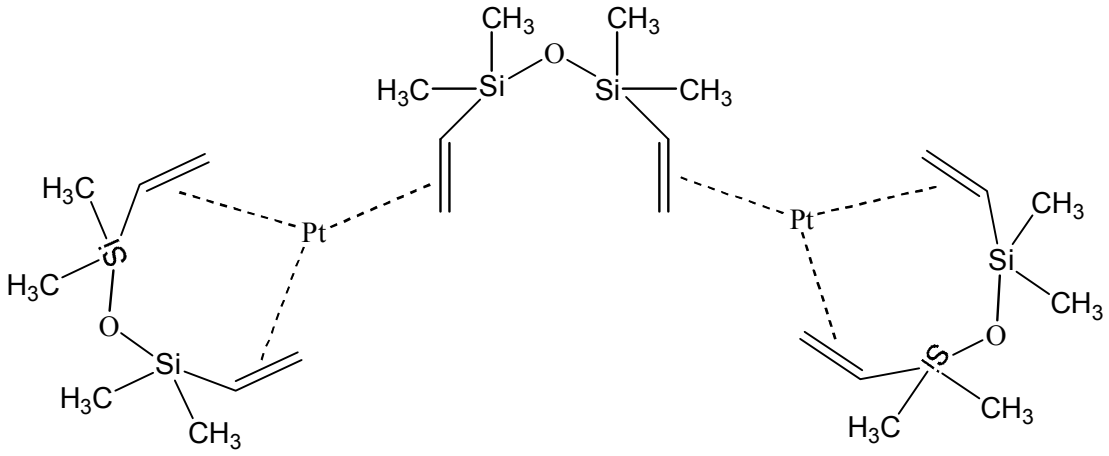

Figure 4.3 Karstedt's catalyst

The polymer precursor, PDMS-*b*-PMVS, was dried under vacuum overnight to remove any water that might cause premature reaction of the alkoxysilyl groups. The hydrosilation reactions were monitored via ^{1}H NMR by observing the disappearance of the Si-H peaks (δ = 4.5 ppm) and an upfield shift and broadening of the triethoxysilyl methylene peaks (figure 4.4). Normal (β) and reverse addition (α) of the Si-H across the double bond are known to occur. [155]Both α (13 %) and β (87 %) addition products were obtained (figure 4.5). Two signals [δ 1.4 –CH_3 (f) and δ 1.3 –CH (c)] corresponding to α addition across the double bonds appeared as the reactions proceeded (figure 4.6).

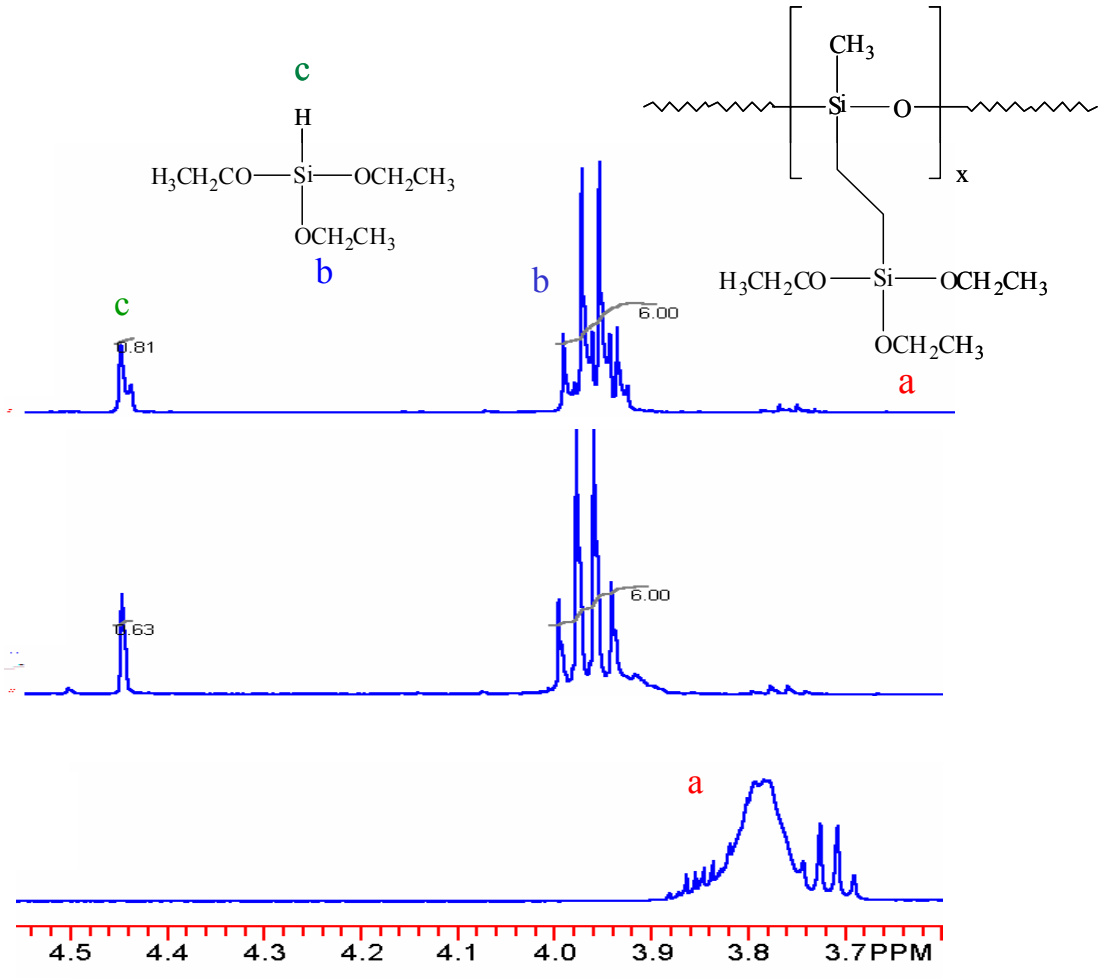

Figure 4.4 Reaction progress of a functionalization reaction via ^{1}H NMR

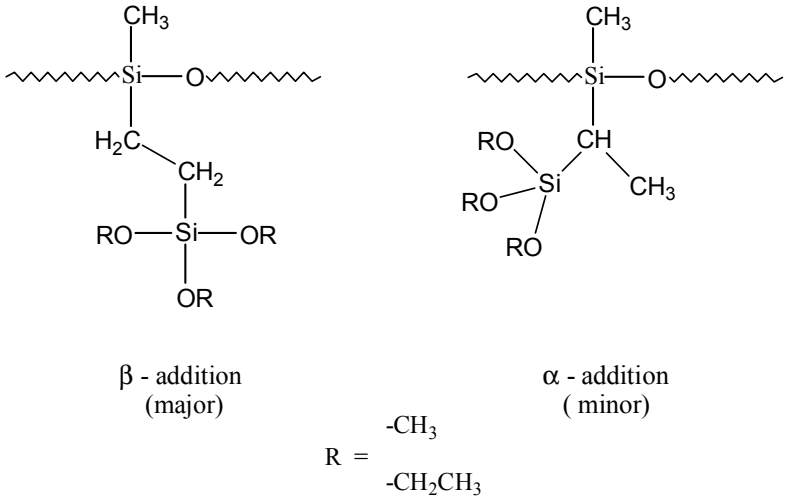

Figure 4.5 β and α addition products.

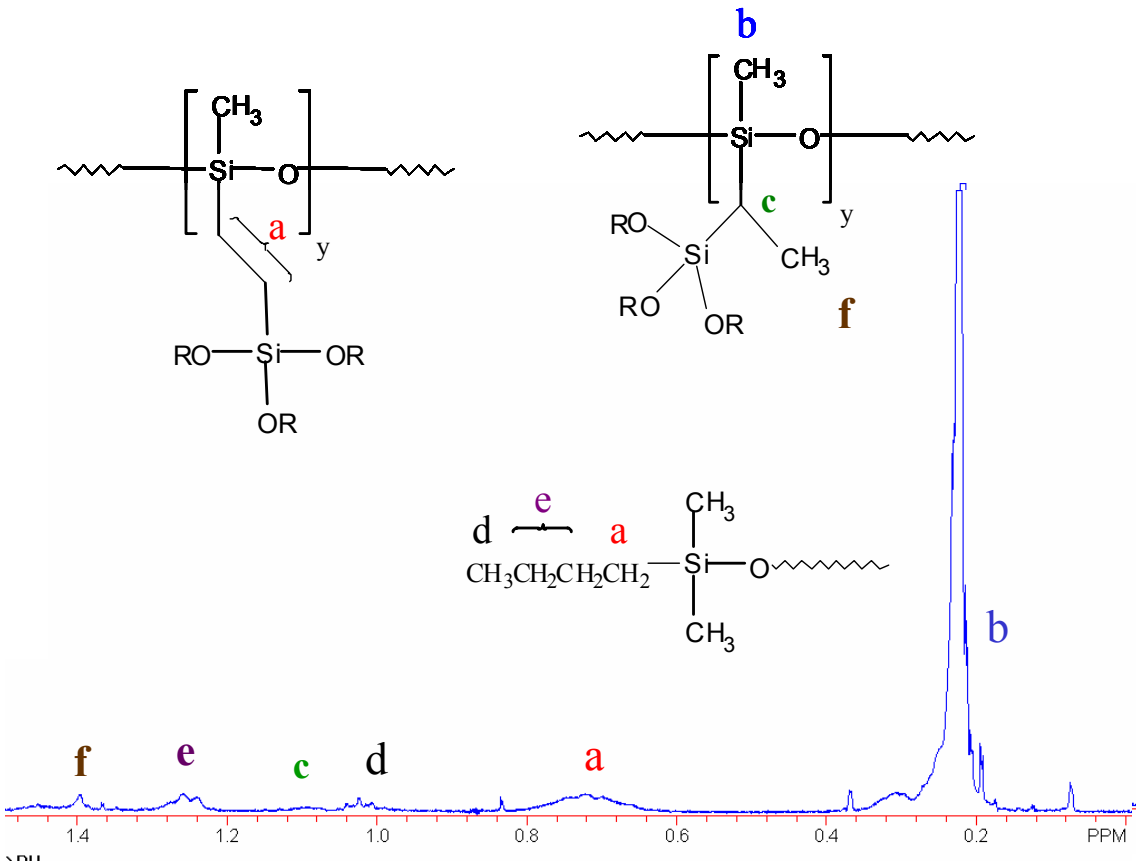

Figure 4.6 ^{1}H NMR α and β addition peak assignments

4.3.2 Thermal characterization

The thermal properties of these functionalized diblock copolymers were investigated to probe their morphologies. The thermal transitions of polymers are based on molecular motion at a given kT. Increased molecular rigidity of the polymer backbone increases the glass transition temperature. Microphase separation in a block copolymer depends on relative block polarities and block molecular weights. PDMS-*b*-PCPMS-*b*-PDMS triblock copolymers were microphase separated even at low block molecular weights (5000 g mol^{-1} PDMS-*b*-2000 g mol^{-1} PCPMS-*b*-5000 g mol^{-1} PDMS). [40] The nitrile containing central block (PCPMS) was significantly more polar than the PDMS tail blocks.

A 1000 g mol^{-1} PMVS homopolymer was quantitatively functionalized to from a PMTES homopolymer and their T_g's were compared. The T_g of the unfunctionalized PMVS homopolymer was -137 °C and the T_g of the PMTES homopolymer was -95 °C (figure 4.7). This probably reflects less rotational mobility in the PMTES.

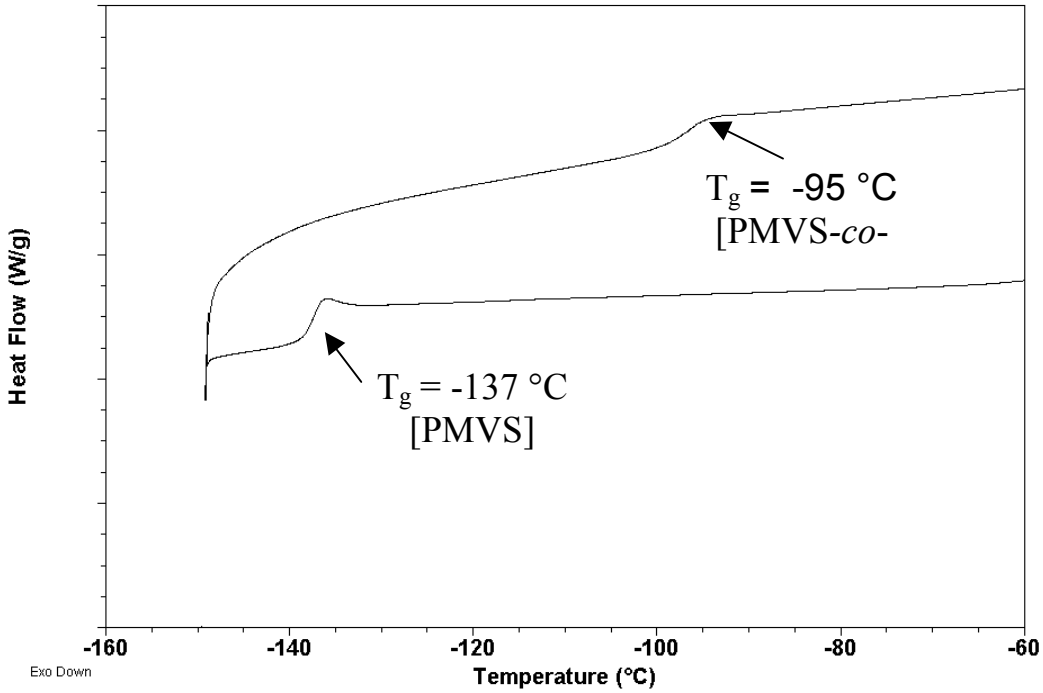

Figure 4.7 T_g's of PMTES and PMVS homopolymers

The thermal of the PDMS-*b*-PMTES diblock copolymers were also determined by DSC (figure 4.8). The PMVS block lengths were kept constant at 2000 g mol^{-1} (pre-functionalization) or 5800 g mol^{-1} (post-functionalization). Only one T_g was observed for each of these diblock copolymers (table 4.1). This implies that the blocks in both types of structures are miscible (even with triethoxysilyl groups pendent on the polymer backbone).

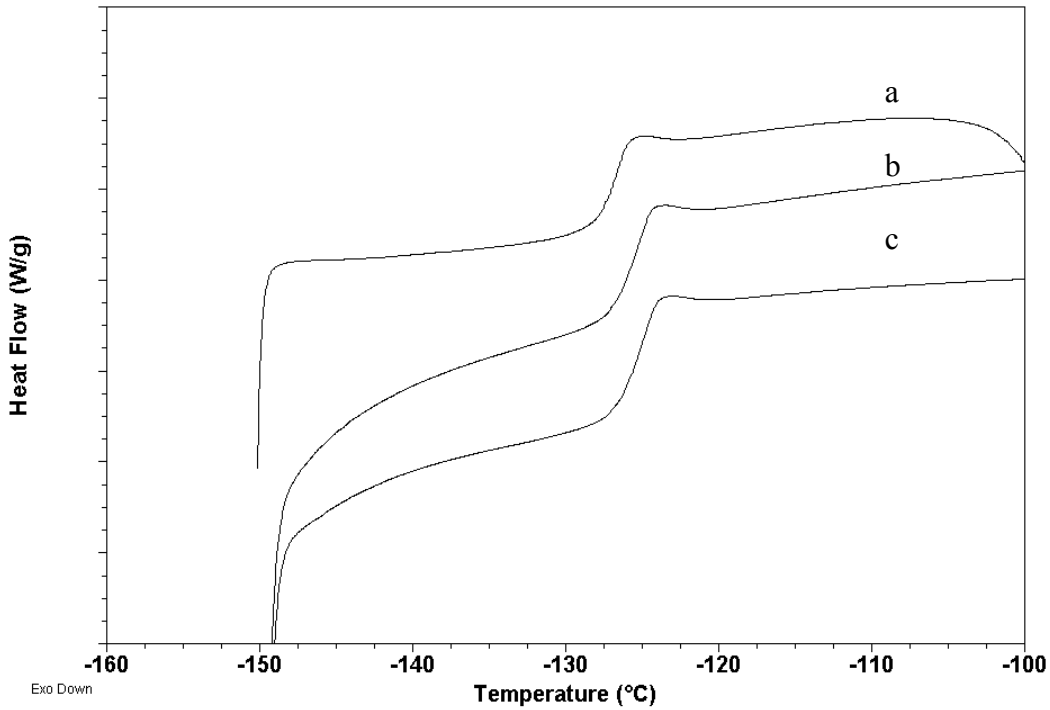

Figure 4.8 DSC scan of PDMS-PMTES diblock copolymer; a.) 5000 g mol^{-1} PDMS-*b*-3900 g mol^{-1} [PMVS-*co*-PMTES], b.) 10,000 g mol^{-1} PDMS-*b*-3900 g mol^{-1} [PMVS-*co*-PMTES], c.) 16000 g mol^{-1} PDMS-*b*-3900 g mol^{-1} [PMVS-*co*-PMTES]

Table 4.1 Diblock copolymer T_g's before and after functionalization with triethoxysilyl groups.

M_n PDMS (g mol^{-1})	M_n PMTES (g mol^{-1})	T_g (PDMS-*b*-PMVS) (°C)	T_g (PDMS-*b*-PMTES) (°C)
5000	5800	-129	-124
10,500	5800	-128	-125
16,000	5800	-127	-126

4.3.3 Solution characterization

One goal of this research has been to design micellar reaction solutions where the micelle cores might be used to template the formation and size of cobalt nanoparticles. Both PDMS and PMVS homopolymers are readily soluble in toluene. It is proposed that the PDMS-*b*-PMTES diblock copolymers form aggregates in toluene solutions where the aggregate structure may depend on the degree of functionalization and the block molecular weights.

Surface tension measurements of block copolymer solutions in toluene support the formation of copolymer aggregates. Solutions of two sets of polymers were investigated: 1.) copolymers with a 5000 g mol^{-1} PDMS block and a 2000 g mol^{-1} PMVS block which had been functionalized with 0, 50, or 100% triethoxysilyl units, and 2.) copolymers with a 16,000 g mol^{-1} PDMS block and a 2000 g mol^{-1} PMVS block which had been functionalized with 0, 50, and 100% triethoxsilyl units. The surface tensions of solutions of all of these materials approached that of pure toluene (28.5 mN/m) at sufficiently low copolymer concentrations.

For the copolymer solutions containing the 5000 g mol^{-1} PDMS, surface tensions gradually decreased with increasing concentration, but the copolymer 100% of the vinyl groups functionalized exhibited lower values (figure 4.9). This suggests that increased functionalization with triethoxysilethyl groups drives the systems toward aggregates. For the copolymer solutions containing the 16,000 g mol^{-1} PDMS, distinct breaks in the surface tension curves between 0.001 and 0.01 g L^{-1} suggest micellization (figure 4.10).

1.)

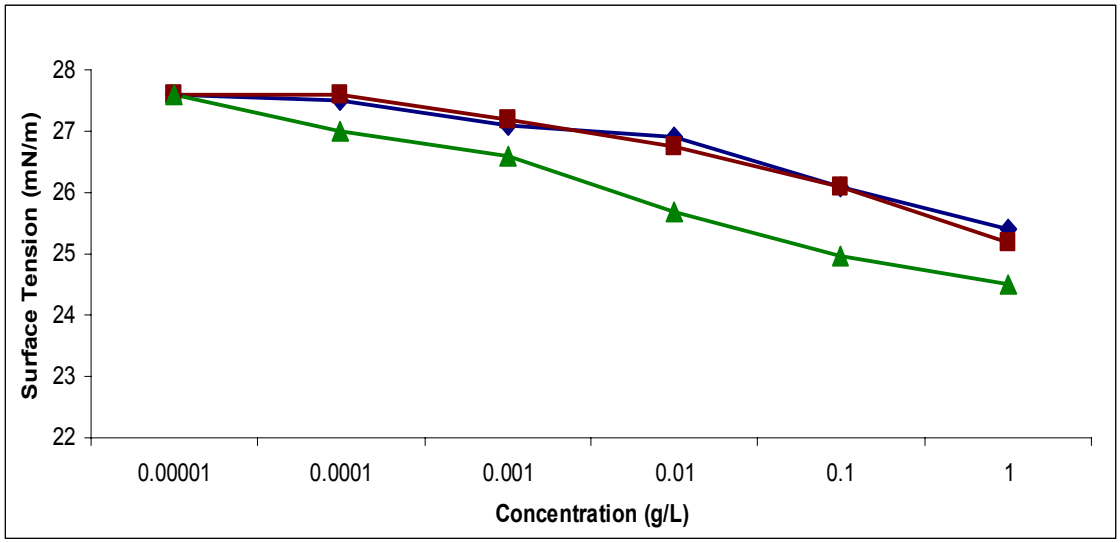

Figure 4.9 Surface tension of a 5000 g mol^{-1} PDMS-*b*-3900 g mol^{-1}[PMVS-*co*-PMTES] copolymer

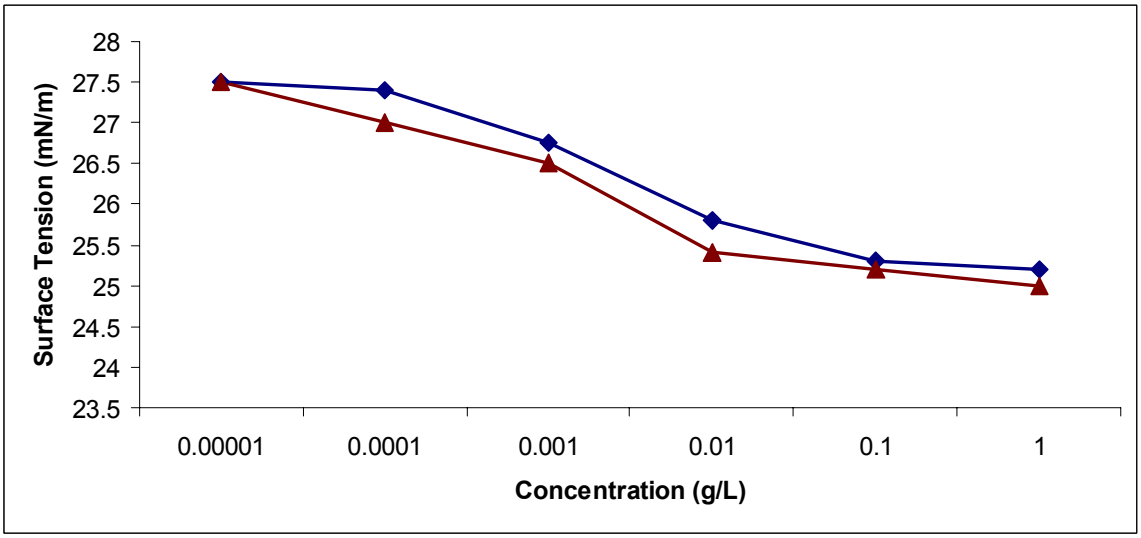

Figure 4.10 Surface tension of a 16,000 g mol^{-1} PDMS-*b*-3900 g mol^{-1}[PMVS-*co*-PMTES] copolymer

CHAPTER 5 Sol-gel reactions with functionalized copolysiloxanes

5.1 Synopsis

This chapter discusses hydrolysis and condensation reactions of trialkoxysilyl pendent groups on the polysiloxane block copolymers utilizing sol-gel techniques. The first section describes hydrolyses of copolysiloxanes functionalized with pendent tri*methoxy*silyl groups. Due to the enhanced reactivity of tri*methoxy*silanes relative to tri*ethoxy*silanes, neutral conditions were utilized in these reactions. This was important because strong acid or basic condensation catalysts could potentially damage the relatively labile polysiloxane backbone. Hydrolyses and condensations of *triethoxy*silyl pendent groups were studied in dichloroacetic acid-water mixtures. The motivation for the sol-gel investigations was to identify reaction conditions wherein the blocks containing the alkoxysilanes could be hydrolyzed and condensed around cobalt particle surfaces.

5.2 Experimental

A Pt^0 [1,3-divinyl-1,1,3,3-tetramethyldisiloxane]$_{1.5}$ complex catalyst in xylene (2.1 – 2.4 wt% Pt) (Gelest, Inc., d 0.885 g mL^{-1}) was used as received. Triethoxysilane and trimethoxysilane (Gelest, Inc.) were used as received. Toluene (Aldrich, 99.8%, FW 92.14 g mol^{-1}, mp -93 °C, bp 110.6 °C, d 0.865 g mL^{-1}) was washed twice with concentrated sulfuric acid and neutralized with water. It was dried over $MgSO_4$ for one hour, then over calcium hydride overnight and distilled just before use.

5.2.1 Hydrolysis and Condensation of poly(dimethylsiloxane)-*b*-[poly(methylvinylsiloxane)-*co*-poly(methyl-(2-triethoxysilethyl)siloxane] copolymer with acetic acid and water.

A sol-gel synthesis of an exemplary 5300 g mol^{-1}- 3900 g mol^{-1} (PDMS-*b*-[PMVS-*co*-PMTES) copolymer is provided. The PMVS-*co*-PMTES block had 50% of the repeat units hydrosilated with triethoxysilane. Copolymers with higher molecular weight PDMS blocks were also investigated using a similar approach. The molecular weights of the PMVS-*co*-PMTES blocks were kept constant at 3900 g mol^{-1}. Acetic acid (0.0011 mol, 1.1 mL of 1 M acetic acid) and H_2O (0.01 mL, 0.00057 mol, stoichiometric) were charged to a flame dried, 6-dram vial along with 0.3g (0.00038 eq triethoxysilethyl groups, 0.0011 eq ethoxy) of the functionalized copolymer in 10 mL toluene. The reaction was stirred at room temperature for five days and monitored by ^1H NMR. These reaction conditions did not result in significant hydrolysis.

5.2.2 Hydrolysis and condensation of poly(dimethylsiloxane)-*b*-[poly(methylvinylsiloxane)-*co*-poly(methyl-(2-triethoxysilethyl)siloxane] (PDMS-*b*-[PMVS-*co*-PMTES]) copolymers with dichloroacetic acid and water.

The reactions were carried out in identical vials as the hydrosilation reactions to prevent any contamination by water caused by transfer between vessels. A sol-gel synthesis of an exemplary 5300 g mol^{-1}-3900 g mol^{-1} (PDMS-*b*-[PMVS-*co*-PMTES) copolymer is provided. The PMVS-*co*-PMTES block had 50% of the repeat units hydrosilated with triethoxysilane. Copolymers with higher molecular weight PDMS blocks were also studied while keeping the molecular weights and mole fractions of PMVS-*co*-PMTES constant. The PDMS-*b*-[PMVS-*co*-PMTES] copolymer (0.3g, 0.00038 eq of triethoxysilethyl groups, 0.0011 eq ethoxy) and toluene (10 mL) were charged to a flame dried, 6-dram vial and the copolymer was dissolved at room temperature. Dichloroacetic acid (0.0011 mol, 0.14g, 0.091 mL,) and H_2O (0.00057 mol, 0.01 mL, 3 eq. per triethoxysilane, stoichiometric) were added to the solution and the mixture was stirred at room temperature for five days. The disappearance of ethoxysilyl groups was monitored by ^1H NMR.

5.2.3 Hydrolysis and condensation of poly[dimethylsiloxane-*b*-(methyl-(2-triethoxysilethyl)siloxane)] (PDMS-*b*-PMTMS)

A series of reactions were conducted wherein the concentration of water per eq of methoxysilyl groups was varied from stoichiometric (1 mol water : 2 mol methoxy), two times stoichiometric (2 mol water : 2 mol methoxy), and four times stoichiometric (4 mol water : 2 mol methoxy). An exemplary sol-gel synthesis of a PDMS-*b*-PMTMS block copolymer having a 10,000 g mol^{-1} PDMS block connected to a 4800 g mol^{-1} PMTMS

block with four times the stiochiometric concentration of water is described. A 3-neck, 250-mL, round bottom flask equipped with a mechanical stirrer, condenser, and nitrogen purge was charged with 1.0 g (0.0016 eq of trimethoxysilethyl groups, 0.0047 eq methoxy) of the PDMS-*b*-PMTMS copolymer. Toluene (15 mL) was transferred via syringe to the reaction vessel to dissolve the copolymer. Water (0.17 mL, 0.0096 mol, 12 eq per trimethoxysilane, 4 times stoichiometric) was added via syringe. The reaction was stirred at 95 °C. The reaction progress was monitored via ^{1}H NMR.

5.2.4 Hydrolysis and condensation of poly(dimethylsiloxane)-*b*-[poly(methylvinylsiloxane)-*co*-poly(methyl-(2-trimethoxysilethyl)siloxane] (PDMS-*b*-[PMVS-*co*-PMTMS]) copolymer with water.

The reactions were carried out in identical vials as the hydrosilation reactions to prevent any contamination by water caused by transfer between vessels. A sol-gel synthesis of a 10,000 g mol^{-1}- 3400 g mol^{-1} PDMS-*b*-[PMVS-*co*-PMTES] copolymer is provided. The PMVS-*co*-PMTMS block had 50% of the repeat units hydrosilated with trimiethoxysilane. A 3-neck, 250-mL, round bottom flask equipped with a mechanical stirrer, condenser, and nitrogen purge was charged with 1.0g (0.00087 eq of trimethoxysilethyl groups, 0.0026 eq methoxy) of the PDMS-*b*-[PMVS-*co*-PMTMS] copolymer. Toluene (15 mL) was transferred via syringe to the reaction vessel. Water (0.09 mL, 0.0052 mol, 12 eq per trimethoxysilane, 4 times stoichiometric) was added via syringe. The reaction was stirred at 95 °C. The reaction progress was monitored via ^{1}H NMR.

5.3 Characterization

5.3.1 ^{1}H NMR

^{1}H NMR spectra were obtained on a Varian Unity 400 MHz NMR spectrometer operating at 400 MHz. The NMR spectra were collected with a pulse width of 28.6° and a relaxation delay of 1.000 sec at ambient temperature. The samples were dissolved in *d*-$CHCl_3$ for obtaining the spectra.

5.4 Results and Discussion

5.4.1 Hydrolysis and condensation reactions of PDMS-*b*-PMTMS

Hydrolysis and condensation reactions have been well studied in recent years.[38,104,112] These reactions are usually conducted with tetraethoxy- or tetramethoxysilanes in their parent alcohol using acidic or basic catalysts. The research described in this thesis involved reactions of trialkoxysilyl functionalized copolysiloxanes. It is known that strong acids or bases can react with the siloxane backbone, and that such reactions can lead to redistributions of the chains and changes in molecular weights. Thus, one motivation for studying the sol-gel reactions of these copolysiloxanes was to identify mild reaction conditions wherein the hydrolyses occured, but wherein any attack on the siloxane backbone was avoided.

Tetramethoxysilane (TMOS) undergoes hydrolysis and condensation in the presence of water and the reactions do not require an additional acid catalyst. [38] It was found that hydrolysis was sensitive to the TMOS:water ratio. Higher water concentrations over the stoichiometric amount (1 mol H_2O : 2 mol methoxy) afforded

faster hydrolysis rates and higher conversions. Tetramethoxysilanes are generally hydrolyzed and condensed in methanol with stoichiometric or higher amounts of water. The overall reactions utilize two methoxysilyl groups for every one water molecule since one water molecule is produced upon condensation.

Model hydrolysis and condensation reactions were conducted with trimethoxysilane in toluene (figure 5.1). The concentrations of water were varied from stoichiometric to four times stoichiometric, and reaction temperatures from 85 to 110 ºC were investigated. The reactions were monitored by ^{1}H NMR by observing the decrease of the methyl resonance corresponding to the methoxysilyl group at 3.7 ppm and the concurrent increase of the methyl resonance of the methanol by-product at 3.55 ppm (figure 5.2). As the reactions proceeded, a white precipitate was observed which increased with conversion. This was believed to be crosslinked "silica-like" species. These reactions were conducted for two hours.

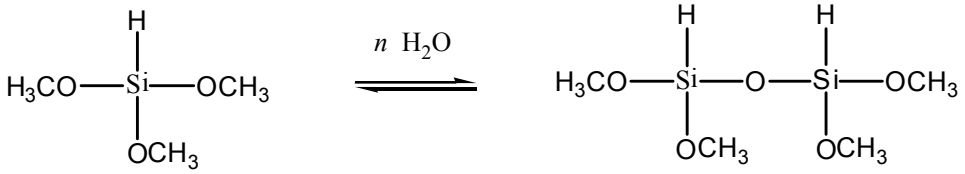

Figure 5.1 Hydrolysis and condensation of trimethoxysilane with varying concentrations of water.

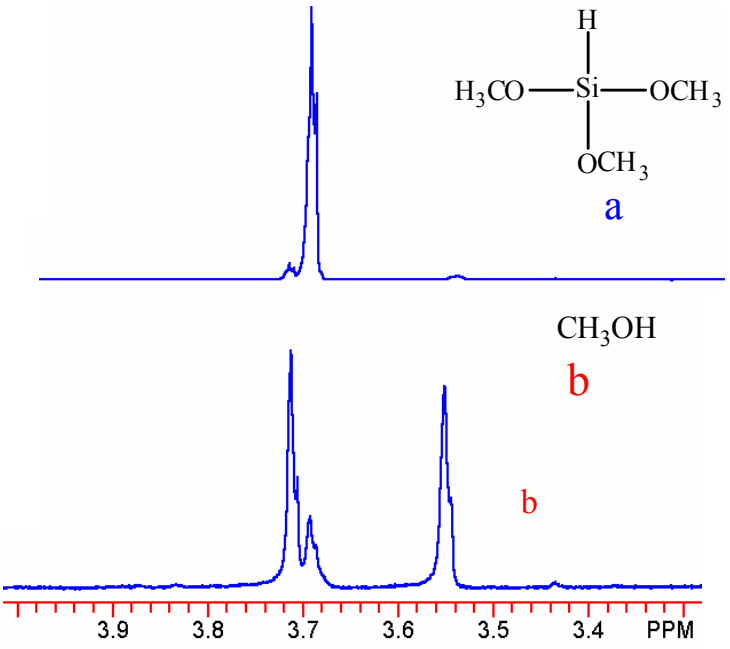

Figure 5.2 ^{1}H NMR reaction progress of the hydrolysis of trimethoxysilane (0.05 g mL^{-1}) at 95 °C in toluene with four times the stoichiometric concentration of water. (top: initial reaction mixture; bottom: reaction mixture after 2 h.)

Increasing the concentration of water over the stoichiometric amount increased conversion of methoxysilyl groups to silanols with elimination of methanol. Methoxysilyl conversion was 95 % with four times stoichiometric concentration of water. Varying the reaction temperatures in this range did not affect conversion but did increase reaction rates (table 5.1). Spinu et. al. has reported similar results (95% hydrolysis of methoxysilyl groups with a TMOS:H_2O ratio of 1:4). [38]

Table 5.1 Conversion of trimethoxysilane groups as a function of water concentration and temperature.

[trimethoxysilane]		water		Temperature (°C)	% Hydrolysis of methoxysilane groups
(g mL^{-1})	mol	(g mL^{-1})	mol		
0.05	0.008	0.007	0.008	95	50
0.05	0.008	0.007	0.008	110	60
0.05	0.008	0.014	0.016	95	90

A study of the hydrolysis and condensation of trimethoxysilyl groups pendent on the polymer backbone was also performed (figure 5.3). It is important to understand these reactions as they are key reactions for the stabilization and oxidative prevention of cobalt nanoparticles.

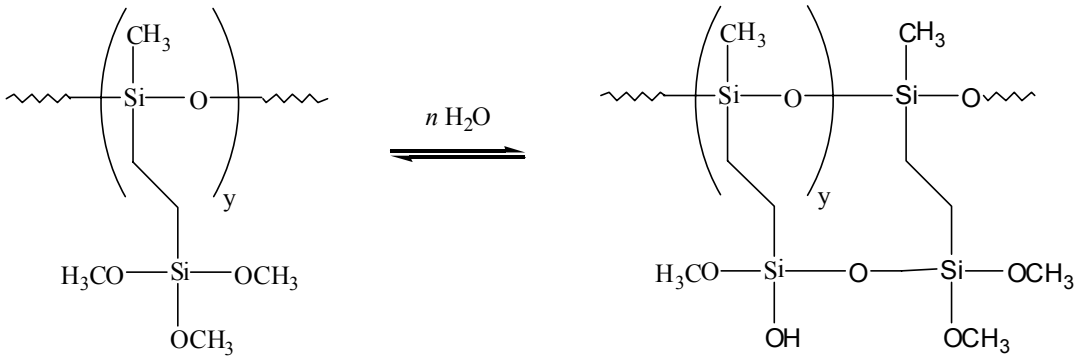

Figure 5.3 Hydrolysis and condensation of a PDMS-*b*-[PMVS-*co*-PMTMS] copolymer with varying concentrations of water.

Hydrolyses of trimethoxysilyl pendent groups on the polymer backbones were investigated under similar conditions utilized for the model studies (table 5.2). The study included copolymers wherein the extent of functionalization of the PMVS block was

varied from 50% to 100%. The PDMS block was 10,000 or 4000 g mol^{-1} and the [PMVS-*co*-PMTMS] block was prepared from a 2000 g mol^{-1} PMVS with varying degrees of functionalization.

The reactions were conducted for 2 hours in toluene and hydrolyses of the methoxy groups were monitored by ^{1}H NMR. The methyl resonance corresponding to the trimethoxysilyl group at 3.72 ppm decreased with the concurrent increase of methyl protons of methanol at 3.68 ppm (figure 5.4). Increasing the degree of functionalization from 50% to 100% increased the conversion regardless of molecular weight. As with the model studies, variations of temperature in this range affected the reaction rates but did not significantly alter conversion (table 5.2). With a quantitatively functionalized copolymer and four times the stoichiometric concentration of water, 75% hydrolysis of methoxysilyl groups was achieved within the two hour period. This was consistent with the results derived from the model studies.

Table 5.2 Results for the hydrolysis and condensation reactions of pendent trimethoxysilyl groups as a function of water concentration and temperature.

M_n PDMS-*b*-[PMVS-*co*-PMTMS] (g mol^{-1})	Functionalization (%)	polymer		[water]		T (°C)	% Hydrolysis
		(g mL^{-1})	mol	(g mL^{-1})	mol		
4000 – 3400	50	0.05	0.0016	0.0026	0.0024	85	0
4000 – 5800	100	0.05	0.0016	0.005	0.0048	110	16
10,000 – 3400	50	0.05	0.0009	0.0013	0.0014	95	0
10,000 -5800	100	0.05	0.0015	0.0026	0.0023	110	16
10,000 – 5800	100	0.05	0.0015	0.005	0.0045	95	25
10,000 – 5800	100	0.05	0.0015	0.005	0.0045	110	25
10,000 – 5800	100	0.07	0.0015	0.014	0.0090	95	75

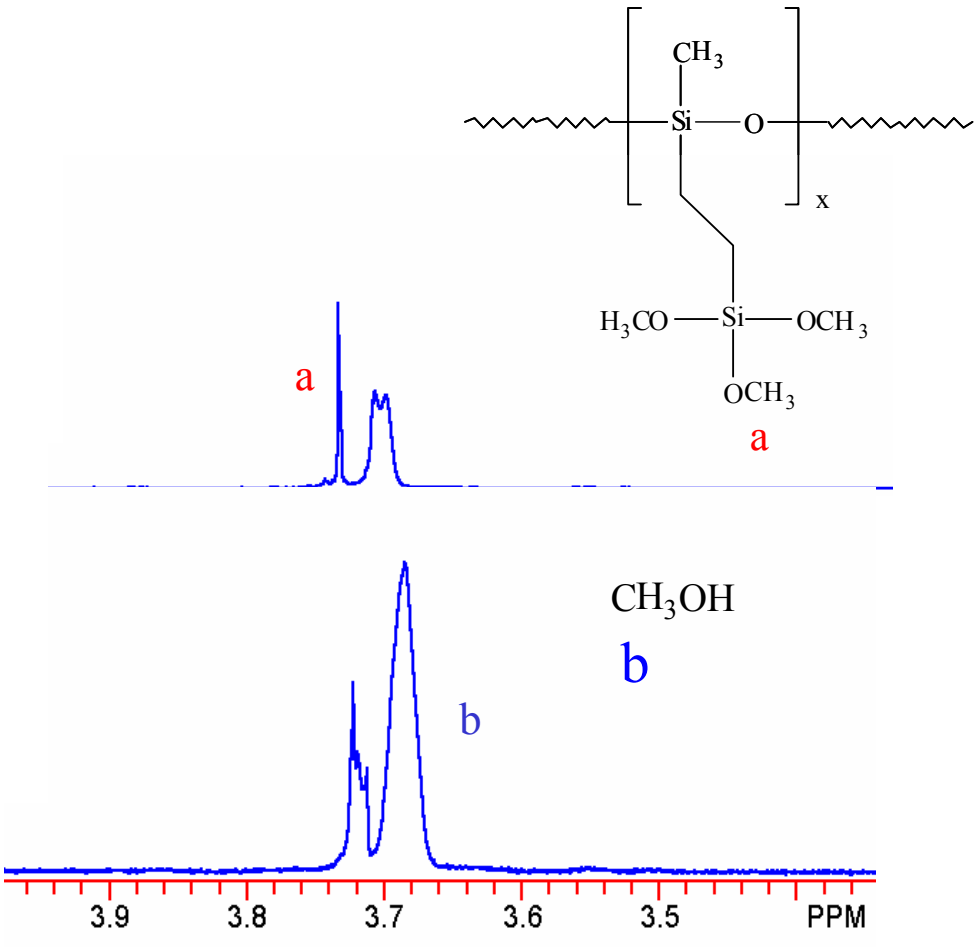

Figure 5.4 ^{1}H NMR of the hydrolysis and condensation of trimethoxysilyl groups pendent on the polysiloxane backbone. Four times the stoichiometric concentration of water was used.

5.4.2 Hydrolysis and condensation of poly(dimethylsiloxane)-*b*-[poly(methylvinylsiloxane)-*co*-poly(methyl-(2-triethoxysilethyl)siloxane] (PDMS-*b*-[PMVS-*co*-PMTES])

The reactivities of triethoxysilyl groups are lower than the previously described trimethoxysilyl substituents, and thus, the sol-gel conditions that were investigated included acidic catalysts (acetic or dichloroacetic acid). Acetic acid is a moderate acid with a pK_a of approximately 4.7. This acid is biocompatible which offers potential in biomedical applications. Acetic acid is readily found in the human body in controlled

amounts. [156] It is involved both in the biosynthesis of fatty acids and of acetyl coenzyme A, an important biomolecule in the Kreb's Cycle (figure 5.5). This cycle is the main pathway for adenosine triphosphate (ATP) production in the body.

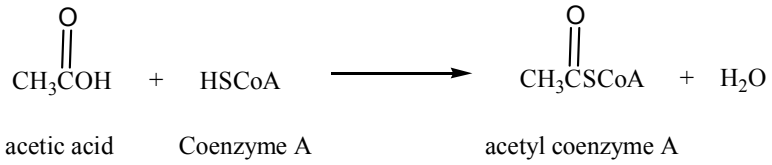

Figure 5.5 Biosynthesis of acetyl CoA

The hydrolysis is initiated by protonation of the oxygen of the triethoxysilyl group with the acidic proton of the acid (figure 5.6). [116] This creates a good leaving group on the siloxane (i.e., ethanol). Water functions as a nucleophile and attacks the electropositive silicon in an S_N2 type mechanism. Ethanol is released as a by-product and a protonated silanol forms. The conjugate base from the first step (acetate anion) removes the proton from the protonated silanol species resulting in a silanol.

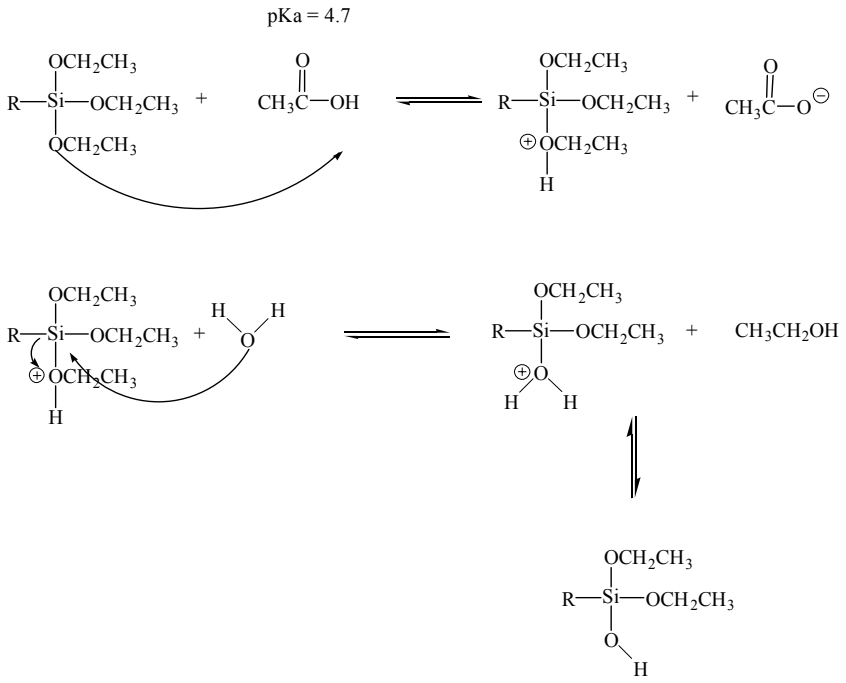

Figure 5.6 Hydrolysis mechanism of triethoxysilyl functional groups pendent on the siloxane backbone.

Hydrolysis is followed by condensation of the resultant silanols. It is believed that this is initiated by attack of a silanol on another silanol or a protonated ethoxysilane (figure 5.7). A silanol may function as a nucleophile and attack a silicon with the elimination of ethanol to form a siloxane dimer.

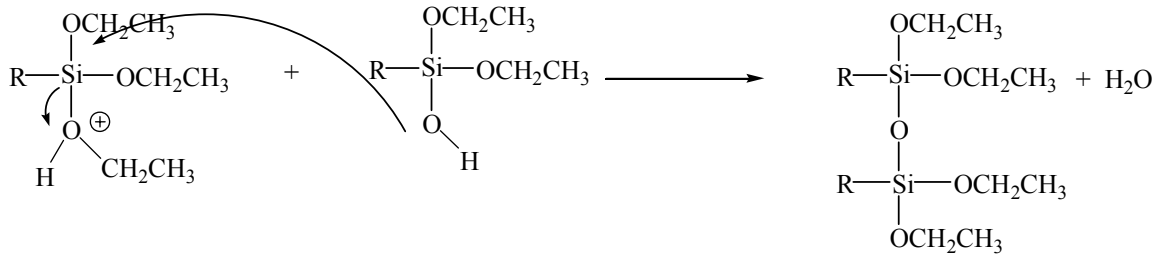

Figure 5.7 Condensation of pendent triethoxysilyl groups on the siloxane backbone.

A series of reactions were conducted with triethoxysilyl functionalized copolymers, acid, and stoichiometric concentrations of water at room temperature. The reactions were monitored over 5 days and it was found that the conversion of ethoxysilyl groups plateaued after about 3 days. The PDMS block was 5000, 10,000, or 16,000 g mol^{-1} and the [PMVS-*co*-PMTES] block was prepared from a 2000 g mol^{-1} PMVS wherein 50% of the units were functionalized (table 5.3). Proton NMR was utilized to monitor the disappearance of the ethoxysilyl methylene resonance (peak b, figure 5.8). No hydrolysis was observed for reactions conducted with acetic acid even after 5 days.

These results suggested that these functionalized copolymers required a stronger catalyst to hydrolyze triethoxysilyl groups. Thus, the use of dichloroacetic acid (pK_a 2.5) was investigated (table 5.3). Up to approximately 60% conversion was achieved after 3 days with dichloroacetic acid. As expected higher conversions were achieved with higher concentrations of polymer in toluene.

Table 5.3 Hydrolysis and condensation reactions with PMTES blocks with acid.

M_n PDMS (g mol^{-1})	M_n (PMVS-*co*-PMTES) (g mol^{-1})	Acid	Concentration (polymer : toluene) (mL^{-1})	% Hydrolysis of ethoxysilyl groups
5000	3900	Acetic acid	0.05	0
5000	3900		0.05	0
5000	3900		0.05	0
10,000	3900		0.05	0
10,000	3900		0.05	0
10,000	3900		0.05	0
16,000	3900		0.05	0
16,000	3900		0.05	0
16,000	3900		0.05	0
5000	3900	Dichloroacetic acid	0.06	55
5,000	3900		0.03	45
5,000	3900		0.015	50
16,000	3900		0.06	62
16,000	3900		0.03	30
16,000	3900		0.015	30

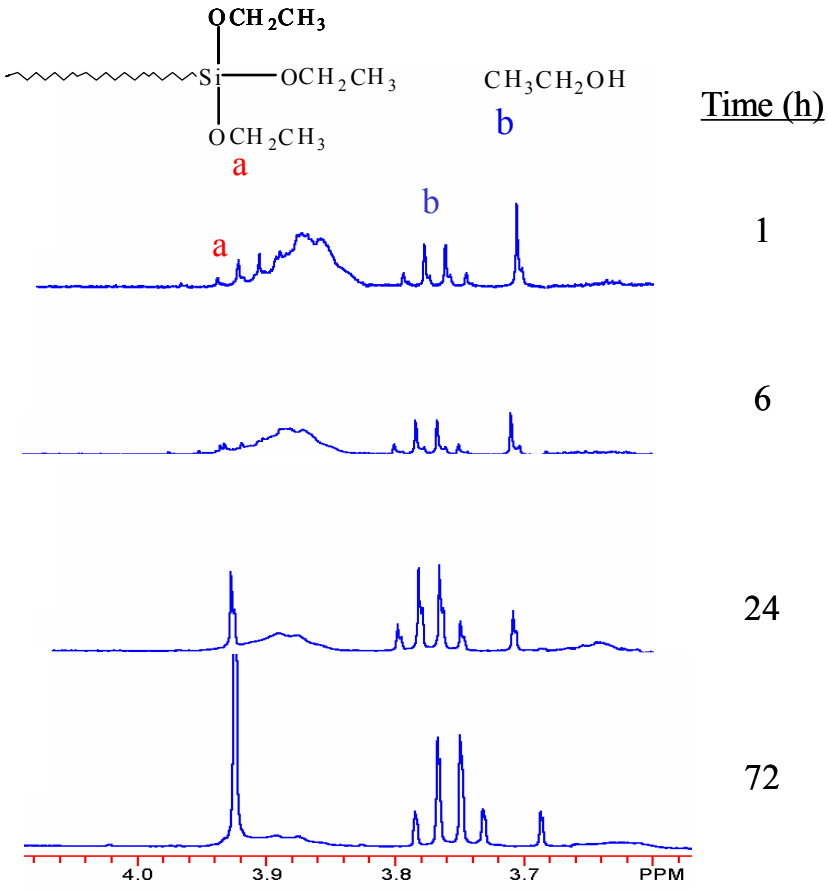

Figure 5.8 Hydrolysis of triethoxysilyl groups on PDMS-*b*-[PMVS-*co*-PMTES] (0.06 g mL^{-1}) at room temperature with dichloroacetic acid and stoichiometric concentrations of water.

The polymer/toluene/water mixtures utilized in the sol-gel investigations were hazy, suggesting inhomogeneity. Thus, a 90% toluene/10% methanol solvent was investigated with PDMS-*b*-[PMVS-*co*-PMTES], acetic acid, and a stoichiometric concentration of water at room temperature. The solutions were clear, but no conversion was achieved.

CHAPTER 6. Synthesis and characterization of polysiloxane-cobalt complexes

6.1 Synopsis

This chapter focuses on the synthesis and characterization of cobalt nanoparticle-polysiloxane complexes dispersed in toluene. These fluids were synthesized by thermolyzing dicobalt octacarbonyl in the presence of PDMS-*b*-[PVMS-*co*-PMTMS] or PDMS-*b*-[PVMS-*co*-PMTES] copolymers (figure 6.1). Thermolysis reactions in the presence of select copolymer compositions produced stable dispersions of cobalt nanoparticles with significant saturation magnetization. FTIR was used to monitor the reactions of dicobalt octacarbonyl to form the cobalt nanoparticles encased in the block copolymers. The dispersions and cobalt-polymer complexes were analyzed via TEM, vibrating sample magnetometry, and elemental analysis.

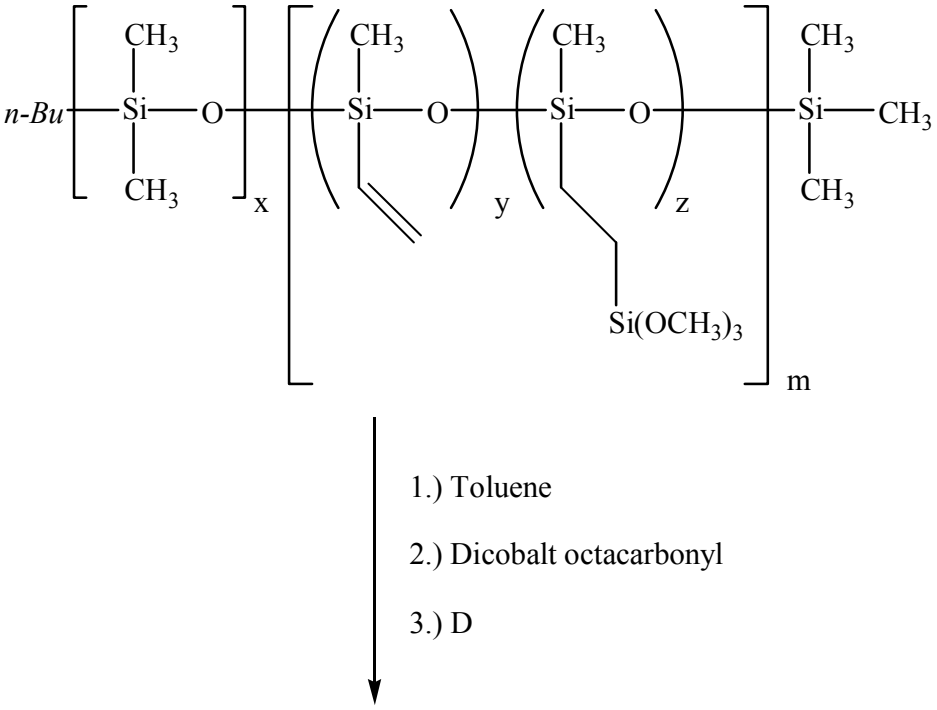

Figure 6.1 Thermolysis of dicobalt octacarbonyl in toluene in the presence of PDMS-*b*-[PMVS-*co*-PMTMS] or PDMS-*b*-[PMVS-*co*-PMTES] diblock copolymers.

6.2 Experimental

Toluene (Aldrich, 99.8%, FW 92.14 g mol^{-1}, mp -93 °C, bp 110.6 °C, d 0.865 g mL^{-1}) was washed twice with concentrated sulfuric acid and neutralized with water. It was dried over $MgSO_4$ for one hour, then over calcium hydride overnight and distilled just before use. $Co_2(CO)_8$ with 1-5% hexane (Alpha Easar) was stored under argon in the freezer without further purification. This compound is a bright orange solid at room temperature.

6.2.1 Synthesis of a cobalt nanoparticle fluid in the presence of a PDMS-*b*-[PMVS-*co*-PMTES] diblock copolymer.

An exemplary reaction is described utilizing a 5300 g mol^{-1}-PDMS-*b*- 3900 g mol^{-1} [PMVS-*co*-PMTES] copolymer. The [PMVS-*co*-PMTES] block had 50% of the repeat units hydrosilated with triethoxysilane. Dispersions with other copolymers were prepared in an analogous manner. A 500-mL, three-neck, round bottom flask equipped with a condenser, mechanical stirrer with a vacuum ready adapter, and argon purge was flame dried under argon. The apparatus was placed in a temperature controlled silicone oil bath over a hot plate (in the absence of a magnetic stirrer). The PDMS-*b*-[PMVS-*co*-PMTES] copolymer (1.0 g, 0.0013 eq triethoxysilethyl groups) in 10 mL toluene was transferred to the reaction vessel via cannula. An additional 10 mL of toluene was added via syringe to the reaction flask. The reaction mixture was stirred at 45 °C (the temperature of the thermocouple in the oil bath) for approximately 15 minutes. Dicobalt octacarbonyl (1.0 g, ≈ 0.0035 mol) was weighed into the reaction vessel and dissolved

under argon. A greenish-brown gas filled the flask immediately upon adding the dicobalt octacarbonyl. The reaction temperature was raised to approximately 110 °C (toluene reflux) and maintained at that temperature until complete reaction of the dicobalt octacarbonyl was determined via FT-IR. After cooling, a stable magnetic dispersion of cobalt particles resulted.

6.2.2 Synthesis of a cobalt nanoparticle fluid stabilized with a diblock PDMS-*b*-PMTES copolymer.

An exemplary reaction is described utilizing a diblock PDMS-*b* –PMTES copolymer having a 5000 g mol^{-1} PDMS block connected to a 5800 g mol^{-1} PMTES block. Dispersions with other copolymers were prepared in an analogous manner. A 500-mL, three-neck, round bottom flask equipped with a condenser, mechanical stirrer with a vacuum ready adapter, and argon purge was flame dried under argon. The aforementioned procedure was followed exactly. After cooling, an unstable dispersion of cobalt particles resulted.

6.2.3 Synthesis of a cobalt fluid stabilized with a diblock PDMS-*b*-[PMVS-*co*-PMTMS] copolymer.

An exemplary reaction is described utilizing a diblock PDMS-*b*-[PMVS-*co*-PMTMS] copolymer having a 5000 g mol^{-1} PDMS block connected to a random, 3400 g mol^{-1} [PMVS-*co*-PMTMS]. The [PMVS-*co*-PMTES] block had 50% of the repeat units hydrosilated with trimethoxysilane. A 500-mL, three-neck, round bottom flask equipped with a condenser, mechanical stirrer with a vacuum ready adapter, and argon purge was

flame dried under argon. The apparatus was placed in a temperature controlled silicone oil bath over a hot plate (in the absence of a magnetic stirrer). The procedure follows that described above in 6.2.1. The decomposition of dicobalt octacarbonyl was monitored by FTIR. After cooling, a magnetic dispersion of cobalt particles sterically stabilized with the functionalized diblock copolymer resulted.

6.2.4 Synthesis of a cobalt fluid stabilized with a diblock PDMS-*b*-PMTMS copolymer.

An exemplary reaction is described utilizing a diblock PDMS-*b*-PMTMS copolymer having a 5000 g mol^{-1} PDMS and 4800 g mol^{-1}PMTMS block. A 500-mL, three-neck, round bottom flask equipped with a condenser, mechanical stirrer with a vacuum ready adapter, and argon purge was flame dried under argon. The apparatus was placed in a temperature controlled silicone oil bath over a hot plate (in the absence of a magnetic stirrer). The procedure follows that described above in 6.2.1. The decomposition of dicobalt octacarbonyl was monitored by FTIR. After cooling, an unstable magnetic dispersion of cobalt particles resulted.

6.2.5 Characterization of Magnetic Fluids

FTIR spectra were obtained using a Nicolet Impact 400 FTIR spectrometer with two drops of the samples run neat between salt plates. Transmission electron micrographs were acquired using a Philips 420T TEM run at 100kV. TEM samples containing cobalt stabilized with copolymers were prepared by diluting toluene dispersions with additional toluene until they had the appearance of “weak tea”. A drop was syringed onto a carbon

coated copper grid and the toluene was evaporated. A Standard 7300 Series Lakeshore Vibrating Sample Magnetometer (VSM) was used to determine the magnetic properties of the cobalt samples including saturation magnetization and any hysteresis. The magnetic moment of each dried sample was measured over a range of applied fields from -8000 to +8000 Oe with a sensitivity of 0.1 emu. Elemental analysis for cobalt was performed by Desert Analytics Laboratory (Tucson, AZ) by treating the samples with hot concentrated nitric acid followed by concentrated perchloric acid until complete dissolution was achieved. These solutions were analyzed by inductively coupled plasma to determine cobalt. Cobalt was calculated from sample response relative to standards and blanks.

6.3 Results and Discussion

6.3.1 Synthesis of cobalt magnetic fluids in the presence of trialkoxysilyl functionalized polysiloxane diblock copolymers

Thermolyses of dicobalt octacarbonyl in the presence of block copolysiloxanes have been investigated in our laboratories for several years[1,2]. These reactions utilized poly(dimethylsiloxane-*b*-cyanopropylmethylsiloxane-*b*-dimethylsiloxane) (PDMS-*b*-PCPMS-*b*-PDMS) triblock copolymers in toluene, D_4, or PDMS solvents to generate cobalt nanoparticles in-situ. The central block containing the nitrile unit was only sparingly soluble in the solvents employed, whereas the PDMS endblocks were soluble. These solutions were micellar in nature with the PCPMS forming the micelle cores and the PDMS endblocks protruding into the solvents. It was reasoned that the lone pair of electrons of the nitrogen complexed with the cobalt to form a so-called anchor block, and

the PDMS tails provided steric stabilization of these nanoparticle dispersions. These cobalt dispersions had specific saturation magnetizations of 90-110 emu g^{-1} of cobalt and TEM micrographs showed well-dispersed cobalt nanoparticles[1,2]. The oxidative durability of the cobalt nanoparticles was poor, however, and their magnetization decreased slowly with time[1,40].

Cobalt carbonyl reactions in the presence of a series of pentablock copolymers (figure 6.2), were also investigated as steric dispersion stabilizers for cobalt nanoparticles.[40] The motivation for this approach was to protect the cobalt surfaces with "silica-like" shells formed around the nanoparticles by hydrolyzing and condensing trialkoxysilyl pendent groups. Thermolyses of dicobalt octacarbonyl in solutions of the pentablock copolymers also resulted in stable dispersions of ≈10 nm cobalt with specific magnetizations of 90-110 emu g^{-1} Co. The pendent triethoxysilyl groups were hydrolyzed with dibutyltin diacetate (catalyst) and stoichiometric concentrations of water at room temperature. Unfortunately, this method required high concentrations of the tin catalyst to achieve quantitative hydrolysis, and preliminary cell survival studies suggested that the resultant complexes had some toxicity.[4]

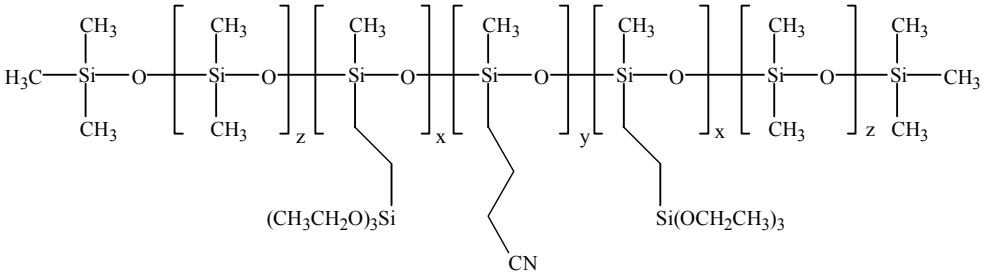

Figure 6.2 Pentablock copolymers were investigated as steric dispersion stabilizers for cobalt nanoparticles. The nitrile containing central block functioned as the anchor block to bind to cobalt; PDMS tail blocks provided dispersion stability; PMTES blocks were precursors for sol-gel reactions to form "silica-like" shells around the nanoparticles.[157,158]

This thesis describes the synthesis and characterization of well-defined diblock copolymers wherein the PMTES or PMTMS blocks complexed with cobalt nanoparticles and the PDMS blocks protruded into the toluene solvent. PDMS-*b*-[PMVS-*co*-PMTES] or PDMS-*b*-[PMVS-*co*-PMTMS] copolymers were investigated as steric dispersion stabilizers.

Dicobalt octacarbonyl and the copolymer were dissolved in toluene and the reaction mixtures were heated to toluene reflux to displace the carbon monoxide and form cobalt nanoparticles. The reactions were monitored by FTIR by observing changes in structure and the decrease of carbonyl peaks. The carbon monoxide region around 2000 cm^{-1} initially showed three absorbance bands at 2020, 2050, and 2070 cm^{-1} attributed to terminal CO, and a peak at 1860 cm^{-1} due to the bridging carbonyls (figure 6.3). [1,159] Two new peaks at 2055 and 2065 cm^{-1} appeared in the IR spectra as the reactions proceeded (figure 6.3). These peaks were attributed to a $Co_4(CO)_{12}$ intermediate based on previous assignments.[159] The reactions were continued at approximately 110 °C until the complete disappearance of the carbonyl peaks (figure 6.3).

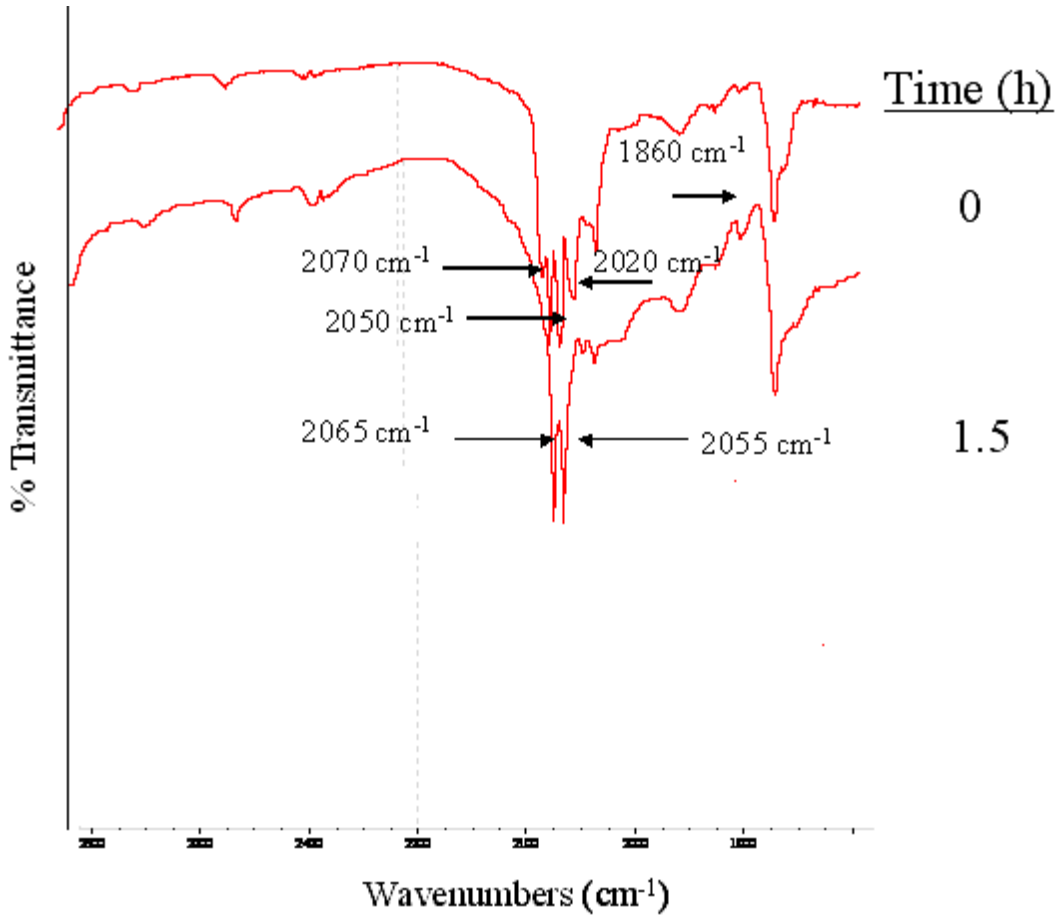

Figure 6.3 Thermolysis of dicobalt octacarbonyl: a.) initial reaction mixture showing peaks 2020, 2050, and 2070 cm^{-1} corresponding to terminal CO and 1860 cm^{-1} attributed to bridging CO; b.) a spectrum respresenting the intermediate reaction stage showing new peaks at 2065 and 2055 cm^{-1} corresponding to $Co_4(CO)_{12}$.

Dispersions prepared with PDMS-*b*-[PMVS-*co*-PMTES] or PDMS-*b*-[PMVS-*co*-PMTMS] copolymers (wherein half the repeat units in the anchor blocks were functionalized) were dark homogeneous fluids without any visible precipitates. However, cobalt dispersions prepared with PDMS-*b*-PMTES or PDMS-*b*-PMTMS copolymers (wherein the anchor block was fully functionalized) exhibited some precipitate that was attributed to larger cobalt particle sizes and aggregates.

Dispersions were prepared for microscopy by casting dilute suspensions of cobalt-copolymer complexes from toluene onto carbon-coated copper grids. TEM micrographs of the cobalt-polymer complexes prepared with PDMS-*b*-[PMVS-*co*-PMTES] or PDMS-*b*-[PMVS-*co*-PMTMS] showed dark, ≈10-15-nm diameter cobalt particles (figure 6.4). Copolymer block lengths of 16,000 g mol^{-1} PDMS-*b*-3900 g mol^{-1} [PMVS-*co*-PMTES], 16,000 g mol^{-1} PDMS-*b*-3400 g mol^{-1} [PMVS-*co*-PMTMS] and 5000 g mol^{-1} PDMS-*b*-3400 g mol^{-1} [PMVS-*co*-PMTMS] were investigated in these reactions. However, TEM micrographs showed no discernible differences in particle sizes. The copolymer sheaths surrounding each particle were visible but it was not possible to determine their thickness due to contrast issues associated with the technique. Further investigations of these in-situ syntheses will be conducted to ascertain whether particle sizes can be correlated with block lengths and micelle sizes in the reaction solutions.

It was reasoned that the polymer coating sterically stabilized the cobalt dispersions. The compositions of these cobalt-copolymer complexes were determined by elemental analysis (table 6.1). The charged ratios of cobalt-copolymer were 0.25 in the first four entries in table 6.1 and 0.15 for the last entry. If one assumes all of the copolymers were recovered, the cobalt yields were 60-70%. It is not yet clear whether one can correlate the cobalt surface areas to number of anchor sites on the copolymer stabilizers. Thus, developing an understanding of the parameters that control the cobalt to polymer ratios in these complexes will also require further research.

1.)

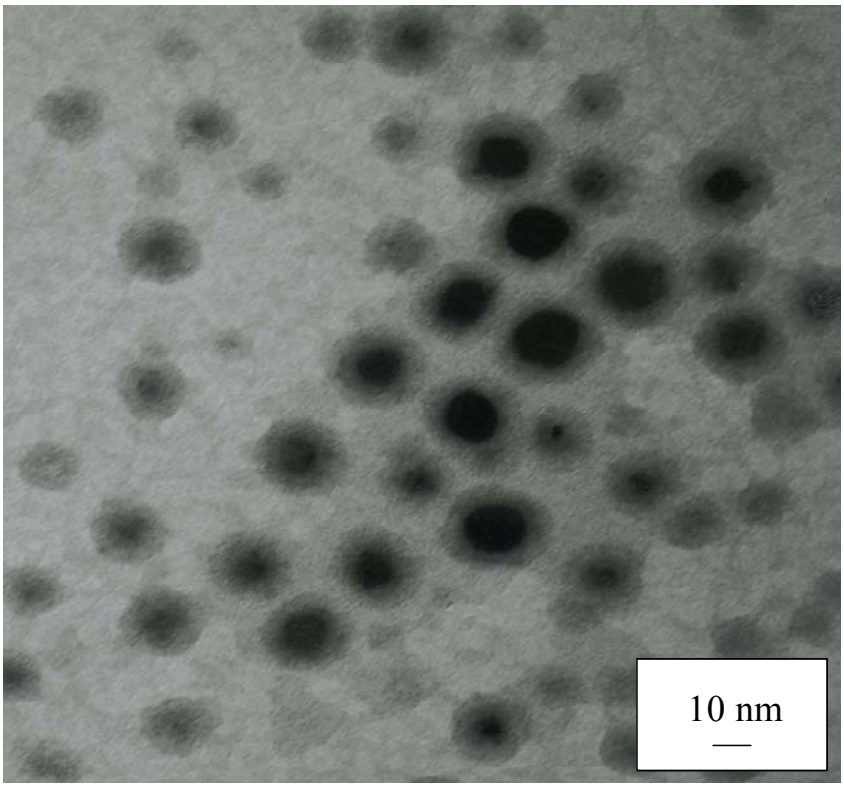

2.)

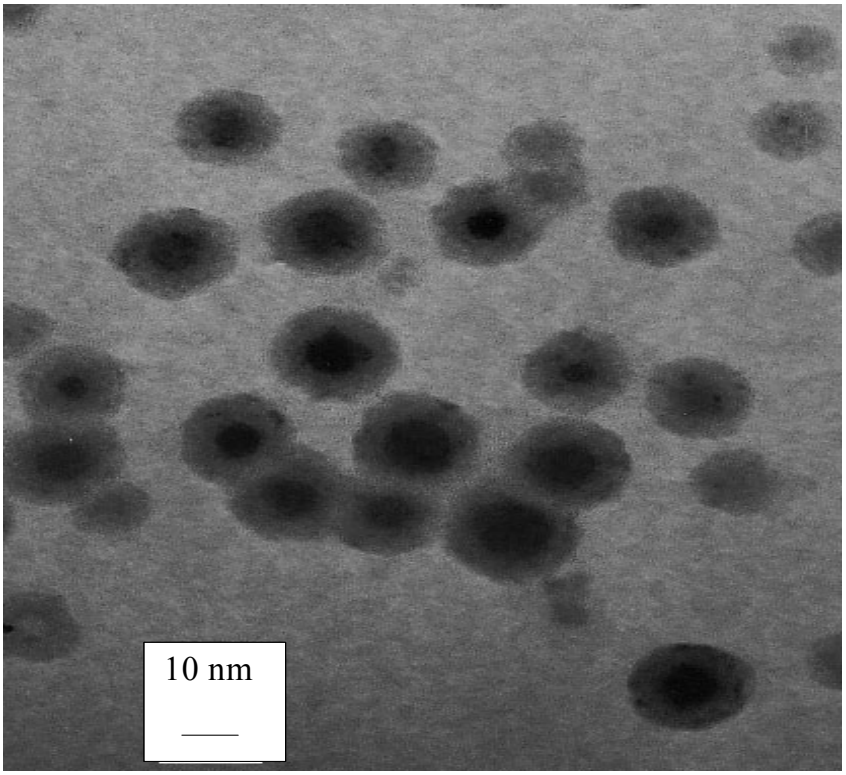

3.)

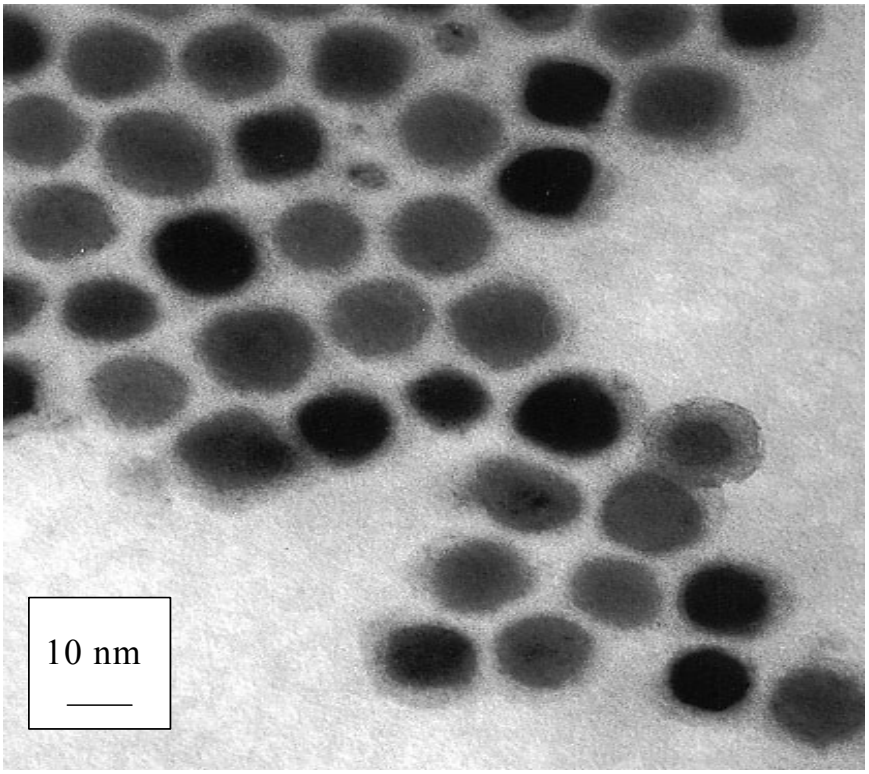

Figure 6.4 Cobalt fluids comprised of 1.) 16,000 g mol^{-1} PDMS-*b*-3400 g mol^{-1} [PMVS-*co*-PMTMS], 2.) 5000 g mol^{-1} PDMS-*b*-3400 g mol^{-1} [PMVS-*co*-PMTMS] 2.) 16,000 g mol^{-1} PDMS-*b*-3900 g mol^{-1} [PMVS-*co*-PMTES]

Specific magnetizations of dispersions prepared with PDMS-*b*-[PMVS-*co*-PMTES] or PDMS-*b*-[PMVS-*co*-PMTMS] copolymers ranged from 90-110 emu g^{-1} Co (table 6.1). Previously reported values for PDMS-cobalt complexes were in the range of 97-116 emu g^{-1} Co. [1,2] Exemplary magnetization curves of cobalt-polymer complexes prepared with a 5000 g mol^{-1} PDMS-*b*-3900 g mol^{-1} [PMVS-*co*-PMTES] and a 16,000 g mol^{-1} PDMS-*b*-3400 g mol^{-1} [PMVS-*co*-PMTMS] copolymers are provided in figure 6.5. These copolymer-cobalt dispersions displayed some magnetic hysteresis. Pileni et. al. has reported hysteresis for cobalt particles organized in a two dimensional lattice on a graphite substrate with mean particle diameters of approximately 6-8 nm. [160]

Table 6.1 Specific magnetizations of the cobalt-polymer complexes

M_n (g mol^{-1})	Wt. % Co	Specific Saturation Magnetizations*	
		emu g^{-1} sample	emu g^{-1} Co
PDMS-*b*-[PMVS-*co*-PMTES]			
16,000 – 3900	16	14	87
5000 – 6800	16	15	90
PDMS-*b*-[PMVS-*co*-PMTMS]			
16,000 – 3400	17	18	109
16,000 – 3,400	16	16	104
5000 – 3400	7	8	115

* These were the saturated values taken at +8000 Oe.

1.)

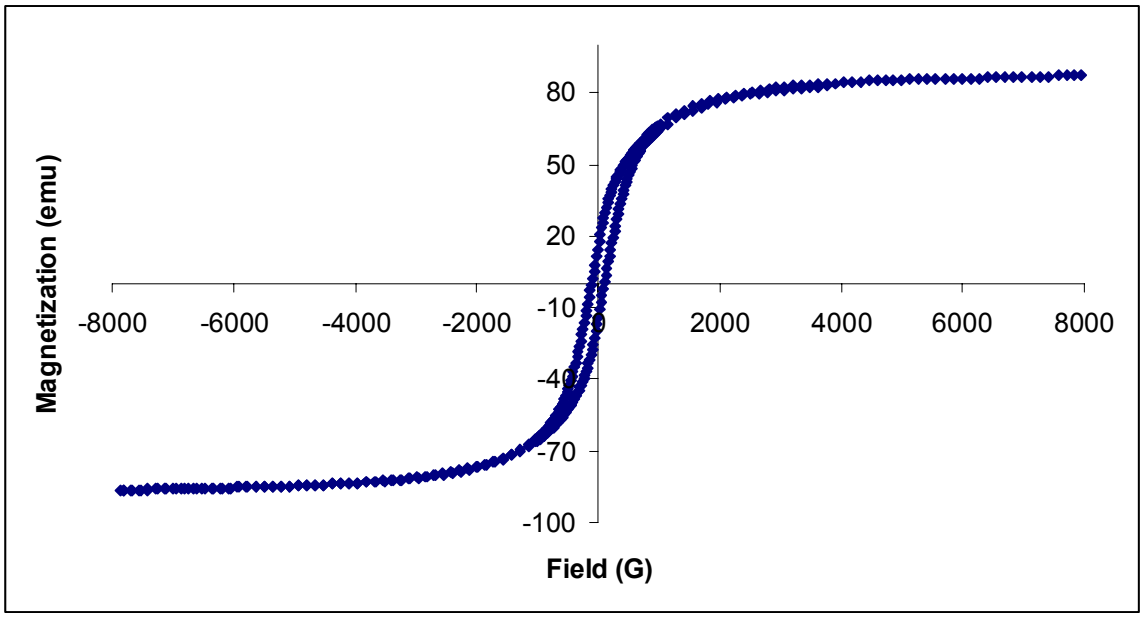

2.)

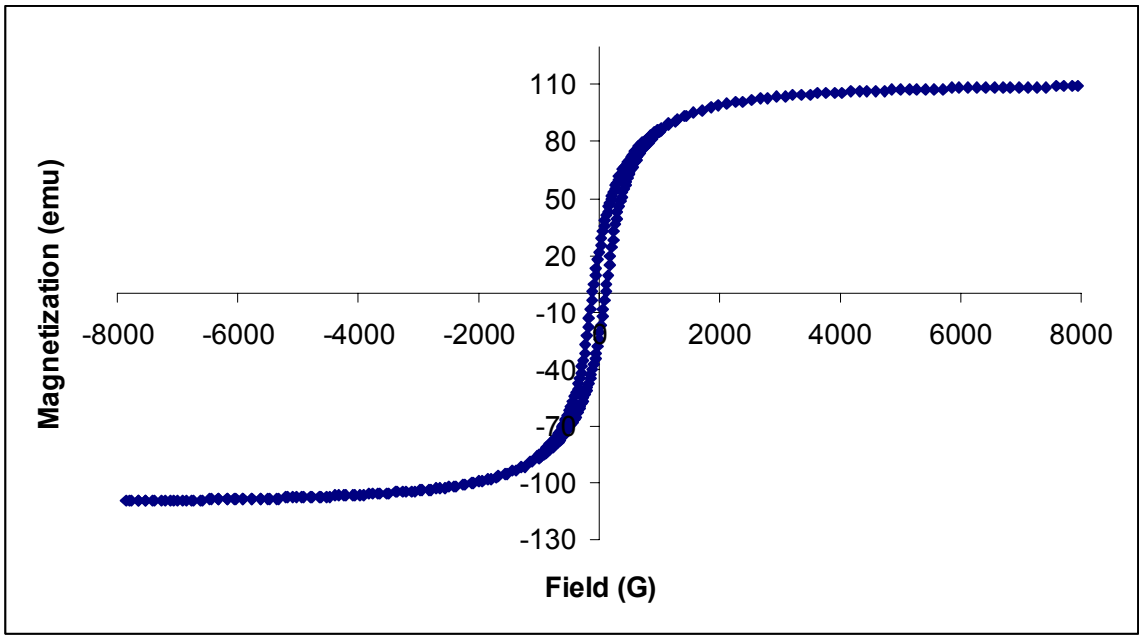

Figure 6.5 Specific magnetization curves for cobalt-polymer complexes prepared with 1.) 5000 g mol^{-1} PDMS-*b*-3900 g mol^{-1} PMVS-*co*-PMTES], and 2.) 16,000 g mol^{-1} PDMS-*b*-3400 g mol^{-1} [PMVS-*co*-PMTES]

CHAPTER 7 Conclusions and Recommendations for Further Investigations

Well-defined poly(dimethylsiloxane-*b*-methylvinylsiloxane) diblock copolymers can be prepared with controlled molecular weights and narrow molecular weight distributions. This suggested that the polymerizations of both monomers were living. Thermal analysis indicated that these materials do not phase separate in the bulk.

The PMVS block can be either partially or fully functionalized with triethoxysilethyl and trimethoxysilethyl pendent moieties using hydrosilations. Thermal characterization suggested that the blocks in the derivatized copolymers were also miscible. Surface tension measurements of block copolymer solutions in toluene suggested that aggregates of these materials were present. Small angle X-ray scattering and dynamic light scattering measurements are recommended to further probe the solution structures. This may be important since it is reasoned that the micelle sizes and shapes may relate to the cobalt particle sizes when cobalt nanoparticles are formed in these solutions.

Hydrolyses of trimethoxysilethyl pendent groups on fully functionalized PDMS-*b*-PMTMS copolymers proceeded to high conversions with four times the stoichiometric concentrations of water and no added catalyst. These mild conditions may be important for condensing "silica-like" shells around the cobalt without chemically damaging the copolymer backbone.

Solutions of the partially hydrosilated PDMS-*b*-[PMVS-*co*-PMTMS] or PDMS-*b*-[PMVS-*co*-PMTES] copolymers can be used to form sterically stabilized cobalt nanoparticle dispersions without any observed aggregation. Cobalt yields in the dispersed complexes were approximately 60-70 wt % of the amount charged.

Considerable additional work will be required to understand the parameters that control the cobalt to copolymer ratio in these complexes. It is desirable to maximize the concentration of cobalt to obtain polymer-cobalt particles with enhanced magnetic responses. To date, formation of cobalt in solutions of the fully functionalized analogues of these polymers has resulted in some aggregation. This may be attributable to having too many functional units on the anchor blocks.

The cobalt nanoparticles prepared in this research were approximately 10-15 nm in diameter as determined by TEM. Further TEM analyses are recommended to quantify the size distributions. Also, scattering measurements (SANS) may provide insight into the sizes and size distributions of the complexes in the dispersions.

Specific saturation magnetization of the cobalt-copolymer complexes ranged from 90-115 emu g^{-1} Co, comparable to previously reported values. The deviation from the bulk cobalt value of 162 emu g^{-1} was at least partially attributed to some surface oxidation. It will be important to determine whether the sol-gel reactions can protect the cobalt surface against oxidation, particularly without damaging the cobalt during the actual sol-gel reaction. Oxidative stabilities of these cobalt-copolymer complexes whereby the "silica-like" shells have been formed will be investigated as functions of copolymer structures, sol-gel conditions, and cobalt-copolymer complex compositions.

Bibliography

(1) Rutnakornpituk M; Thompson MS; Harris LA; Farmer KE; Esker AR; Riffle JS; Connolly J; St. Pierre TG; P*olymer* 2002, *43*, 2337-2348.

(2) Stevenson JP; Rutnakornpituk M; Vadala M; Esker AR; Riffle JS; Charles SW; Wells S; Dailey JP; *J. Mag. Mag. Mater.* 2001, *225*, 47-58.

(3) Chojnowski J; Cypryk M; Fortuniak W; Rozga-Wijas K; Scibiorek M; *Polymer* 2002.

(4) Hafeli U.; Private Communication, 2002.

(5) Mazumder B; *Silicon and its Compounds*; Science Publishers, Inc.: Enfield, NH, 2000.

(6) Noll W.; *Chemistry and Technology of Silicones*; Academic press Inc.: New York, 1968.

(7) Bruins PF.; *Silicone Technology*; Interscience Publisher: New York, 1970.

(8) Rochow EQ; *Silicon and Silicones*; Springer-Verlag: Germany, 1987.

(9) LiebauF.; *Stuctural Chemistry of Silicates : Structure, Bonding, Classification*; Springer-Verlag: Berlin, Heidelberg, NY, Tokyo, 1985.

(10) Newman E.; *Separated Isotope : Vital Tool for Science and Medicine*; National Academy Press: Washington, D.C, 1982.

(11) Sommer LH.; *Stereochemistry, Mechanism, and Silicon*; Pergamon Press: New York, 1962.

(12) Eaborn C.; *Organosilicon compounds*; Buttersworth Scientific Publication: London, 1962.

(13) Barrett C; Massalski TB.; *Structure of Metals, Crystallographic Methods, Principles and Data*; 3 ed.; Pergamon Press: Oxford, 1980.

(14) Cottrell T.; *The Strength of the Chemical Bonds*; 2nd ed.; Butterworths: London, 1958.

(15) Flory PJ; Crescenzi V; Mark JE *J Am Chem. Soc.* 1964, *86*, 146.

(16) Rochow EQ.; *An Introduction to the Chemistry of Silicones*; Wiley and Sons, Inc.: New York, 1962.

(17) Chen X; Gardella JR.; *Macromolecules* 1994, *27*, 12.

(18) Roe RJ.; *J. Phys. Chem.* 1968, *72*, 2013.

(19) Myshlyaeva LV; Krasnoshchekov; *Analytical Chemistry of Silicon*; Wiley and Sons, Inc.: New York, 1974.

(20) Brook MA.; *Silicon in Organic, Organometallic, and Polymer Chemistry*; John Wiley and Sons, Inc: New York, 2000.

(21) Kipping; Lloyd LL.; *J. Chem. Soc.* 1901, *91*, 209.

(22) Hyde and DeLong.; *J Am Chem. Soc.* 1941, *63*, 1194.

(23) Frisch KC.; *Cyclic Monomers*; Wiley and Sons, Inc.: NY, London, Sydney, 1972.

(24) Sommer LH.; *J Am Chem. Soc.* 1954, *76*, 1030.

(25) Patnode WI; Wilcock DF *J Am Chem. Soc.* 1946, *68*, 362.

(26) Sokolov NN; Akimova SM *J. Gen. Chem (USSR)* 1956, *26*, 2276.

(27) Dobay DG.; U.S. Patent 2,769,829; 1956.

(28) Prescott PI; Selon TG.; US Patent 3,317,578,*General Electric Company*: USA, 1967.

(29) Grassie N; Francey KF, M.; MacFarlane IG.; *Polym. Degrad. and Stab.* 1993, *3*, 67.

(30) Takiguchi T; Sakurai M; Kishi T; *J. Org. Chem* 1960, *25*, 310.

(31) Momper B; Wagner T; Maschke U; Ballauf M; Fisher EW; *Polym. Commun.* 1990, *31*, 186.

(32) Weber WP; Cai G; *Polymer* 2001, *43*, 1753-1759.

(33) Weber WP; Cai G; *Macromolecules* 2000, *33*, 6310.

(34) Goossens JC.; French Patent 1456981, 1964.

(35) Nagasawa K; Yoneta A; Umezawa T; Ito K.; *Heterocycles* 1987, *26*, 2607-2609.

(36) Scott DW; *J Am Chem. Soc.* 1946, *68*, 2294.

(37) Chojnowski J; *Siloxane Polymers*; PTR Prentice Hall: Englewood Cliffs, NJ, 1993.

(38) Spinu M; McGrath JE; *J. Polym Sci. Part A* 1991, *29*, 657-670.

(39) Painter PC; Coleman M.; *Fundamentals of Polymer Science, an Introduction Text*; 2nd. ed.; Technomic Publishing: Pennsylvania, 1997.

(40) Rutnakornpituk M; Riffle JS; PhD Dissertation, *Department of Chemistry*; Virginia Polytechnic Institute and State University: Blacksburg, Virginia, 2002.

(41) Cantor SW; Grubb WT; Osthoff RC; *J Am Chem. Soc.* 1954, *76*.

(42) Brunelle DJ; *Ring-Opening Polymerization : Mechansims, Catalysis, Structure, Utility*; Hanser Publishers: Munich, Vienna, New York, Barcelona, 1993.

(43) Carmichael JB; Gordon DJ; Isackson FJ; *J. Phys. Chem.* 1967, *71*, 2011.

(44) McGrath JE; *American Chemical Society*; McGrath, J. E., Ed.: Washington, D.C., 1985; Vol. ACS Monograph 286.

(45) Sauvet G; Lebrun JJ; Sigwalt P, Stannett V.; *Cationic Polymerization and Related Processes*; Academic: NY, 1984.

(46) Sormani PM; McGrath JE; *Polym. Prepr. (Am. Chem. Soc. Div. Polym. Chem)*. 1985, *26 (1)*, 258-259.

(47) Elsbernd; Spinu M; Kilic S; McGrath JE; *Polym. Prepr. (Am. Chem. Soc. Div. Polym. Chem.)* 1986, *29 (1)*, 255-357.

(48) Yilgor I; Riffle JS; McGrath JE; *American Chemical Society*; HJ, H. F. a. S., Ed.: Washington, D.C., 1985; Vol. 282, Reactive Difunctional Siloxane Oligomers, p p. 161.

(49) McGrath JE; Riffle JS; Yilgor I; Banthia AK; Sormani P; *Org. Coat. Appl. Polym. Sci.* 1981, *46*, 693-700.

(50) Bryk MT; *Vysokomol. Soedi* 1978, *A20*, 147.

(51) Noshay; McGrath JE; *Block Copolymers : Overview and Critical Survey*; Academic Press: NY, San Francisco, London, 1977.

(52) Chojnowski J; Mazurek M; *Makromol. Chem.* 1975, *176*, 2999.

(53) Frye CL; Salinger RM; Fearon RM; *J. Org. Chem* 1970, *35*, 1308.

(54) Suzuki T; *Polymer* 1989, *30*, 333.

(55) Li C and Riffle JS; PhD Dissertation, *Department of Chemistry*; Virginia Polytechnic Institute and State University: Blacksburg, Virginia, 1996.

(56) Williard PG.; *Comprehensive Organic Synthesis*; Pergamon: New York, 1991; Vol. 1.

(57) Szwarc M.; *ACS Symposium Series 166*; McGrath, J. E., Ed.; American Chemical Society: Washington, D.C., 1981.

(58) Smid J.; *ACS Symposium Series*; JE, M., Ed.; American Chemical Society: Washington, DC, 1981.

(59) Lee CL; Frye CL; Johansson OK; *Polym. Prepr.* 1969, *10*, 1361.

(60) Holle HJ; Lehnen BR; *Eur. Polym. J.* 1975, *11*, 663.

(61) Veith CA; Cohen RE; *J. Polym Sci. Part A* 1989, *27*, 1241-1258.

(62) Zilliox JG; Roovers JEL; Bywater S, *Macromolecules* 1975, *8*, 573 - 578.

(63) Yu JM; Teyssie D; Khalifa RB; Boileau S.; *Polymer Bulletin* 1994, *32*, 35-40.

(64) Hedden RC; Cohen C.; *Polymers* 2000, *41*, 6975.

(65) Ziegler K; Bahr K.; *Chem. Ber.* 1928, *61*, 253.

(66) Dostal H; Mark H *Z.; Phys. Chem. B* 1935, *29*, 299.

(67) Flory PJ, Crescenzi V, Mark JE.; *Principiles of Polymer Chemistry*; Cornell Press:, 1953.

(68) Chojnowski J; *Inorg. Organomet. Polym.* 1991, *1*, 299.

(69) Sigwalt P, Stannett V.; *Polym. J.* 1987, *19*, 597.

(70) Sigwalt P; Stannett V; *Makromol. Chem.* 1990, *32*, 217.

(71) Wilczek L; Kennedy JP; *Polymer Journal* 1987, *19*, 531-538.

(72) Boileau S; *American Chemical Society, Polymer Division*; McGrath, J., Ed.: Washington, D.C., 1980; Vol. 166, pp 283-306.

(73) Dang Ngoc H; Porte H; Hemery P; Boileau S; *International Symposium on Macromolecules;* Mainz, Germany, 1979; Vol. Prep. Vol. I, p 137.

(74) Tanford C.; *The Hydrophobic Effect*; Wiley and Sons: New York, 1974.

(75) Schollenberger CS; Scott H; Moore GR; *Rubber World* 1958, *137*, 549.

(76) Schlick S; Levy M; *J. Phys. Chem.* 1960, *64*, 883.

(77) Milkovich R; S. African Patent No. 280, 712, *Assigned to the Shell Oil Company*: S. Africa, 1963.

(78) McGrath JE; *Ninth Midland Macromolecular Meeting*; Meier, D., Ed.; Harwood Academic Publishers: Midland, Michigan, 1983.

(79) Allport DC; Janes WH.; *Block Copolymers*; Applied Science Publishers Ltd: London, 1973.

(80) Bostick EE.; *Polym. Prepr.* 1969, *10*, 877.

(81) Chojnowski J; Rozga-Wijas K.; *Macromolecules* 1996, *29*, 2711-2720.

(82) Kickelbick G; Husing N; Bauer J, Kickelbick G.; *J. Polym Sci. Part A* 2002, *40*, 1539-1551.

(83) Benham JL; Kinstle JE (Eds.); *ACS Symposium Series*; American Chemical Society: Washington, D.C., 1988.

(84) Mittal JL; *Micellization, Solubilization, and Microemulsions*; Plenum: New York, 1977.

(85) Selb J; Gallot Y; *Developments in Block Copolymers*; Elsevier Applied Science Publishers: London, 1985.

(86) Tanford C; *J. Phys. Chem.* 1974, *78*, 2469.

(87) Preston WC; *J. Phys. Chem.* 1948, *52*, 84.

(88) Hiemenz PC; Rajagopalan R; *Principles of Colloid and Surface Chemistry*; Marcel Dekker, Inc.: New York, Basel, Hong Kong, 1997.

(89) Chen SH; Rajagopalan R; *Micellar Solutions and Microemulsions : Structure, Dynamics, and Statistical Thermodynamics*; Springer-Verlag: New York, Berlin, 1990.

(90) Moroi Y; *Micelles : Theoretical and Applied Aspects*; Plenum Press: New York and London, 1992.

(91) Ruckenstein E; Nagarajan R; *J. Phys. Chem.* 1981, *85*, 3010.

(92) Shinoda K; Hutchinson E; *J. Phys. Chem.* 1962, *66*, 577.

(93) Cutler SG; Meares P; Hall DG; *J. Chem. Soc. Faraday Trans. 1* 1978, *74*, 1758.

(94) Hartle GS; *Aqueous Solutions of Paraffin-Chain Salts*; Hermann: Paris, 1936.

(95) Mattoon RH; Stearns RS; Harkins WD *J. Phys. Chem.* 1947, *15*, 209.

(96) McBain JW; *Colloid Chemistry, Theoretical and Applied*; Reinhold: New York, 1944.

(97) Debye P; Anacker EW; *J. Phys. Colloid Chem.* 1951, *55*.

(98) Hayter JB; Penfold J; *J. Chem. Soc. Faraday Trans. 1* 1981, *77*, 1851.

(99) Cabane B; Duplessix R; Zemb T; *J. Phys* 1985, *89*, 146.

(100) Birdi KS; *Prog. Colloid Polym. Sci* 1985, *70*, 23.

(101) Iyama K; Nose T *polymer* 1998, *39*, 651.

(102) Mahdi SM; Skold RO; *Colloid Surf.* 1992, *66*, 203-214.

(103) Pope E; Sumio S; Klein L; *Sol-Gel Science and Technology*; The American Ceramic Society: Ohio, 1995.

(104) Brinker CJ; Scherer G; *Sol-Gel Science : The Physics and Chemistry of Sol-Gel Processing*; Academic Press: Boston, NY, London, 1990.

(105) Ebelmen; *Annales de Chimie et de Physique* 1846, *57*, 319.

(106) Geffcken W; Berger E In;, 1939.

(107) Schroeder H; *Phys. Thin Films* 1969, *5*, 87-141.

(108) Levene L; Thomas IM In;, 1972.

(109) Dislich H.; *Angewandt Chemie* 1971, *10*, 363-370.

(110) Keefer KD; *Better Ceramics through Chemistry*; Wiley and Sons, Inc.: New York, 1986.

(111) Rankin SE; McCormick AV *Chemical Engineering Science* 2000, *55*, 1955-1967.

(112) McGrath JE; Pullockaren JP; Riffle JS; Kilic S; Elsbernd CS; *Ultrastructure Processing of Advanced Ceramics*; Wiley and Sons, Inc.: New York, 1988.

(113) Plueddemann EP; *Silane Coupling Agents*; Plenum: New York, 1982.

(114) Pohl ER; *38th Annual Tech. Conf.*, 1983; pp Section 4-B.

(115) McNeil KJ; DiCaprio JA; Walsh OA; Pratt RJ; *J Am Chem. Soc.* 1980, *102*, 1859.

(116) Pohl ER; Osterholtz FD; In *Molecular Characterization of Composite Interfaces*; G, I. H. a. K., Ed.; Plenum Press: New York, 1985.

(117) Swain CH; Esteve RM; Jones RH; *J Am Chem. Soc.* 1949, *11*, 965.

(118) Grubb WT; *J Am Chem. Soc.* 1954, *76*, 3408.

(119) Jakubovics J;P *Magnetism and Magnetic Materials*; 2nd ed.; The Institute of Materials: Londong, 1994.

(120) Craik DJ; Tebble RS; *Magnetic Materials*; Wiley-Interscience: London, 1969.

(121) Cullity BD; *Introduction to Magnetic Materials*; Addison-Wesley Publishing Company: Reading, Mass., 1972.

(122) Bashtovoy VG; Berkovsky BM; Vislovich AN *Introduction to Thermomechanics of Magnetic Fluids*; Hemisphere Publishing Corporation: Washington, New York, 1988.

(123) Scholten PC; *Chem. Eng.Comm.* 1988, *67*, 331.

(124) Fertman VE; *Magnetic Fluids Guidebook : Properties and Applications*; Hemisphere Publishing Corporation: New York, 1990.

(125) Berkovsky BM; Medvedev VF; Krakov MS *Magnetic Fluids : Engineering Applications*; Oxford Science Publications: New York, 1993.

(126) Martinet A.; In *Thermomechanics of Magnetic Fluids*; Berkovski, B., Ed.; Hemisphere Publishing Corporation: New York, 1977.

(127) Berkovski B.; *Thermomechanics of Magnetic Fluids*; Hemisphere Publishing Corporation: New York, 1977.

(128) Special Issue, *Chem. Mater.* 1996, *8*.

(129) Pileni MP; *J. Phys. Chem.* 1993, *97*, 9661.

(130) Eastoc J; *Curr. Opinion Colloid Interface Sci.* 1996, *1*, 800.

(131) Sorensen CM; Klabunde KJ; Hajipanayis GC; *J. Mater. Res.* 1999, *14*, 1542.

(132) Bonneman H; Brijoux W; Joussen T; *Angnew. Chem. Int. Ed. Engl.* 1990, *29*, 273.

(133) Reike RD; *Acc. Chem. Res.* 1977, *10*, 301.

(134) Fievet F; Lagier JP; Figlarz M; *MRS Bulletin* 1989, *29*.

(135) Hoffman D; Schlinder W; Krischner J; *Appl. Phys. Lett.* 1998, *73*, 3279.

(136) Petit C; Pileni MP; *Journal of Magnetism and Magnetic Materials* 1997, *166*, 82-90.

(137) Lu J; Dreisinger DB; Cooper WC; *Hydrometallurgy* 1997, *45*, 305-322.

(138) Glavee GN; Klabunde KJ; Sorensen CM; *Langmuir* 1992, *8*, 771.

(139) Mochalov KN; Volkov NV; *Trud Kazan Khim. Techn. Inst.* 1969, *40*, 48-55.

(140) Petit C; Taleb A; Pileni MP; *J. Phys. Chem. B.* 1999, *103*, 1805-1810.

(141) Gomez-Lahoz C; Garcia-Herruzo F; Rodriguez JJ; *Water Res.* 1993, *27*, 985-992.

(142) Blums E; Cebers A; Maiorov MM; *Magnetic Fluids*; Walter de Gruyter: New York, Berlin, 1997.

(143) Hess PH; Parker Jr. PH; *J. Appl Polym Sci* 1966, *10*, 1915-1927.

(144) Riffle JS; Rutnakornpituk M; Vadala M; Wilson KS; J, H. *Polymer Preprints* 2000, *41*, 1368-1369.

(145) Papirer E; Horny P; Balard H; Anthore R; Petipas C; Martinet A; *J. Colloid Interface Sci* 1983, *94*, 207-219.

(146) Smith TW; US Patent 4,252,674; Xerox Corporation, 1981.

(147) Miller RD; Renaldo AF; Ito H; *J. Org. Chem* 1988, *53*, 5571-5573.

(148) Dilanjan Soysa HS; Hiroshige O; Weber WP; *J. Organometallic Chemistry* 1977, *133*.

(149) Chojnowski J; Scibiorek M; Gladkova N; *Polymer Bulletin* 2000, *44*, 377.

(150) Jones R; Ando W; Chojnowski J; *Silicon-Containing Polymers*; Kluwer Academic: Dordrecht, 2000.

(151) Clarson SJ; Dodgson K; Semlyen JA; *Polymer* 1985, *26*, 930.

(152) Hoyt-Lalli J; Riffle JS; PhD Dissertation; *Department of Chemistry*; Virginia Polytechnic Institute and State University: Blacksburg, 2002.

(153) Paulasaari JK; Weber WP; *Macromolecules* 1999, *32*.

(154) Lewix LN; Stein J; Gao Y; Coborn RE; Hutchins G; *Platinum Metals Rev.* 1997, *41*.

(155) Clarson SJ; Semlyen JA; *Siloxane Polymers*; PTR Prentice Hall: New Jersey, 1993.

(156) Horton HR; Moran LA; Ochs RA; Rawn JD; Scrimgeour KG; *Principles of Biochemistry*; Prentice Hall: New Jersey, 1996.

(157) Rutnakornpituk M; Baranauskas VV; Riffle JS; Connolly J; St Pierre TG; Dailey JP; *European Cells and Materials* 2002, *3*, 102-105.

(158) Connolly J; St Pierre TG; Rutnakornpituk M; Riffle JS; *European Cells and Materials* 2002, *3*, 106-109.

(159) Tannenbaum R; *Inorganica Chimica Acta* 1994, *227*, 223-240.

(160) Russier V; Petit C; Legrand J; Pileni MP; *Appl. Surf. Sci.* 2000, *164*, 193-199.

VITA

Michael Lawrence Vadala, son of Captain Lawrence and Patricia Vadala, was born on August 2, 1978 in Orlando, Florida. He is the second child with two sisters, Nicole and Lindsay, and one brother, Timothy. He was raised all over the U.S. due to his father's career in the Navy. His parents currently reside in Richmond, Virginia where he attended Mills E. Godwin high school and graduated with honors in 1996. That same fall, he began his studies at Virginia Polytechnic Institute and State University where he became interested in polymer chemistry and its biological applications. He pursued this interest with CASS under the advisement of Dr. Judy Riffle during the summer of 1998. He continued as an undergraduate researcher under Dr. Riffle for the remainder of his undergraduate career. He graduated with a Bachelor of Science degree in Biochemistry, a Bachelor of Arts in Spanish, and a minor in Chemistry on May 13, 2000. During the fall of 2000, he entered the graduate program at Virginia Polytechnic Institute and State University in pursuit of a Master's degree in Chemistry. His Mater's thesis focused on novel copolysiloxane cobalt complexes for use in biological applications under the advisement of Dr. Judy Riffle. Upon completion of this degree, he will pursue a Doctor of Philosophy degree in Macromolecular Science and Engineering at Virginia Tech.